MODELING AND PROTECTION SCHEME FOR IEEE 34 RADIAL DISTRIBUTION FEEDER WITH AND WITHOUT DISTRIBUTED GENERATION

by

Sidharth Parmar Ashok

A Thesis Submitted in

Partial Fulfillment of the

Requirements for the Degree of

Master of Science

in Engineering

at

The University of Wisconsin-Milwaukee

May 2014

ABSTRACT

MODELING AND PROTECTION SCHEME FOR IEEE 34 RADIAL DISTRIBUTION FEEDERWITH AND WITHOUT DISTRIBUTED GENERATION

by

Sidharth Parmar Ashok

The University of Wisconsin-Milwaukee, 2014
Under the Supervision of Professor Adel Nasiri

The existing power system was not designed with distribution generation (DG) in mind. As DG penetration is being considered by many distribution utilities, there is a rising need to address many incompatibility issues which puts a big emphasis on the need to review and implement suitable protection scheme. The usual practice for existing distribution feeders is the Overcurrent scheme which includes coordination between fuses and reclosers. But when DG is added to the distribution feeder, the configuration is no more radial as there is contribution of fault currents from the DG's and if the existing protection scheme is applied then this could lead to various issues like fuse misoperation or nuisance tripping considering temporary and permanent fault conditions.

This thesis presents a study on the modeling of existing IEEE 34 radial distribution feeder and scaling of the system from 24.9kV to 12.47kV keeping in mind the existing conditions and also proposes a protection scheme with and without the addition of DG's to the feeder nodes. The protection scheme involves providing appropriate relaying with suitable fuse selection and Current transformer settings. Considerations for proper transformer grounding and capacitor bank fusing protection is

also simulated and reviewed. When DG's added, the results show increase in fault contribution and hence causing misoperations which needs to avoided. Relaying considerations are also provided when an islanded mode occurs. The entire analysis has been simulated by a combination of various tools like Aspen One liner, CYMDist and Wavewin with occasional simulations and calculations performed in MATLAB environment.

Dedicated to my grandmother

TABLE OF CONTENTS

LIST OF FIGURES

LIST OF TABLES

ACKNOWLEDGEMENTS

I would like to thank God for providing me the strength and patience to study and perform this thesis. I would also like to sincerely thank my advisor Dr. Adel Nasiri for his continuous guidance and mentorship throughout this project. Without my Professor's support, it would not be possible to study this project and be a part of the research group.

I also sincerely thank my colleagues Dean Sorensen, Harsh Thakkar and Larry Nelson from the Protection Engineering department who have enormously helped me in understanding the mathematical and simulation ideas behind the basics of Protection Engineering and its applications. The support of my colleagues has come at a very crucial stage of my thesis and I owe them many thanks. I would also like to take this opportunity to thank my supervisor Kasia Kulbacka for mentoring me.

Many thanks to all my colleagues from my Research lab and special thanks to Ashish Solanki, Qiang Fu and Luke Webber who have helped me in providing useful inputs and suggestions for my thesis. Lastly, I would like to thank my parents and my closest friends for their continuous support and words of advice.

CHAPTER I: INTRODUCTION

1.1 Summary:

Distribution Generation sources like Photovoltaic, Wind turbines, fuel cells, micro turbines, energy storage technologies, etc are fast finding their importance today to solve environmental issues and serve as alternates to rising energy demand. This thesis is to introduce the modeling of the IEEE 34 radial distribution feeder system structure and study the impacts of Distribution Resources (DR) when integrating with Distribution systems and relaying considerations when it is in islanded mode. Many different distribution structures exist like networked or radial systems or based on grounding configurations. Radial distribution systems consist of a main substation with multiple feeders. They key feature about this system is it has only one source. The nominal phase-to-phase voltage levels of most primary distribution circuits used in the United States ranges between 4.16kV to 34.5kV or between 120/240V secondary voltage levels [1].

For radial power flow on distribution system, faults can be cleared based on the magnitude of fault current using fuses and reclosers, but if there are multiple sources on the distribution network, it is no longer radial in nature and this would require appropriate interconnection protection at the point of common coupling (PCC) between the source and the node at which it is being interconnected with possible requirement of directional or distance based relaying depending on the location of the source.

Faults can be either temporary or permanent in nature and when a fault occurs protection equipment is designed to clear the fault within a few seconds or less. Most of the faults are temporary in nature and hence reclosing would be ideal choice to restore

service immediately rather than the fuse operating to de-energize a permanent fault. Fuses should be coordinated with other protective devices to clear the fault. If the distribution network is radial, fuse saving, which is discussed in detail later, would be a good choice but if network is non-radial, then many issues could arise causing misoperation of fuses leading to nuisance tripping, which ultimately affect the customers. Hence there is a need to decide on a reliable protection scheme with accurate coordination settings.

1.2 Research Objective:

The goal behind this thesis is to model the IEEE 34 bus radial distribution network from scratch with the existing data and scale it down from 24.9kV to 12.47kV system, based on symmetrical components while keeping most of the system parameters unchanged. This is done with the addition of DG's to specific feeders which have already been studied [2]. Then an overall protection scheme is proposed based on the addition of DG's and the impact study is performed which is compared with the existing protection scheme that includes fuse saving practice. This thesis includes a unique approach to protection study that involves appropriate transformer connection and grounding, Capacitor fusing and selection of fuses to CT ratio calculations. Coordination simulation results show the accuracy of the relaying scheme adopted.

1.3 Microgrid:

A microgrid is a part of a large utilitypower system in which sources, usually attached to a power electronic converter, and loads are clustered so that the microgrid can operate independent of the main network being electrically isolated from the power system and also continues to energize thus supplying power to the loads

connected to it. [3], [4]. Research lab at University Services Building at the University ofWisconsin-Milwaukee are progressing to build the Microgrid and controls and thus this thesis includes DG's from this project which includes a 240kW Photovoltaic , two 750kW Wind turbines, one 500kW energy storage and 1.5MVA diesel generator and are connected to the scaled down IEEE 34 bus radial distribution network. Through email correspondence, required citation is provided for the use of Aspen, CYMDist and Wavewin for the modeling of this feeder with and without DG's.

1.4 Problem Statement:

Issues created by adding DG's to distribution network are protective device coordination, potential formation of islanded systems and ground fault detection. The problemstatement is defined as to how to mitigate some of these issues when DG's are added to the distribution feeder system by the approach of interconnection protection and coordination study. The thesis aims to cover a step by step approach from modeling the distribution feeder to coordination of various protective devices on various nodes of the feeder and the impact DG's can have on the system.

CHAPTER II:IEEE 34 BUS RADIAL TEST FEEEDER

2.1 Existing IEEE 34 Bus Radial feeder Model:

In order to add DG's to a distribution network, the existing IEEE 34 bus system was adopted as a test case. The IEEE Distribution Analysis Subcommittee has data for numerous test cases and hence the data for IEEE 34 bus was chosen for the radial distribution feeder [5]. The original system is 60Hz, 24.9kV, 12 MVA with various fixed loads and distributed loads connected to a main utility substation. The load type includes constant current, constant impedance and constant power models (three phase and single phase). The line impedances are calculated from their geometric data and given as configurations which contains details of impedance and capacitance matrices in ohms/mile and Siemens/mile. The entire configuration is as shown below in figure 1 [6] and the model details are found in the same description.

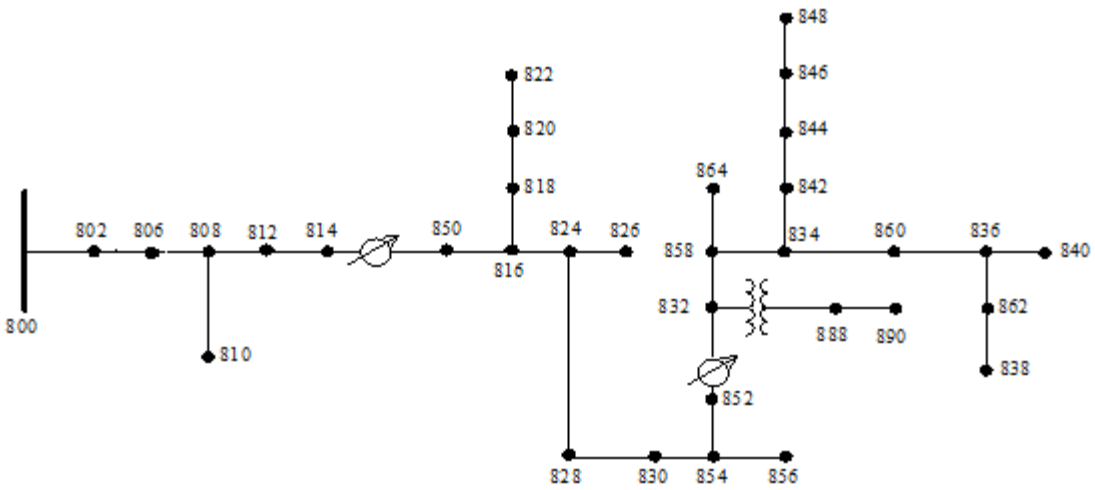

Figure 1: Existing IEEE 34 Bus Radial Distribution Feeder (Adopted from [6])

From the IEEE 34 Distribution feeder committee [5], [6], the information about line impedances, transformer connection and impedances, load data is obtained and tabulated as shownbelow.

Line Segment Data

Node A	Node B	Length(ft.)	Config.
800	802	2580	300
802	806	1730	300
806	808	32230	300
808	810	5804	303
808	812	37500	300
812	814	29730	300
814	850	10	301
816	818	1710	302
816	824	10210	301
818	820	48150	302
820	822	13740	302
824	826	3030	303
824	828	840	301
828	830	20440	301
830	854	520	301
832	858	4900	301
832	888	0	XFM-1
834	860	2020	301
834	842	280	301
836	840	860	301
836	862	280	301
842	844	1350	301
844	846	3640	301
846	848	530	301
850	816	310	301
852	832	10	301
854	856	23330	303
854	852	36830	301
858	864	1620	303
858	834	5830	301
860	836	2680	301
862	838	4860	304
888	890	10560	300

Transformer Data

	kVA	kV-high	kV-low	R - %	X - %
Substation:	2500	69 - D	24.9 -Gr. W	1	8
XFM -1	500	24.9 - Gr.W	4.16 - Gr. W	1.9	4.08

Spot Loads

Node	Load Model	Ph-1 kW	Ph-1 kVAr	Ph-2 kW	Ph-2 kVAr	Ph-3 kW	Ph-4 kVAr
860	Y-PQ	20	16	20	16	20	16
840	Y-I	9	7	9	7	9	7
844	Y-Z	135	105	135	105	135	105
848	D-PQ	20	16	20	16	20	16
890	D-I	150	75	150	75	150	75
830	D-Z	10	5	10	5	25	10
Total		344	224	344	224	359	229

Distributed Loads

Node A	Node B	Load Model	Ph-1 kW	Ph-1 kVAr	Ph-2 kW	Ph-2 kVAr	Ph-3 kW	Ph-3 kVAr
802	806	Y-PQ	0	0	30	15	25	14
808	810	Y-I	0	0	16	8	0	0
818	820	Y-Z	34	17	0	0	0	0
820	822	Y-PQ	135	70	0	0	0	0
816	824	D-I	0	0	5	2	0	0
824	826	Y-I	0	0	40	20	0	0
824	828	Y-PQ	0	0	0	0	4	2
828	830	Y-PQ	7	3	0	0	0	0
854	856	Y-PQ	0	0	4	2	0	0
832	858	D-Z	7	3	2	1	6	3
858	864	Y-PQ	2	1	0	0	0	0
858	834	D-PQ	4	2	15	8	13	7
834	860	D-Z	16	8	20	10	110	55
860	836	D-PQ	30	15	10	6	42	22
836	840	D-I	18	9	22	11	0	0
862	838	Y-PQ	0	0	28	14	0	0
842	844	Y-PQ	9	5	0	0	0	0
844	846	Y-PQ	0	0	25	12	20	11
846	848	Y-PQ	0	0	23	11	0	0
Total			262	133	240	120	220	114

Shunt Capacitors

Node	Ph-A kVAr	Ph-B kVAr	Ph-C kVAr
844	100	100	100
848	150	150	150
Total	250	250	250

Regulator Data

Regulator ID:	1		
Line Segment:	814 - 850		
Location:	814		
Phases:	A - B -C		
Connection:	3-Ph,LG		
Monitoring Phase:	A-B-C		
Bandwidth:	2.0 volts		
PT Ratio:	120		
Primary CT Rating:	100		
Compensator Settings:	Ph-A	Ph-B	Ph-C
R - Setting:	2.7	2.7	2.7
X - Setting:	1.6	1.6	1.6
Volltage Level:	122	122	122

Regulator ID:	2		
Line Segment:	852 - 832		
Location:	852		
Phases:	A - B -C		
Connection:	3-Ph,LG		
Monitoring Phase:	A-B-C		
Bandwidth:	2.0 volts		
PT Ratio:	120		
Primary CT Rating:	100		
Compensator Settings:	Ph-A	Ph-B	Ph-C
R - Setting:	2.5	2.5	2.5
X - Setting:	1.5	1.5	1.5
Volltage Level:	124	124	124

2.2 Scaled down IEEE 34 Bus model for Microgrid

In order to match Microgrid system parameters, the existing IEEE radial distribution feeder is scaled to 12.47kV, 6MVA with other scaling parameters in consistence with the model developed [7]. The wye-wye grounded transformer is scaled from 24.9kV/4.16kV to 12.47kV/4,16kV. The voltage regulators are scaled to 7.2kV. The power ratings of the constant power loads and impedance loads are reduced to half. The method involved for scaling down line impedances is reducing the length of lines to half and quadrupling the capacitance matrix [7]. Hence the Wind turbines are connected to the nodes 840 and 848. Solar Photovoltaic is connected to node 890. Energy storage system is connected to node 828 and the Synchronous generator is connected to node 800. The conversion of ohmic values to sequence values involves symmetrical component analysis which is shown in Appendix A and Appendix B. This step is critical as changes to existing model is been done. The main tools used for this simulation are Aspen one liner and CYMDist. Since CYMDist has the feature to use geometric data based on line spacing, GMR, etc, computation of sequence values is accurate as it takes into account the effect of mutual impedances between lines, except for configuration 302, 303 and 304 where it had to be mathematically computed due to the matrix property. The calculations involving sequence components and conversion to per unit system so that the equivalent impedance can be entered in Aspen One liner is shown in Appendix B.

The use of symmetrical components is to obtain sequence components that can be used to model impedances in both the simulation tools.

Equation (3.2.1) to (3.2.3) represents phase quantities represented in terms of their symmetrical components. $I_{0,}$ $I_{1,}$ I_2 represent zero, positive and negative sequence quantities respectively and *a* is defined as $1\angle 120$.

$$I_{a} = I_0 + I_1 + I_2 \quad (3.2.1)$$

$$I_{b} = I_0 + a^2 I_1 + aI_2 \quad (3.2.2)$$

$$I_{c} = I_0 + aI_1 + a^2 I_2 \quad (3.2.3)$$

Equation (3.2.4) represents in a matrix form

$$\begin{pmatrix} I_a \\ I_b \\ I_c \end{pmatrix} = \begin{pmatrix} 1 & 1 & 1 \\ 1 & a^2 & a \\ 1 & a & a^2 \end{pmatrix} * \begin{pmatrix} I_0 \\ I_1 \\ I_2 \end{pmatrix} \quad (3.2.4)$$

Simplifying equation (3.2.4), the following equations are obtained for conversion to symmetrical components which are used in MATLAB for line impedance calculations.

$$(I_{abc}) = (A) * (I_{012})$$

$$(I_{012}) = (A^{-1}) * (I_{abc})$$

$$\begin{pmatrix} I_0 \\ I_1 \\ I_2 \end{pmatrix} = \left(\frac{1}{3}\right) \begin{pmatrix} 1 & 1 & 1 \\ 1 & a^2 & a \\ 1 & a & a^2 \end{pmatrix} * \begin{pmatrix} I_a \\ I_b \\ I_c \end{pmatrix}$$

In the similar fashion, similar procedure is obtained for conversion of phase to symmetrical components in voltage domain as shown in the equations below

$$V_{a} = V_0 + V_1 + V_2$$

$$V_{b} = V_0 + a^2 V_1 + aV_2$$

$$V_{c} = V_0 + {}_{aV1} + a^2 V_2$$

$$\begin{pmatrix} V_a \\ V_b \\ V_c \end{pmatrix} = \begin{pmatrix} 1 & 1 & 1 \\ 1 & a^2 & a \\ 1 & a & a^2 \end{pmatrix} * \begin{pmatrix} V_0 \\ V_1 \\ V_2 \end{pmatrix}$$

$$(V_{abc}) = (A) * (V_{012})$$

$$(V_{012}) = (A^{-1}) * (V_{abc})$$

$$\begin{pmatrix} V_0 \\ V_1 \\ V_2 \end{pmatrix} = \left(\frac{1}{3}\right)\begin{pmatrix} 1 & 1 & 1 \\ 1 & a^2 & a \\ 1 & a & a^2 \end{pmatrix} * \begin{pmatrix} V_a \\ V_b \\ V_c \end{pmatrix}$$

For unbalanced networks, independent networks are created and connected where the unbalance occurs or the fault location. The above process is to verify the positive and negative sequence impedances for the Z and B matrix based on the configurations from the IEEE 34 bus configuration. Then it is converted to per-unit to be scaled down to 12.47kV system. The scaling method used is the perunit method. Equations (3.2.5) to (3.2.7) represent the equations to calculate impedances in per unit (pu) value using base and actual quantities.

$$I_{base} = \frac{kVA_{base}}{\sqrt{3} * kV_{base}} \quad (3.2.5)$$

$$Z_{base} = \frac{V_{base}}{I_{base}} = \frac{kV_{base}^2 \ \ X\ 1000}{kVA_{base}} = \frac{kV_{base}^2}{MVA_{base}} \quad (3.2.6)$$

$$pu = \frac{actual\ value}{base\ value}$$

$$V_{pu} = I_{pu} * Z_{pu}$$

$$Z_{pu} \ = \frac{Z_{actual}}{Z_{base}} = \frac{kVA_{base}}{1000 * kV_{base}^2} Z_{actual} (3.2.7)$$

It is necessary for impedance values to be converted to new base quantities from pu system from an old base quantity calculated in the pu system. The conversion is accomplished in the following equations.

$$Z_{pu}^{new} \ = \ Z_{pu}^{old}\left(\frac{Z_{base}^{old}}{Z_{base}^{new}}\right)$$

$$Z_{pu}^{new} = Z_{pu}^{old}\left(\frac{kVA_{base}^{new}}{kVA_{base}^{old}}\right) * \left(\frac{kV_{base}^{old}}{kV_{base}^{new}}\right)^2$$

$$Also, \ \ Z_{actual}^{new} = Z_{actual}^{old} * \left(\frac{kV_{base}^{new}}{kV_{base}^{old}}\right)^2$$

Using the above equations [8], the p.u impedance is obtained in the scaled down system and hence the model is built accordingly.

2.3 Comparison of both models to validate the Model Accuracy:

Once the model is built in CymDIST, it is critical to validate the 24.9kV IEEE 34 bus system with IEEE results, so that the final model is accurate enough to perform protection studies. The results for comparison of these models is shown in the includes the simulation studies that compares the load flow studies of the model built in CYMDist and IEEE results obtained from [9]. Once the model is built and verified in CYMDist, the next step is to extract the same model to Aspen One-liner and perform the protection schemes for coordination studies. Table 1, Table 2, Table 3 and Table 4 are the cases for the 24.9kV IEEE 34 bus modeled distribution feeder from CYMDist Validation cases and they show the accuracy of this tool when compared with IEEE results. The error and average differences in various results validate this tool and have enabled to model the scaled down version of the IEEE 34 bus network.

The regulators were modeled as fixed taps in this model not for the model in the scaled down system as the tap settings change for the addition of Distributedgeneration (DG) sources which is discussed in the rest of the chapters.

Table 1: Comparison cases of Line Voltages of IEEE 34 Bus from CYME QA Validation test[9]

NODE	CYMDIST VA (pu)	IEEE VA (pu)	Diff VA(%)	Diff VA(pu)	CYMDIST VB (pu)	IEEE VB (pu)	Diff VB(%)	Diff VB(pu)	CYMDIST VC (pu)	IEEE VC (pu)	Diff VC(%)	Diff VC(pu)
MAIN	1.05	1.0500	0.0000	0	1.05	1.0500	0.0000	0	1.05	1.0500	0.0000	0
802	1.047	1.0475	0.0477	0.0005	1.048	1.0484	0.0382	0.0004	1.048	1.0484	0.0382	0.0004
806	1.046	1.0457	0.0287	0.0003	1.047	1.0474	0.0382	0.0004	1.047	1.0474	0.0382	0.0004
808	1.014	1.0136	0.0395	0.0004	1.03	1.0296	0.0388	0.0004	1.029	1.0289	0.0097	1E-04
810					1.029	1.0294	0.0389	0.0004				
812	0.976	0.9763	0.0307	0.0003	1.01	1.0100	0.0000	0	1.007	1.0069	0.0099	1E-04
814	0.947	0.9467	0.0317	0.0003	0.994	0.9945	0.0503	0.0005	0.989	0.9893	0.0303	0.0003
RG10	1.018	1.0177	0.0295	0.0003	1.026	1.0255	0.0487	0.0005	1.02	1.0203	0.0294	0.0003
850	1.018	1.0176	0.0393	0.0004	1.026	1.0255	0.0487	0.0005	1.02	1.0203	0.0294	0.0003
816	1.017	1.0172	0.0197	0.0002	1.025	1.0253	0.0293	0.0003	1.02	1.0200	0.0000	0
818	1.016	1.0163	0.0295	0.0003								
820	0.993	0.9926	0.0403	0.0004								
822	0.99	0.9895	0.0505	0.0005								
824	1.008	1.0082	0.0198	0.0002	1.016	1.0158	0.0197	0.0002	1.012	1.0116	0.0395	0.0004
826					1.016	1.0156	0.0394	0.0004				0
828	1.007	1.0074	0.0397	0.0004	1.015	1.0151	0.0099	1E-04	1.011	1.0109	0.0099	1E-04
830	0.989	0.9894	0.0404	0.0004	0.998	0.9982	0.0200	0.0002	0.994	0.9938	0.0201	0.0002
854	0.989	0.9890	0.0000	0	0.998	0.9978	0.0200	0.0002	0.993	0.9934	0.0403	0.0004
852	0.958	0.9581	0.0104	1E-04	0.968	0.9680	0.0000	0	0.964	0.9637	0.0311	0.0003
RG11	1.036	1.0359	0.0097	1E-04	1.035	1.0345	0.0483	0.0005	1.036	1.0360	0.0000	0
832	1.036	1.0359	0.0097	1E-04	1.035	1.0345	0.0483	0.0005	1.036	1.0360	0.0000	0
858	1.034	1.0336	0.0387	0.0004	1.032	1.0322	0.0194	0.0002	1.034	1.0338	0.0193	0.0002
834	1.031	1.0309	0.0097	1E-04	1.03	1.0295	0.0485	0.0005	1.031	1.0313	0.0291	0.0003
842	1.031	1.0309	0.0097	1E-04	1.029	1.0294	0.0389	0.0004	1.031	1.0313	0.0291	0.0003
844	1.031	1.0307	0.0291	0.0003	1.029	1.0291	0.0097	1E-04	1.031	1.0311	0.0097	1E-04
846	1.031	1.0309	0.0097	1E-04	1.029	1.0291	0.0097	1E-04	1.031	1.0313	0.0291	0.0003
848	1.031	1.0310	0.0000	0	1.029	1.0291	0.0097	1E-04	1.031	1.0314	0.0388	0.0004
860	1.03	1.0305	0.0485	0.0005	1.029	1.0291	0.0097	1E-04	1.031	1.0310	0.0000	0
836	1.03	1.0303	0.0291	0.0003	1.029	1.0287	0.0292	0.0003	1.031	1.0308	0.0194	0.0002
840	1.03	1.0303	0.0291	0.0003	1.029	1.0287	0.0292	0.0003	1.031	1.0308	0.0194	0.0002
862	1.03	1.0303	0.0291	0.0003	1.029	1.0287	0.0292	0.0003	1.031	1.0308	0.0194	0.0002
838					1.029	1.0285	0.0486	0.0005				
864	1.034	1.0336	0.0387	0.0004								
XFM1_XFO	1	0.9997	0.0300	0.0003	0.998	0.9983	0.0301	0.0003	1	1.0000	0.0000	0
888	1	0.9996	0.0400	0.0004	0.998	0.9983	0.0301	0.0003	1	1.0000	0.0000	0
890	0.917	0.9167	0.0327	0.0003	0.924	0.9235	0.0541	0.0005	0.918	0.9177	0.0327	0.0003
856					0.998	0.9977	0.0301	0.0003				
			Avg.Diff VA(%)	0.03			Avg.Diff VB(%)	0.03			Avg.Diff VC(%)	0.02
			Max.Diff VA(%)	0.05			Max.Diff VB(%)	0.05			Max.Diff VC(%)	0.04
			Avg.Diff VA(pu)	0.0003			Avg.Diff VB(pu)	0.0003			Avg.Diff VC(pu)	0.0002
			Max.Diff VA(pu)	0.0005			Max.Diff VB(pu)	0.0005			Max.Diff VC(pu)	0.0004

Table 1 shows the results of line voltages compared to the IEEE results and gives a small error margin of less than 0.5%. It is interesting to note the cases of nodes 890,844,848 as they are one of the few nodes where DG's are placed as their line voltages changes.

Table 2: Comparison cases of Voltage Angles of IEEE 34 Bus from CYME QA Validation test [9]

NODE	CYMDIST Angle VA	IEEE Angle VA	Diff VA(%)	Diff VA(deg)	CYMDIST Angle VB	IEEE Angle VB	Diff VB(%)	Diff VB(deg)	CYMDIST Angle VC	IEEE Angle VC	Diff VC(%)	Diff VC(deg)
MAIN	0.00	0.00	0.00	0.00	-120.00	-120.00	0.00	0.00	120.00	120.00	0.00	0.00
802.00	-0.05	-0.05	0.00	0.00	-120.07	-120.07	0.00	0.00	119.95	119.95	0.00	0.00
806.00	-0.08	-0.08	0.00	0.00	-120.11	-120.11	0.00	0.00	119.92	119.92	0.00	0.00
808.00	-0.75	-0.75	0.00	0.00	-120.95	-120.95	0.00	0.00	119.30	119.30	0.00	0.00
810.00					-120.95	-120.95	0.00	0.00				
812.00	-1.57	-1.57	0.00	0.00	-121.92	-121.92	0.00	0.00	118.58	118.59	0.01	0.01
814.00	-2.26	-2.26	0.00	0.00	-122.70	-122.70	0.00	0.00	118.00	118.01	0.01	0.01
RG10	-2.26	-2.26	0.00	0.00	-122.70	-122.70	0.00	0.00	118.00	118.01	0.01	0.01
850.00	-2.26	-2.26	0.00	0.00	-122.70	-122.70	0.00	0.00	118.00	118.01	0.01	0.01
816.00	-2.27	-2.26	0.44	0.01	-122.71	-122.71	0.00	0.00	117.99	118.01	0.02	0.02
818.00	-2.27	-2.27	0.00	0.00								
820.00	-2.33	-2.32	0.43	0.01								
822.00	-2.33	-2.33	0.00	0.00								
824.00	-2.38	-2.37	0.42	0.01	-122.93	-122.94	0.01	0.01	117.74	117.76	0.02	0.02
826.00					-122.93	-122.94	0.01	0.01				
828.00	-2.39	-2.38	0.42	0.01	-122.95	-122.95	0.00	0.00	117.72	117.75	0.03	0.03
830.00	-2.64	-2.63	0.38	0.01	-123.39	-123.39	0.00	0.00	117.23	117.25	0.02	0.02
854.00	-2.65	-2.64	0.38	0.01	-123.40	-123.40	0.00	0.00	117.21	117.24	0.03	0.03
852.00	-3.12	-3.11	0.32	0.01	-124.18	-124.18	0.00	0.00	116.31	116.33	0.02	0.02
RG11	-3.12	-3.11	0.32	0.01	-124.18	-124.18	0.00	0.00	116.31	116.33	0.02	0.02
832.00	-3.12	-3.11	0.32	0.01	-124.18	-124.18	0.00	0.00	116.31	116.33	0.02	0.02
858.00	-3.18	-3.17	0.32	0.01	-124.27	-124.28	0.01	0.01	116.20	116.22	0.02	0.02
834.00	-3.25	-3.24	0.31	0.01	-124.38	-124.39	0.01	0.01	116.07	116.09	0.02	0.02
842.00	-3.26	-3.25	0.31	0.01	-124.39	-124.39	0.00	0.00	116.06	116.09	0.03	0.03
844.00	-3.28	-3.27	0.31	0.01	-124.41	-124.42	0.01	0.01	116.04	116.06	0.02	0.02
846.00	-3.32	-3.32	0.00	0.00	-124.46	-124.46	0.00	0.00	115.99	116.01	0.02	0.02
848.00	-3.33	-3.32	0.30	0.01	-124.46	-124.47	0.01	0.01	115.98	116.00	0.02	0.02
860.00	-3.24	-3.24	0.00	0.00	-124.38	-124.39	0.01	0.01	116.07	116.09	0.02	0.02
836.00	-3.24	-3.23	0.31	0.01	-124.38	-124.39	0.01	0.01	116.07	116.09	0.02	0.02
840.00	-3.24	-3.23	0.31	0.01	-124.38	-124.39	0.01	0.01	116.07	116.09	0.02	0.02
862.00	-3.24	-3.23	0.31	0.01	-124.38	-124.39	0.01	0.01	116.07	116.09	0.02	0.02
838.00					-124.39	-124.39	0.00	0.00				
864.00	-3.18	-3.17	0.32	0.01								
XFM1_XFO	-4.64	-4.63	0.22	0.01	-125.73	-125.73	0.00	0.00	114.79	114.82	0.03	0.03
888.00	-4.64	-4.64	0.00	0.00	-125.73	-125.73	0.00	0.00	114.79	114.82	0.03	0.03
890.00	-5.20	-5.19	0.19	0.01	-126.77	-126.78	0.01	0.01	113.95	113.98	0.03	0.03
856.00					-123.41	-123.41	0.00	0.00				
			Avg.Diff VA(%)	0.20			Avg.Diff VB(%)	0.00			Avg.Diff VC(%)	0.02
			Max.Diff VA(%)	0.44			Max.Diff VB(%)	0.01			Max.Diff VC(%)	0.03
			Avg.Diff VA(deg)	0.01			Avg.Diff VB(deg)	0.00			Avg.Diff VC(deg)	0.02
			Max.Diff VA(deg)	0.01			Max.Diff VB(deg)	0.01			Max.Diff VC(deg)	0.03

Table 2 gives a comparison of voltage angles obtained from this tool compared to the IEEE results in order to validate the model accuracy and the motivation behind using this tool and again the difference in error is less than 0.55%.

Table 3: Comparison cases of Line currents of IEEE 34 Bus from CYME QA Validation test [9]

NODE	CYMDIST IA (A)	IEEE IA (A)	Diff IA(%)	Diff IA(A)	CYMDIST IB(A)	IEEE IB (A)	Diff IB(%)	Diff IB(A)	CYMDIST IC(A)	IEEE IC(A)	Diff IC (%)	Diff IC(A)
MAIN	51.547	51.56	0.03	0.01	44.568	44.57	0.00	0.00	40.922	40.95	0.07	0.03
802	51.561	51.58	0.04	0.02	44.569	44.57	0.00	0.00	40.927	40.93	0.01	0.00
806	51.571	51.59	0.04	0.02	42.468	42.47	0.00	0.00	39.237	39.24	0.01	0.00
808	51.744	51.76	0.03	0.02	42.463	42.46	0.01	0.00	39.28	39.28	0.00	0.00
810					0	0.00	0.00	0.00				
812	51.94	51.95	0.02	0.01	41.293	41.29	0.01	0.00	39.328	39.33	0.01	0.00
814	52.089	52.10	0.02	0.01	41.287	41.29	0.01	0.00	39.365	39.37	0.01	0.00
RG10	52.089	52.10	0.02	0.01	41.287	41.29	0.01	0.00	39.365	39.37	0.01	0.00
850	48.455	48.47	0.03	0.02	40.036	40.04	0.01	0.00	38.172	38.17	0.01	0.00
816	48.457	48.47	0.03	0.01	40.036	40.04	0.01	0.00	38.172	38.17	0.01	0.00
818	13.013	13.03	0.13	0.02								
820	10.607	10.62	0.12	0.01								
822	0	0.00	0.00	0.00								
824	35.871	35.87	0.00	0.00	39.824	39.82	0.01	0.00	38.048	38.05	0.01	0.00
826					0	0.00	0.00	0.00				
828	35.874	35.87	0.01	0.00	36.928	36.93	0.01	0.00	37.77	37.77	0.00	0.00
830	35.435	35.43	0.01	0.01	36.914	36.91	0.01	0.00	37.794	37.79	0.01	0.00
854	34.226	34.23	0.01	0.00	36.195	36.19	0.01	0.01	36.486	36.49	0.01	0.00
852	34.35	34.35	0.00	0.00	35.902	35.90	0.01	0.00	36.524	36.52	0.01	0.00
RG11	34.35	34.35	0.00	0.00	35.902	35.90	0.01	0.00	36.524	36.52	0.01	0.00
832	31.769	31.77	0.00	0.00	33.592	33.59	0.01	0.00	33.976	33.98	0.01	0.00
858	20.855	20.86	0.02	0.00	23.127	23.13	0.01	0.00	24.022	24.02	0.01	0.00
834	20.293	20.29	0.01	0.00	22.366	22.37	0.02	0.00	23.229	23.23	0.00	0.00
842	14.736	14.74	0.03	0.00	16.295	16.30	0.03	0.00	15.111	15.12	0.06	0.01
844	14.464	14.47	0.04	0.01	16.282	16.29	0.05	0.01	15.1	15.11	0.07	0.01
846	9.758	9.76	0.02	0.00	9.394	9.40	0.06	0.01	9.779	9.78	0.01	0.00
848	9.749	9.76	0.11	0.01	9.76	9.77	0.10	0.01	9.771	9.78	0.09	0.01
860	5.866	5.87	0.07	0.00	7.676	7.68	0.05	0.00	5.295	5.29	0.09	0.00
836	1.494	1.49	0.27	0.00	4.419	4.42	0.02	0.00	1.743	1.74	0.17	0.00
840	0.793	0.79	0.38	0.00	0.793	0.79	0.38	0.00	0.793	0.79	0.38	0.00
862	0	0.00	0.00	0.00	2.091	2.09	0.05	0.00	0	0.00	0.00	0.00
838					0	0.00	0.00	0.00				
864	0	0.00	0.00	0.00								
XFM1_XFO	69.887	69.90	0.02	0.01	70.046	70.04	0.01	0.01	69.5	69.50	0.00	0.00
888	69.887	69.90	0.02	0.01	70.046	70.04	0.01	0.01	69.5	69.50	0.00	0.00
890	69.903	69.91	0.01	0.01	70.056	70.05	0.01	0.01	69.514	69.51	0.01	0.00
856					0	0.00	0.00	0.00				
			Avg.Diff IA(%)	0.05			Avg.Diff IB(%)	0.03			Avg.Diff IC(%)	0.04
			Max.Diff IA(%)	0.38			Max.Diff IB(%)	0.38			Max.Diff IC(%)	0.38
			Avg.Diff IA(A)	0.01			Avg.Diff IB(A)	0.00			Avg.Diff IC(A)	0.00
			Max.Diff IA(A)	0.019			Max.Diff IB(A)	0.01			Max.Diff IC(A)	0.028

Table 3 is the comparison of results of line currents of the CYMDist and IEEE model and shows that there are very less errors in this case as compared to the other results and is less than 0.3%.

Table 4: Comparison cases of Current Angles of IEEE 34 Bus from CYME QA Validation test [9]

NODE	CYMDIST Angle IA	IEEE Angle IA	Diff IA(%)	Diff IA(deg)	CYMDIST Angle IB	IEEE Angle IB	Diff IB(%)	Diff IB(deg)	CYMDIST Angle IC	IEEE Angle IC	Diff IC(%)	Diff IC(deg)
MAIN	-12.78	-12.78	0.00	0.00	-127.72	-127.7	0.00	0.02	117.33	117.36	0.00	0.03
802	-12.84	-12.84	0.00	0.00	-127.78	-127.76	0.02	0.02	117.27	117.3	0.03	0.03
806	-12.87	-12.87	0.00	0.00	-126.85	-126.82	0.02	0.03	118.48	118.5	0.02	0.02
808	-13.51	-13.51	0.00	0.00	-127.61	-127.59	0.02	0.02	117.72	117.75	0.03	0.03
810					0	0	0.00	0.00				
812	-14.22	-14.22	0.00	0.00	-128.01	-127.99	0.02	0.02	116.86	116.89	0.03	0.03
814	-14.77	-14.77	0.00	0.00	-128.71	-128.69	0.02	0.02	116.2	116.22	0.02	0.02
RG10	-14.77	-14.77	0.00	0.00	-128.71	-128.69	0.02	0.02	116.2	116.22	0.02	0.02
850	-14.77	-14.77	0.00	0.00	-128.71	-128.69	0.02	0.02	116.2	116.22	0.02	0.02
816	-14.78	-14.78	0.00	0.00	-128.72	-128.69	0.02	0.03	116.19	116.21	0.02	0.02
818	-26.77	-26.77	0.00	0.00								
820	-28.99	-28.99	0.00	0.00								
822	0	0	0.00	0.00								
824	-10.76	-10.76	0.00	0.00	-129.04	-129.02	0.02	0.02	116.21	116.23	0.02	0.02
826					0	0	0.00	0.00				
828	-10.78	-10.78	0.00	0.00	-127.43	-127.4	0.02	0.03	116.39	116.41	0.02	0.02
830	-11.12	-11.12	0.00	0.00	-127.94	-127.92	0.02	0.02	115.92	115.95	0.03	0.03
854	-10.05	-10.05	0.00	0.00	-127.3	-127.48	0.02	0.02	116.21	116.24	0.03	0.03
852	-11.06	-11.06	0.00	0.00	-128.68	-128.65	0.02	0.03	115.37	115.39	0.02	0.02
RG11	-11.06	-11.06	0.00	0.00	-128.68	-128.65	0.02	0.03	115.37	115.39	0.02	0.02
832	-11.06	-11.06	0.00	0.00	-128.68	-128.65	0.02	0.03	115.37	115.39	0.02	0.02
858	0.77	0.77	0.00	0.00	-116.41	-116.38	0.03	0.03	128.43	128.47	0.03	0.04
834	2.15	2.15	0.00	0.00	-116.09	-116.05	0.03	0.04	130.01	130.05	0.03	0.04
842	34.63	34.63	0.00	0.00	-95.67	-95.62	0.05	0.05	150.98	151.02	0.03	0.04
844	37.08	37.08	0.00	0.00	-95.73	-95.69	0.04	0.04	150.91	150.96	0.03	0.05
846	78.79	78.79	0.00	0.00	-52.55	-52.54	0.02	0.01	-161.96	-161.96	0.00	0.00
848	78.78	78.78	0.00	0.00	-42.47	-42.47	0.00	0.00	-161.97	-161.94	0.02	0.03
860	-33.63	-33.63	0.00	0.00	-156.52	-156.52	0.00	0.00	86.08	86.08	0.00	0.00
836	-19.83	-19.83	0.00	0.00	-150.74	-150.75	0.01	0.01	68.07	68.06	0.01	0.01
840	-41.12	-41.12	0.00	0.00	-162.26	-162.26	0.00	0.00	78.19	78.19	0.00	0.00
862	0	0	0.00	0.00	-149.49	-149.5	0.01	0.01	0	0	0.00	0.00
838					0	0	0.00	0.00				
864	0	0	0.00	0.00								
XFM1_XFO	-32.3	-32.3	0.00	0.00	-152.74	-152.74	0.00	0.00	87.37	87.37	0.00	
888	-32.3	-32.3	0.00	0.00	-152.74	-152.74	0.00	0.00	87.37	87.37	0.00	0.00
890	-32.32	-32.32	0.00	0.00	-152.76	-152.76	0.00	0.00	87.35	87.35	0.00	0.00
856					0	0						
			Avg.Diff IA(%)	0.00			Avg.Diff IB(%)	0.01			Avg.Diff IC(%)	0.02
			Max.Diff IA(%)	0.00			Max.Diff IB(%)	0.05			Max.Diff IC(%)	0.03
			Avg.Diff IA(deg)	0.00			Avg.Diff IB(deg)	0.02			Avg.Diff IC(deg)	0.02
			Max.Diff IA(deg)	0			Max.Diff IB(deg)	0.05			Max.Diff IC(deg)	0.05

Table 4 is the comparison made for voltage angles and the differences in error in this model is less than 0.3% in this case. The model assumes fixed taps but for the scaled down model it is not fixed taps but control regulated for the voltage regulators and results show that the taps don't exceed the limit of 16 which are developed from discussion and equation in Chapter VI.

CHAPTER III: PRINCIPLES OF PROTECTION SCHEME

3.1 Protection Philosophy:

Since at distribution level, the most common type of relays used are Magnitude and Directional relays, this thesis focuses on using these relays to mitigate the issues faced when DG's are interconnected to this system. By providing instantaneous and time delay to the relay settings, coordination issues can be mitigated[8], [10]. The reason being there can be nuisance tripping due to backfeed of current when DG's are interconnected to the radial feeders and that makes the existing system more complicated [1]. For simulation purposes close-in faults are considered as they are the worst case scenario situations. Depending on the fault current magnitude, primary and back up protection is selected by giving a time delayed approach to the settings. The following terms are used for the language simplification in performing protection studies:

- *Zones of protection*: They are the portions of the electrical power system where the relay operates for a fault occurrence depending on the occurrence of the fault in the zone defined as primary or secondary for backup or tertiary for load encroachment [11].
- *Minimum fault current magnitude*: $|I_f|$, It is the minimum fault current magnitude seen by the relay for any fault [12]
- *Relay pickup*: $|I_{pu}|$, the current magnitude for which the relay will operate and the Pick-up(PU) setting associated with it or the minimum magnitude of current that will allow a relayed protective device to operate [12]

- *Relay operating time*: T: It is the time associated by the minimum operating time of the relay
- *Circuit Breaker* A protective device used to open or close the electrical circuit during a faulted condition or maintenance condition for that section to be operated. During short circuit condition which results in rise of currents, the breaker will sectionalize that particular equipment and feeder sections associated with it so as to allow other sections to operate normally.
- *Coordinating Time Interval (CTI)*Time delay or differences of time between operation of primary and the next protective element
- *DC Offset :*DC offset is a transient component of AC fault current due to sudden rise of phase current in a fault condition
- *Open Interval:* During reclosing operation, open interval is the time interval till the device remains open until it goes into lockout.
- *Recloser:*Unlike the circuit breaker, the recloser is an interrupting device with reclosing function and much more economical which can be controlled by multifunctional protective devices. It works based on the reclosing function which operates the breaker or recloser for the open interval time till it goes to lockout which is a set number of operations it is supposed to operate and trip the operating device
- *Reclosing Reset Time:* It is the time delay used by the recloser logic. Reset after successful reclose occurs when the recloser or breaker is closed and no overcurrent is detected.
- *Relay* It is an electromechanical or digital controlled component that operated the recloser or breaker or switches

Relays can be classified based on input (current/voltage/etc) or operating principle (phase/restraint/magnitude/etc) or performance characteristics (Overvoltage/Overcurrent/Directional/etc)

Classification by Performance Characteristics:

-Overcurrent

-Over/under voltage

-Distance

-Directional

-Inverse time, definite time

-Ground/phase

-High or slow speed

-Current differential

-Phase comparison

-Directional comparison

3.2 Review of Fault types:

There are four major types of faults [13]:

-Single line to ground (1L-G): Unsymmetrical fault where the trend is to see a depression in the faulted phase voltage and sharp rise in current

-Double line to ground (2L-G): Unsymmetrical fault showing the same trend as 1L-G fault involving two faulted phases

-Three line to ground (3L-G): Symmetrical fault showing sharp rise in all three phase currents and collapse of all three phase voltages.

- Line to Line fault (L-L): Unsymmetrical fault where the trend is to see a depression in phase voltage and sharp rise in currents on all the three phase voltages and currents and does not include any zero sequence components

3.3 Overcurrent Protection for radial feeder:

Consider one section of the distribution feeder containing the main utility and section 800 onwards. The simulation results for the fuse saving scheme as discussed in [1], [14] is implemented and shown in Chapter IV. The thesis aims to understand the implementation of overcurrent protection with settings. For instance,

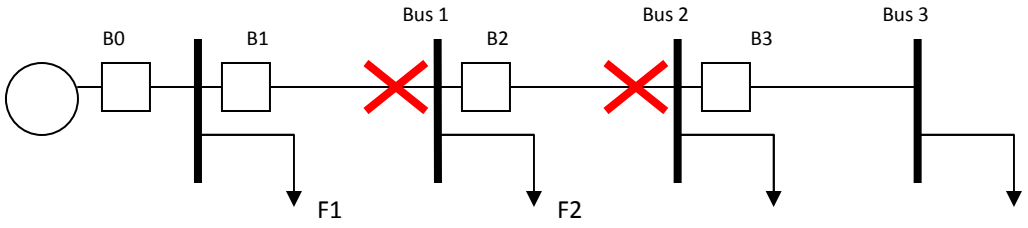

Figure 2 : Section of Overcurrent Protection explanation for various faults represented

In the above figure 2, Let's consider coordination between B1, B2.

F1 and F2 represent feeders and B0, B1, B2 indicate breakers or reclosers or fuses depending on the usage for this example. To set B2, specifying close in fault or specifying classical fault, $|I_{f2}|$, which is for fault located at bus 3 (maximum impedance between source and fault) can be calculated and hence $|I_{pu}|$ can be set to operate faster to trip.

If $|I_f| > |I_{pu}|$ ➔ Trip

If $|I_f| < |I_{pu}|$ ➔ Block

Figure 3 below represents on the current plane

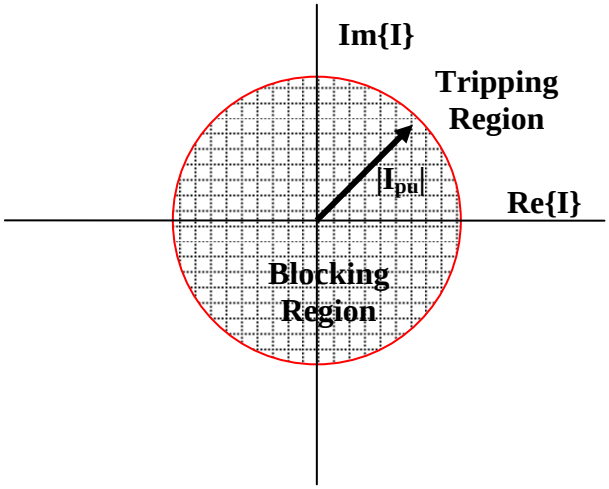

Figure 3: Current plane graph to represent Trip and Block region for a Protective device to operate

If we have $|I_{pu}|$= 6 pu as one of the results from Appendix A, for B1then $|I_{f2}|$ will be higher because the fault is closer and hence say $|I_{pu}|$= 7 pu

But for fault currents pick up set above 7 pu for the line between 1 and 2 has higher chance of misoperation as we want B1 to operate only for faults between buses 1-2, so mitigating between selectivity is useful criteria. Hence we introduce time delay and instantaneous settings. Same pickupswith different time delay will not work as both the relays will operate at different margins

Therefore what we will do is to set B1 to pick up at the same minimum fault current at b2, with time delay, and then apply decreasing time delay for larger currents [15].

$$\frac{I_{Line}}{I_{\mathrm{Re}\,lay}} = \frac{N}{5}, \qquad N > 5$$

And there are limited, discrete choices available for N.

- Using I_p as the minimum current level on the line-side of the CT for which the relay will operate, we have

$$\frac{I_p}{Tap} = \frac{N}{5}, \quad \Rightarrow TAP = \frac{5}{N} I_p$$

where Tap is the pickup setting, in Amps on the relay side of the CT.

To find the appropriate CT ratios, time dial settings and tap ratios, the following scheme is adopted with few modifications from existing scheme from [2],[14].

Possible CT ratios are: 50:5, 100:5, 150:5, 200:5, 250:5, 300:5, 400:5, 450:5, 500:5, 600:5, 800:5, 900:5, 1000:5, and 1200:5. CT ratios and accuracy classes are chosen so that secondary current is limited to 5A and 100A under maximum fault conditions [16]

Possible Taps are 4, 5, 6, 7, and 8.

From correspondence with utility engineers, the coordination time is specified to be T_{CT}=0.3 seconds. To set B1, we have to obtain the sequence components which are shown in the code mentioned in the appendix and calculations shown. The line-to-line voltage: V=12.47/sqrt (3) =7.2 kV. The abc to 012 currents can be obtained from the formulas mentioned above.

Let the minimum fault current be $I_{f,min}$. Let's take a "safety" factor of 3:

$$I_{f,\min} / 3 = I_{p,desired}$$

So based on $Tap_{desired}$ we have to choose the correct CT ratio and then calculate pick up which should be more than load currents in practice. Thus that Tap and pick up current

becomes Tap_{actual} and $I_{p,desired}$. The next step is to select the Time dial which depends on fast it has to operate and the current for which its operation is slowest which is the minimum fault current. Now you need to select the time-dial setting (TDS). To do this, you need two things which is specified by $I_{f,min}/I_{p,actual}$ Also in the above figure if we are setting relays for B2, then we will consider minimum and maximum fault currents in that zone where we want the time delay. For calculations, 3 times pickup is considered as a useful tool to check time dial settings. Therefore, to ensure we get 0.3 time difference between the two relays (each relay having its own TDS and therefore its own time-overcurrent curve), we should perform the design for the maximum current (furthest to the right on the time-overcurrent curves) [17].

Design Summary:

- Choose the taps and CTs (determines relay pickup)
- Then determine the minimum fault current for which the relay should protect. If the relay has back-up responsibility, this will be for a fault outside the primary zone. Employ the safety margin as described above

$$I_{p,desired} = \frac{I_{f,\min}}{3}$$

- Computing the desired tap from for several different values of N and choosing the CT ratio that gives $Tap_{desired}$ close to an available Tap, call it Tap_{actual}.

$$Tap_{desired} = I_{p,desired}\frac{5}{N}$$

Then recomputed the pickup as

$$I_{p,actual} = \left(\frac{N}{5}\right) Tap_{actual}$$

and check if it is close to $I_{p,desired}$.

- Choosing Total operating time for back-up relays is by computing maximum fault current in backed-up zone, $I_{f,max}$. and calculating operation time for primary relay, $T_{P,}$ the total time delay for the relay is calculated as (T_P+T_{CT})

3.4 Coordination Study of Overcurrent Protection:

Overcurrent protection scheme is implemented for coordination of relay of interest with relays to be coordinated upstream which refers to the supply side or higher voltage side of the system. For radial network, since the level of fault current is same, the coordination is done for the feeder protection with upstream protection.

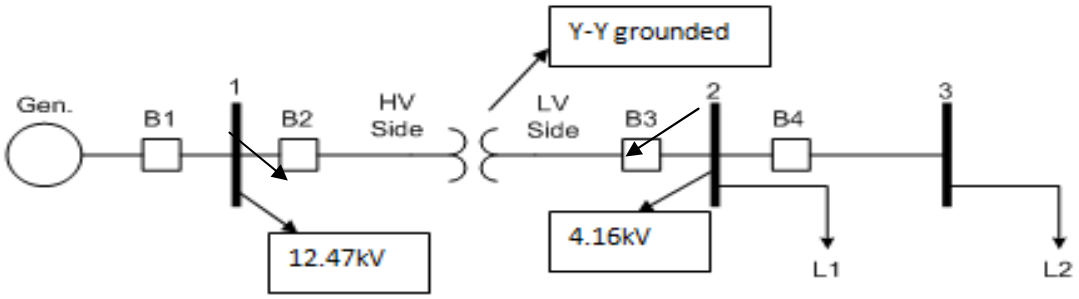

Figure 4: Bus 800 represented as Number 1 to show Coordination study approach

The above figure 5 is one part of the 34 bus radial distribution feeder that shows step down of 12.47kV to 4.16kV. So for a fault between bus 2 and 3, B4 is set to operate faster than B3 by time delayed approach thus defining primary and backup protection zones. The design approach is mentioned in the above pages. Simulation studies show that coordination is done in only for a set of breakers as faults outside that zone could affect normal operation of breaker as it adds more time delay. The figure below shows coordination curves obtained and is compared with standard curves from various relay information documented in Appendix D

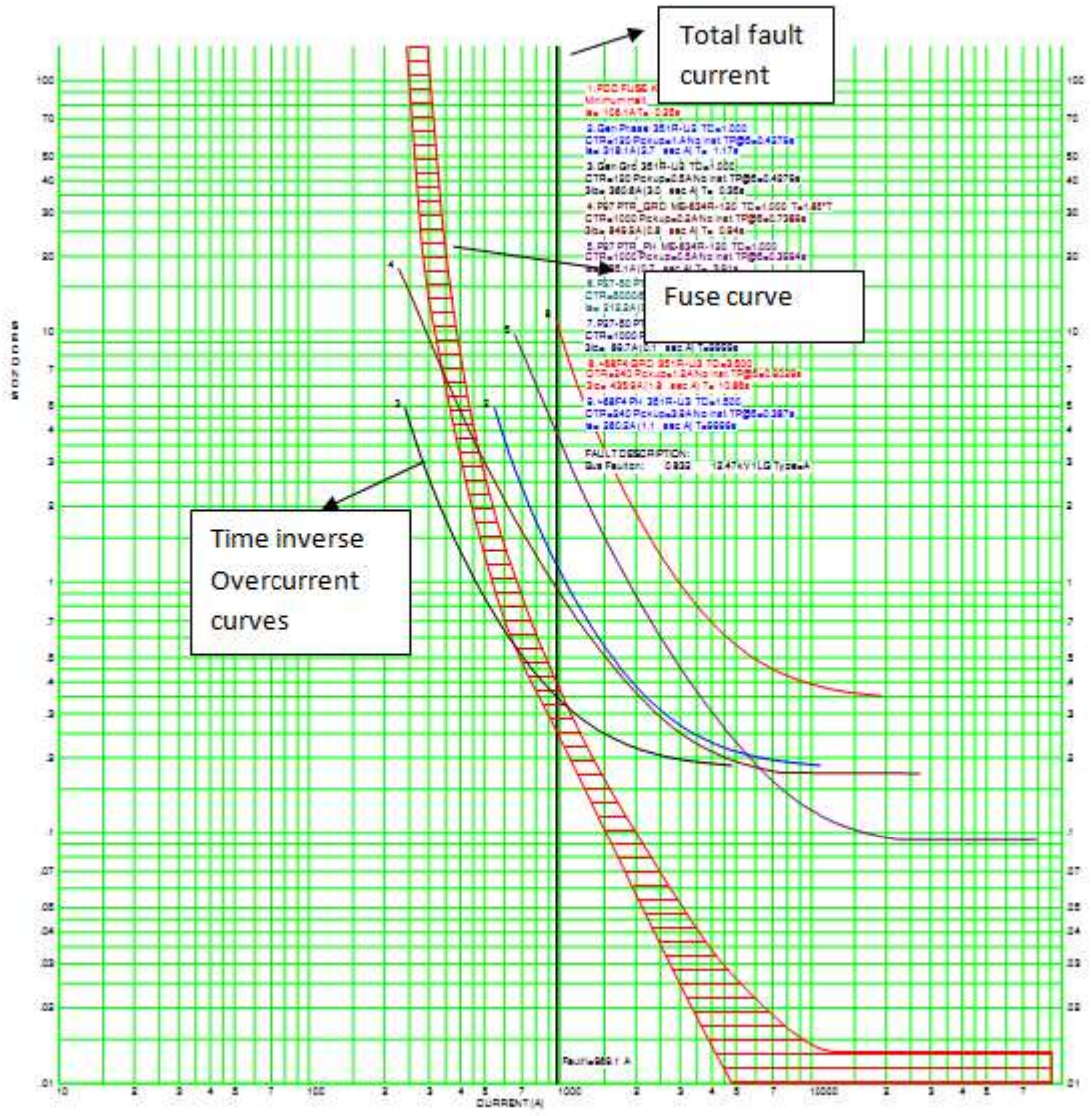

Figure 5: Description of Coordination curve from Aspen One-liner

Figure 6 above shows all types of faults and depending on our interested it can be aligned for a particular fault type.The graph is a log-log graph with time on the vertical axis and current on the horizontal axis. For coordination purposes, the transformer relay curves should intersect with the fault current line at least 0.3 seconds after the feeder relays and the transformer damage curves are always on the higher side if there happens to be any

internal fault.Coordination is also checked for line to line faults as ground curves do not play in a role in this case.Objective of Overcurrent protection is to protect equipment from damages due to fault currents and thus maintain a reliable distribution system.

Fuse Saving: This approach is followed by many utility companies to clear temporary faults on laterals. When fuses are located in laterals, using these approach temporary faults can be cleared by breakers or reclosers and permanent faults can be cleared using the fuses. In this thesis fuses are selected based on time delayed approach rather than instantaneous settings so that temporary faults can be cleared first.

Instantaneous Settings :In general, instantaneous settings are used to limit equipment damage from high magnitude fault conditions. Unlike time inverse overcurrent curves as discussed above, they do not follow these characteristics, but will operate immediately for any value of current set by the user to operate instantaneously. An instantaneous value of 150% of the magnitude of an expected end of zone, bolted fault is recommended if the instantaneous element is sensitive to DC offset[18].

Load Encroachment: When the load current and fault current are similar values then this approach is used by allowing a tripping region and blocking region based on changes in impedance angle, as shown in figure .Load impedance typically has a lower impedance angle (higher power factor) than fault impedance.

Transformer Inrush Current: A transient phenomenon in which there occurs a short-duration inrush of magnetizing current when an unloaded, or loaded, distribution or power transformer is energized. The transformer's primary protective device must be capable of withstanding this inrush current without operating (or, in the case of certain types of fuses, without sustaining damage to their fusible elements).

In the case of a fuse, the minimum-melting curve should be such that the fuse will not operate as a result of this magnetizing-inrush current.

To avoid a nuisance operation of the transformer-primary fuse or relayed protective device, it must be capable of withstanding the magnetizing-inrush current of the transformer superimposed on the transient overcurrent associated with picking up cold load current, the expected overload current associated with the total kVA connected.

The transformer primary fuse or relayed protective device to must be able to withstand the combined magnetizing- and load-inrush current [19]. With consultation with various protection engineers in utility industries and keeping in mind various industry practices, the following guidelines for overcurrent protection settings is tabulated as shown in below flowchart and also for the above rules for coordination purposes.

(Pickup value of Phase/Ground unit)$_{upstream}$ > (Pickup value of Phase/Ground unit)$_{downstream}$

For a 3-phase fault phase pickup should be able to clear the fault in < 1s

Phase settings are set to coordinate with 140K fuse and ground settings are set to coordinate with 100K fuse

For reclosing operation, fuses are set to operate before recloser foes into lockout condition by coordinating with fuse's minimum melt and total clearing time

Load encroachment settings are recommended in case 100K fuses do not clear the fault less than one second

TCI (Time coordination interval) between devices from discussions with utility practices:

Electromechanical relay with electromechanical relay : 0.3s (assuming breaker time <0.1s)

Electromechanical relay to electronic device - 0.3 seconds

Electromechanical device to fuse – 0.2 seconds –

Electronic device to electronic device – 0.2 seconds

Electronic device to fuse – 0.1 seconds

Fuse to fuse – 0.1 seconds

3.5 Fuse Selection Study:

Fuses are required in any circuit to protect the circuit from overcurrent condition due to short circuit or overloaded conditions. In this work, fuses are selected based on various parameters like:

- Normal load current and voltage
- Short circuit current
- In rush currents
-Reliability of fuse in order to be reattachable and resettable

In this thesis, fuses are selected at 135% of normal load current at standard temperatures. If the ambient temperatures are extreme then the fuse ratings have to be re-rated. Another important factor in considering fuses is the total clearing time (Tc) , melting time (Tm) and arcing time(Ta) and these factors are included while performing coordination between the fuses and reclosers.

3.6 Effect of addition of Distributed Generation in Radial feeder:

From the simulation results tabulated in Appendix A, when DG's are connected there is a clear increase in fault current at some of the nodes and also from the load flow study it can be seen that adding DG at 890 increases under voltage at 890 from 0.99 to 0.95 pu. The data used to find the DG impact on the distribution feeder are [18], [20]:

-size and type of DG converter and prime energy source
-Fault current contribution from the DG
-Location of DG which for this system has been discussed in [7]
-Type of interfacing transformer connection used at the point of coupling DG with the distribution feeder

The below figure 6 shows the configuration of microgrid attached to the 34 bus radial distribution feeder. Following general protection scheme and the configuration adopted from [2],[14], which involves only fuse recloser scheme the results seem consistent and is discussed in detail in the simulations

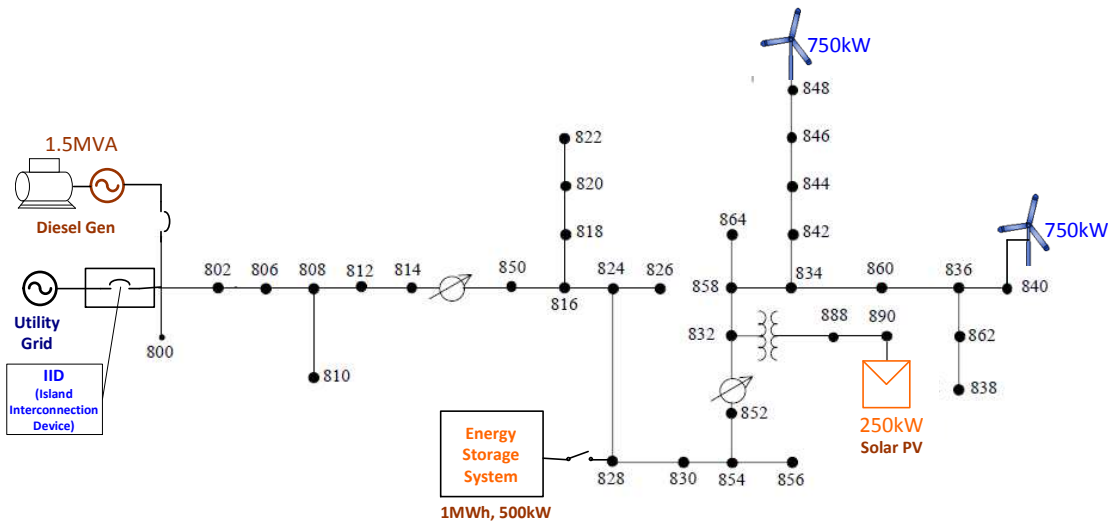

Figure 6: Topology of Distributed Generation Sources added to IEEE 34 Bus network (Adopted from [7])

In our study, for example at node 890 where PV is interconnected there is voltage imbalance and using the existing protection scheme there is also coordination issues as there is increase in fault current, as shown in figure 7

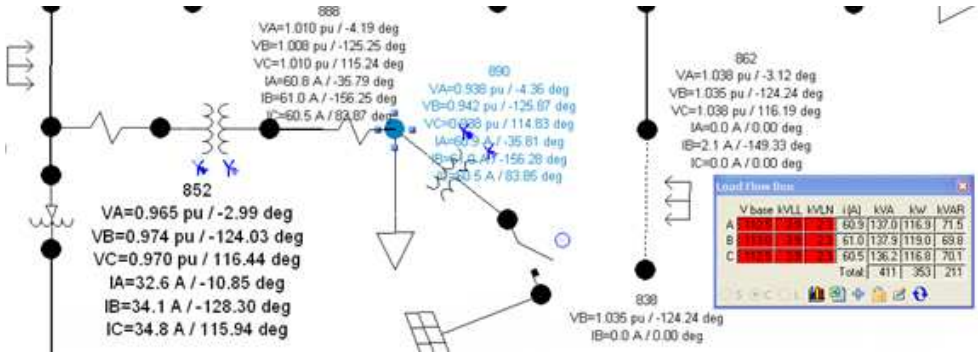

Figure 7: Snapshot of Cyme Fault study at Bus 890 showing voltage imbalance

The following figure 8 is adopted for explanation purposes from [1], shows the impact of DG in an understable procedure. The figure shows that increase in fault current due to addition of DG causes the fuse to melt for a temporary fault before the recloser clears the fault. This leads to misoperation of the fuse. This is a classical demonstration to show one of the main issues while applying Overcurrent Protection for a distribution network and goes to show that when there is high penetration of DG's the existing protection needs to be remodeled and revamped.

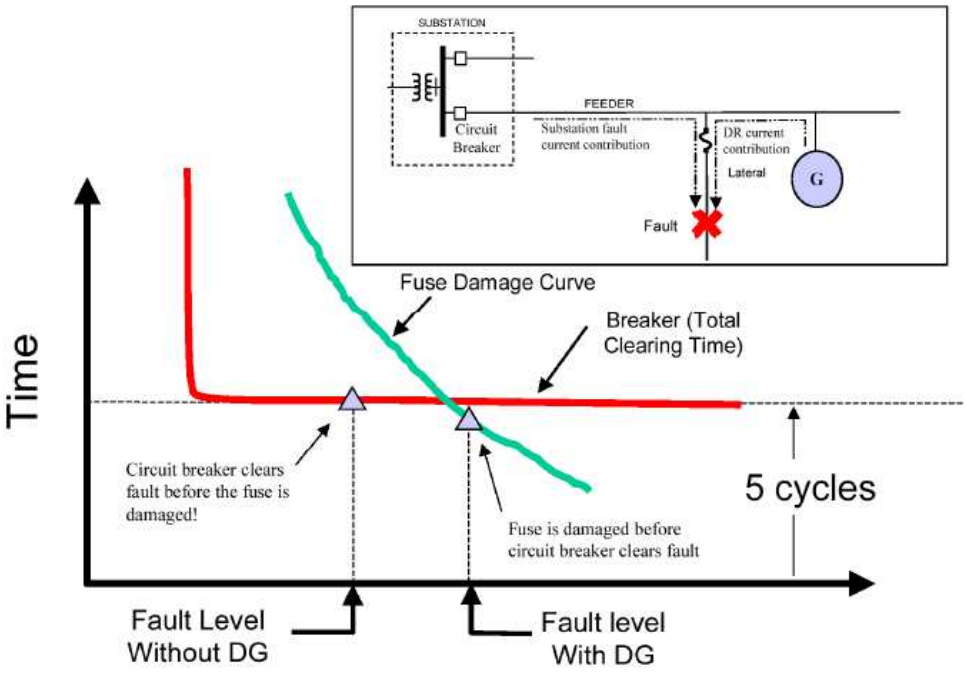

Figure 8: Misoperation of Protective devices due to addition of DG's (Adopted from [1])

CHAPTER IV: INTERCONNECTION PROTECTION

4.1 Issues discussed in addition of DG's to existing Overcurrent Protection:

-Sensitivity of Phase and ground protection of feeder breakers based on addition of DG's

-Based on faults on other feeders, it could lead to current contributions from DG's and hence backfeed is an issue

-Out of sync reclosing due to islanding condition.

Impacts of these issues are shown in the simulation results in Appendix A and Chapter IV deals with the methods to mitigate these issues to a certain extent. For instance in one of the cases considering DG at node 800 as synchronous generator, there is an increase of current to 3273A. Close in fault on node 800 not only accounts for fault contribution from DG's on other nodes but also since it is connected to low voltage side of the main utility transformer it has to be implemented with sufficient interconnection protection.

4.2 Impact of Fault contributions of DG's on Lateral Fusing practice:

Without the DG's the fuse recloser scheme is adopted from [14],[21] and implemented in Aspen for the scaled down version of 12.47kV system In the below figure 9, the laterals are defined as the lines that bifurcate from the nodes and some of the loads are fixed loads and some are distributed loads which are single and three phase as described in the IEEE 34 bus distribution feeder

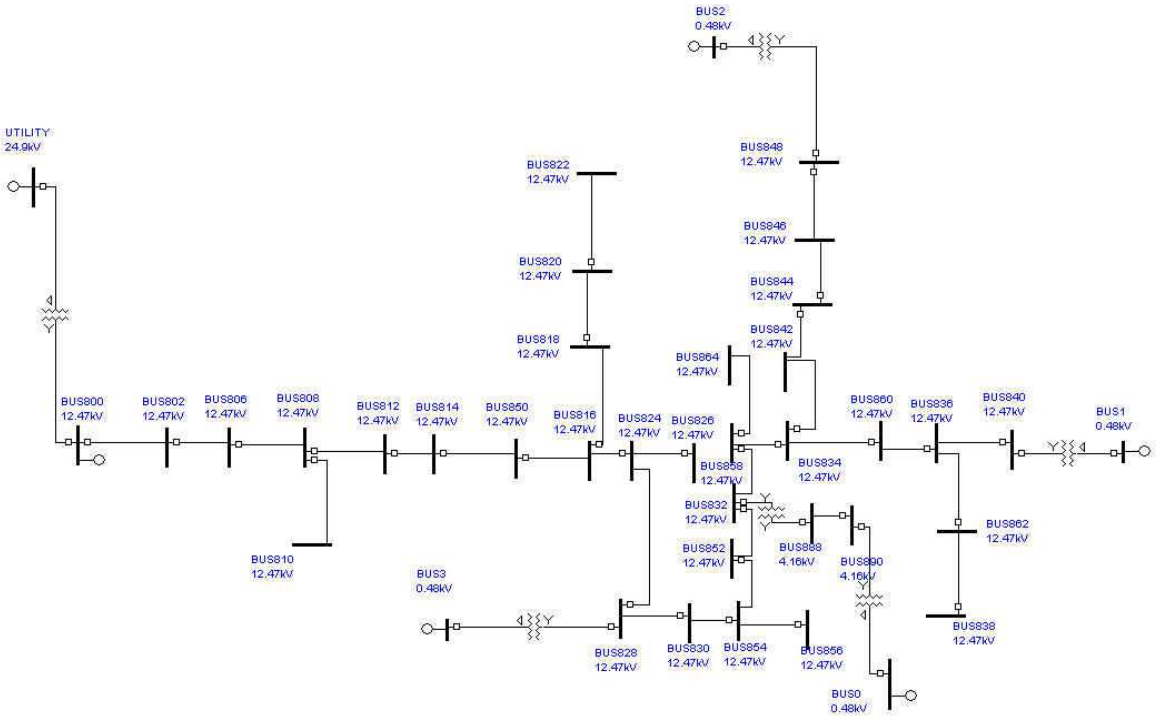

Figure 9: Complete Scaled down model of IEEE 34 Bus distribution network with DG's in Aspen

The below figure 10 shows a case for minimum fault on node 810 which is to validate the result from the reference [2] , but for the scaled down version

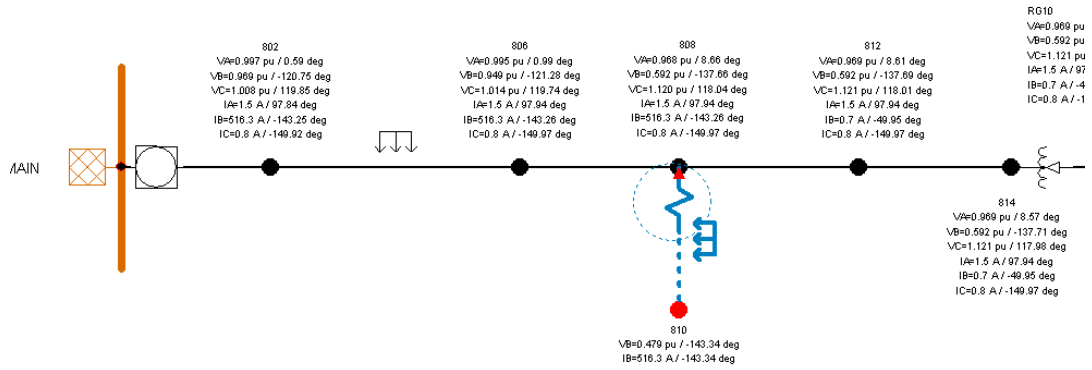

Figure 10: Close in fault at Bus 810 of the 34 bus distribution network

The aim is to achieve the coordination between the recloser and fuse on the lateral for a minimum classical fault on node 810. As expected we would want the recloser to operate first before the fuse melts for the temporary fault. As seen in the graph, the sensitivity is really poor as coordination interval time for any total fault is below its operating margin of 0.3s. Overall adjusting the time dial would yield better coordination. Simulation performed for the fuse recloser scheme shows similar results as obtained in [14], [22], [23], with the scaled down version. Addition of DG's clearly changes the dynamics of the system as it changes the magnitudes of fault currents, direction of power flow , mismatch of fault current leading to misoperation of fuses when fuse is coordinated with fuse or fuse with recloser and the effect of transients from the DG's.

Figure 10 also shows the lateral modeled as three phase as described in the IEEE description and is particularly important for fuse-recloser coordination when the DG is added at node 800. Figure 11 below shows the coordination curve of a fuse recloser scheme with emphasis of fuse saving to show the recloser trips for a temporary fault and then the fuse melts for a permanent fault , but the operating margin is clearly less than 0.3s even after improving the time dial settings.

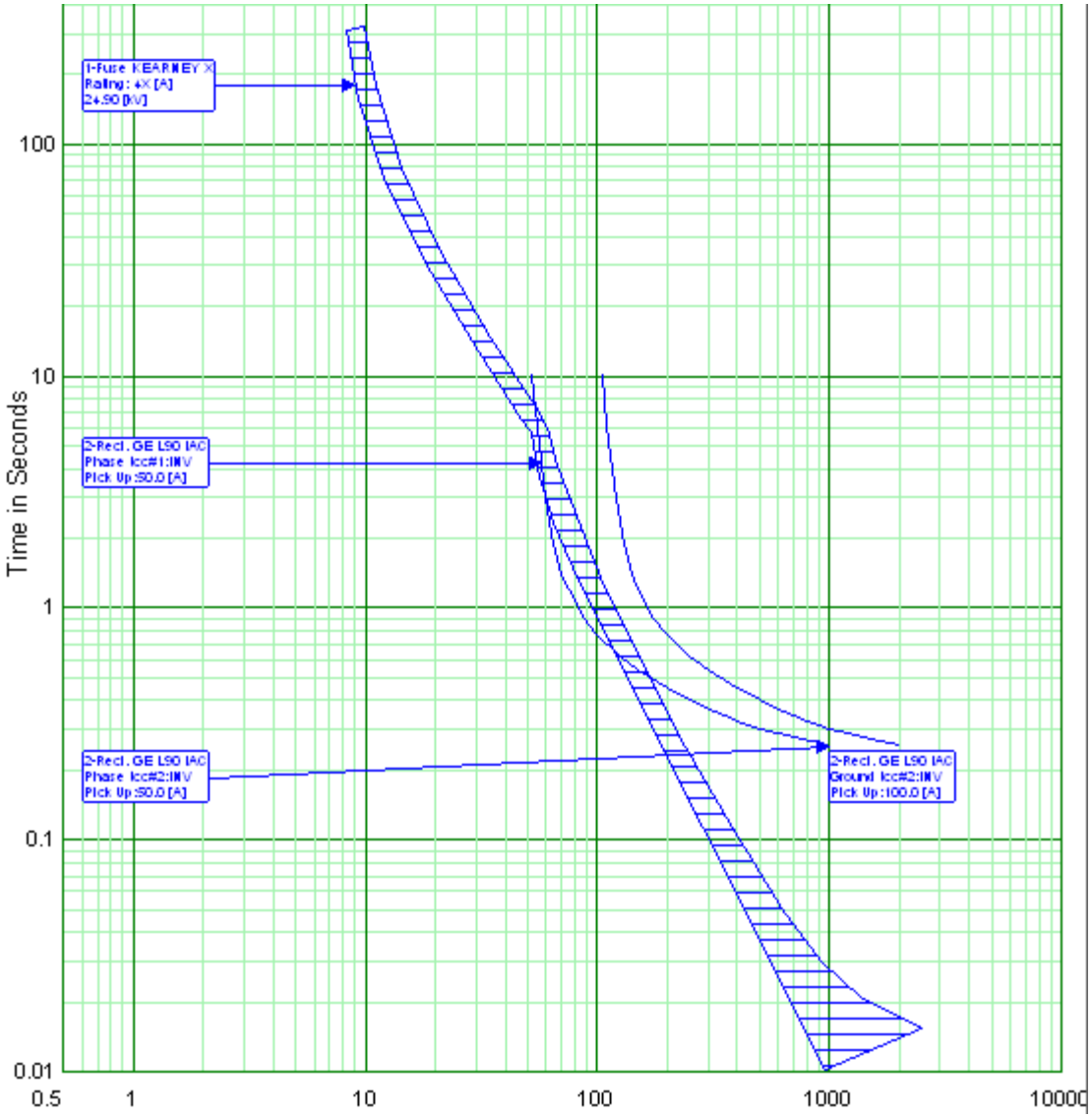

Figure 11: Fuse Recloser coordination study with operating margin less than 0.3s

Hence there is a need to modify the protection scheme and settings by choosing slower phase and ground units while also adding a time multiplier to the recloser settings. These are adopted when interconnection protection scheme is implemented.

4.3 Nuisance tripping of feeder with DG:

From the figure 12 below, if the one line is simplified with DG's and addition of an adjacent feeder, then this could lead to nuisance tripping of feeder due to addition of DG. The fault indicated may cause tripping of both the breakers instead of just the breaker on the adjacent feeder if the breaker on the main utility does not normally have reverse power flow detection . Hence the fault could lead to misoperation of both the breakers leading to the outage of the entire feeder.

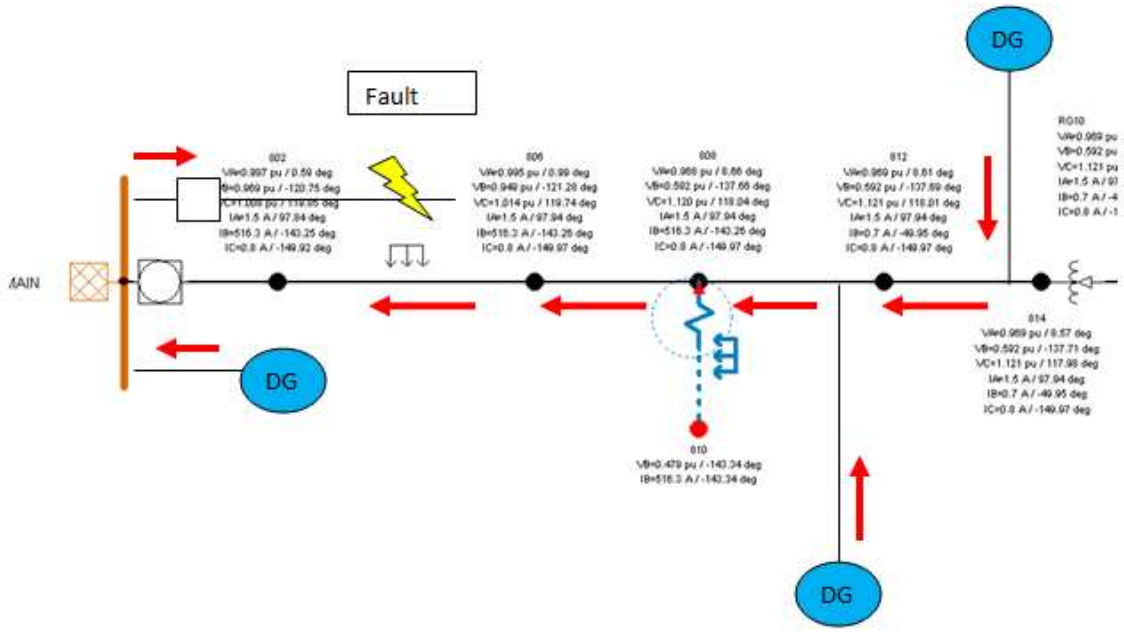

Figure 12: Nuisance tripping of feeder breaker due to multiple sources of current for a faulted condition

Hence appropriate settings can help detect this issue and using fuses and reclosers alone cannot detect the reverse power flow issues and directional issues and hence the breakers have to upgrade.

4.4 Grounding study and Transformer Phasing:

Based on the existing configuration, the transformer is wye-wye grounded for step down of 12.47kV to 4.16kV. The interconnection transformers chosen for this work is delta-wye grounded where the low side which is the DG side is delta connected and the high side is wye grounded.The distribution feeder used is four wire neutral grounded and IEEE standards suggest that the DG should be effectively grounded which is defined between the ratio of sequence impedances of the generator and transformer combined [1], [24]. This study involves analysis involved with the transformer connection and generator grounding. IEEE standard recommends the use of the above transformer connection and hence it is used for this study.

Transformer terminals are usually represented as H1 H2 H3 and X1 X2 X3 and based on the H/X relationship obtained from the transformer name plate details and various combinations allowable for the windings, the transformer rotations and field connections to H and X terminals are tabulated in the table below after discussions with utility substation experts. In our case, the high side leads the low side by 30°. Table 5 is developed after constructing various possibilities using positive and negative sequence networks for the high side leading the low side by 30°. Using the dot convention and approach of rotation of networks while angles rotating always in the counter clockwise direction, Table 5 was developed and were used while modeling the interconnect transformers.

Table 5:Transformer Phasing results for High side leading the low side by 30°

Test Cases	H & X Terminal Inputs and Outputs				Rotation	Phase Connections to H & X Terminals			Rotations after Phase Connection
1	H1/H2/H3	0	120	240	ABC	A	B	C	ABC
	X1/X2/X3	330	90	210	ABC	A	B	C	ABC
2	H1/H2/H3	240	0	120	ABC	C	A	B	ABC
	X1/X2/X3	210	330	90	ABC	C	A	B	ABC
3	H1/H2/H3	120	240	0	ABC	B	C	A	ABC
	X1/X2/X3	90	210	330	ABC	B	C	A	ABC

For this work, the interconnect transformer are chosen based on various consultations from different standards like IEEE 1547 [25] with various merits and demerits. Based on the DG location and fault current contribution, interconnect transformers are chosen as delta on low side and wye grounded on high side. The table below formulates various interconnect transformers for faults F1, F2 and F3 shown in figure 13.

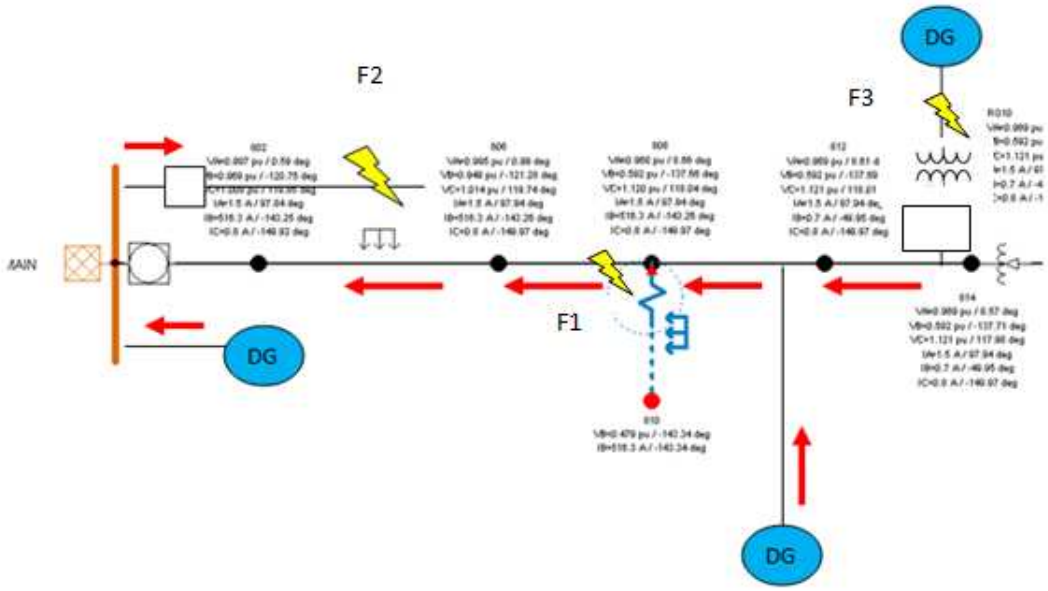

Figure 13: Faults at three locations F1, F2, F3 with Interconnect transformer selection

As seen in figure 13, for faults on various locations, the choices of selecting the right transformer was analyzed. This analysis is studied from various ANSI and IEEE standards and the 2001 EPRI document for integrating DG's to distribution network. Based on discussions from table 6, interconnect transformer chosen was delta-wye grounded, with delta on low voltage DG side. Since overvoltage being a main concern during islanded conditions, delta-wye with proper grounding of the DG's reduces this risk and hence with appropriate Overcurrent protection, for our system, interconnection protection is implemented.

Table 6: Merits and Demerits for choosing Interconnect transformer at point of interconnection

High side	Low side	Merits	Demerits
Δ	Δ	For faults F1 , F2 and F3 there is no ground fault current contribution as high side is delta connected	Overvoltage issues
Δ	Y gr		
Y	Δ		
Δ	Y gr	For fault F3 there is no ground current and no overvoltage for Fault F1 as high side is Y grounded and DG is sufficiently grounded	Ground current contribution for fault F1 and F2 and hence need Overcurrent protection for ground fault
Y gr	Y gr	No overvoltage issues as generator neutral is grounded.	Fault at F3 could cause breaker misoperation

4.5 Capacitor Bank fusing study and Voltage regulator settings:

In the IEEE 34 bus radial system , Capacitor banks are located at Nodes 844 and 848 and proper fusing practice is required as Wind turbine is connected to Node 848. The practice adopted in this model is Single wye grounded Cap Bank protection. This study is to show arrangement of the bank and its study performed in Matlab for fault study.

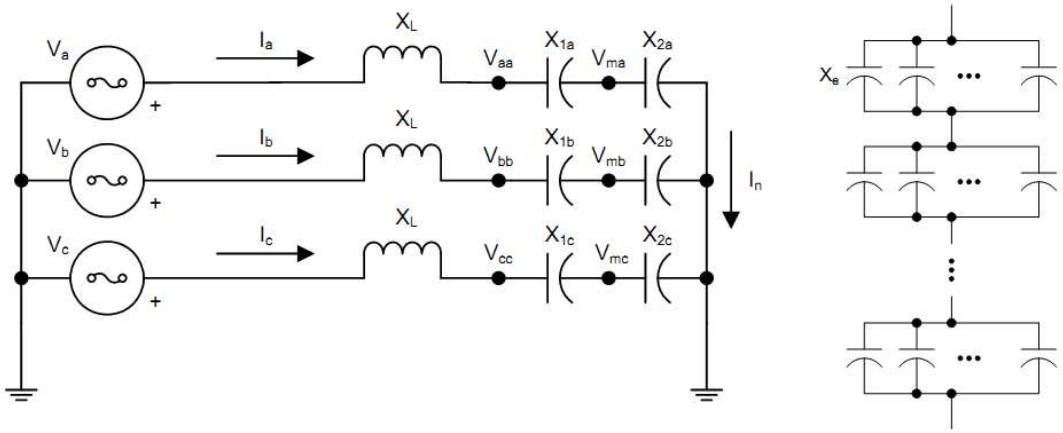

Figure 14: Single Wye grounded Capacitor bank arrangement at nodes 844 and 848 (Adopted from [25], [28])

With the assistance from utility companies to know the calculations involved for the single wye grounded banks, IEEE standard [25], [26], [27], [28] suggests some limitations, which are:

-135% of nameplate kVAr

-180% of rated RMS current, including fundamental and harmonic currents. Many fuse manufacturers specify the fuse curve versus full load current and case rupture curves. For a model developed in Matlab Simulink for the above Capacitor Bank arrangement of rating 12.47kV and 150kVAR. The following arrangement was used as shown in figure 15 and 16. With assistance from Protection Engineers at Utility industries, single wye grounded configuration is chosen as the model in this case to avoid ground faults which is a major concern while practicing capacitor fusing practice.

Four fuses shown with switches are used to simulate blown fuses for faulty conditions. Figure 17, 18 and 19 are various current and voltages obtained from the protected elements. Only one parallel arrangement is used in this case. The capacitor

banks are rated at 250kVar with operating voltage of 12.47kV. As seen from figure 17, the first switch opens in 0.1s relating to an operation of 6 cycles and the successive elements in multiples of 6 cycles. This study and the model were developed with consultation and citation from Protection Engineer at Utility companies.

Blown Fuses Analysis:

Figure 15: Current and Voltages on Protected Element (at t=0.1s)

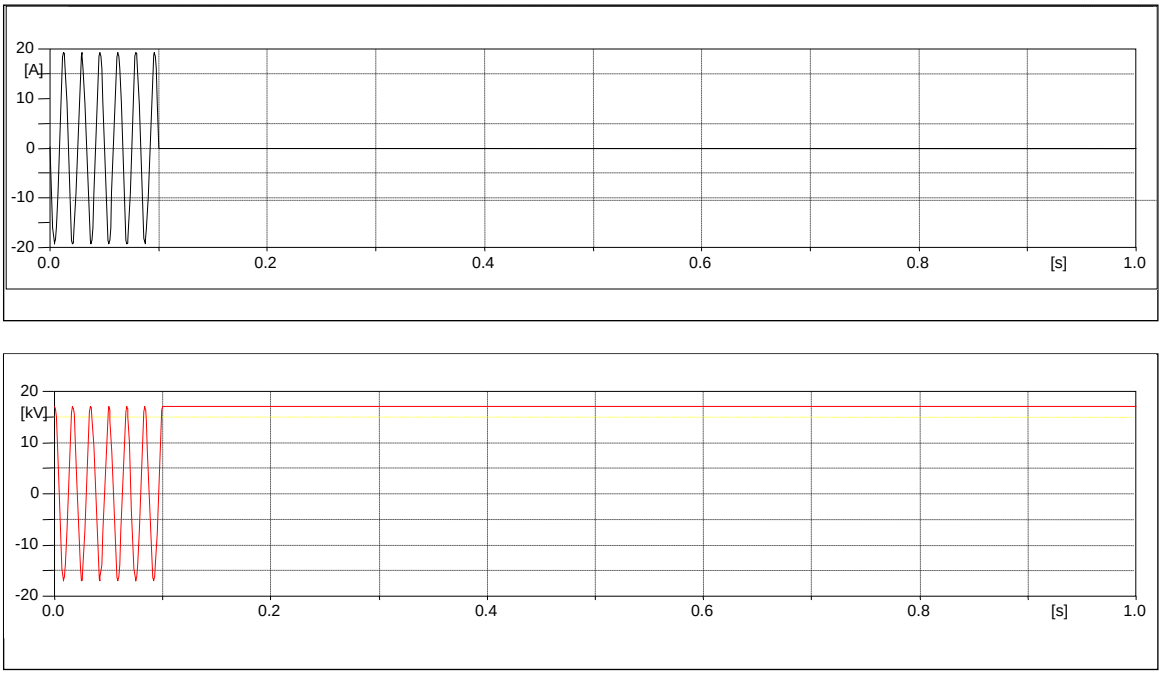

Figure 16: Bank neutral current after BF1 - BF4 open in succession

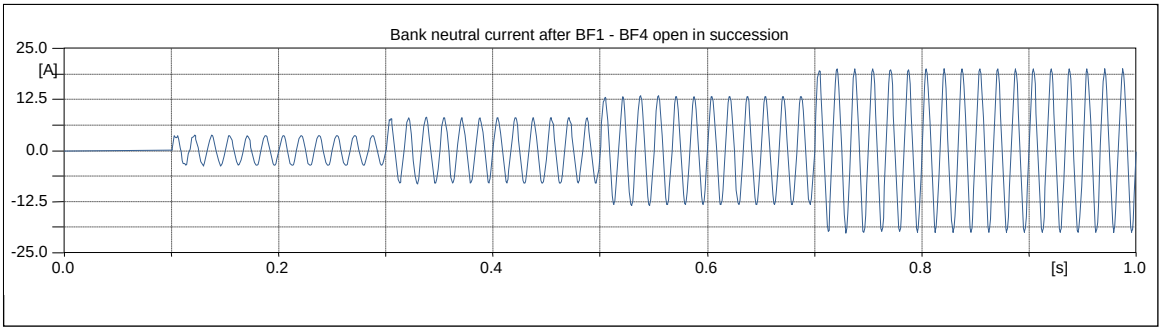

Figure 16 uses the fuse operation for the capacitor neutral current 3Io and the successive intervals it operates. Using CYMDist, the operation of Fuse during a capacitor fault at node 848 on cap side is simulated and the coordination is performed as shown in figure 17below . For a specific line to ground fault there is enough coordination time for the fuse to operate. The fuses represent the fuse at Capacitor bank at node 848 and 844 for existing fuse recloser arrangement. As seen for this arrangement, the capacitor fuses melt for a three phase to ground fault as there is a higher fault contribution and the aim is to protect the cap buses from further damage and hence faster melting time operation is adopted.

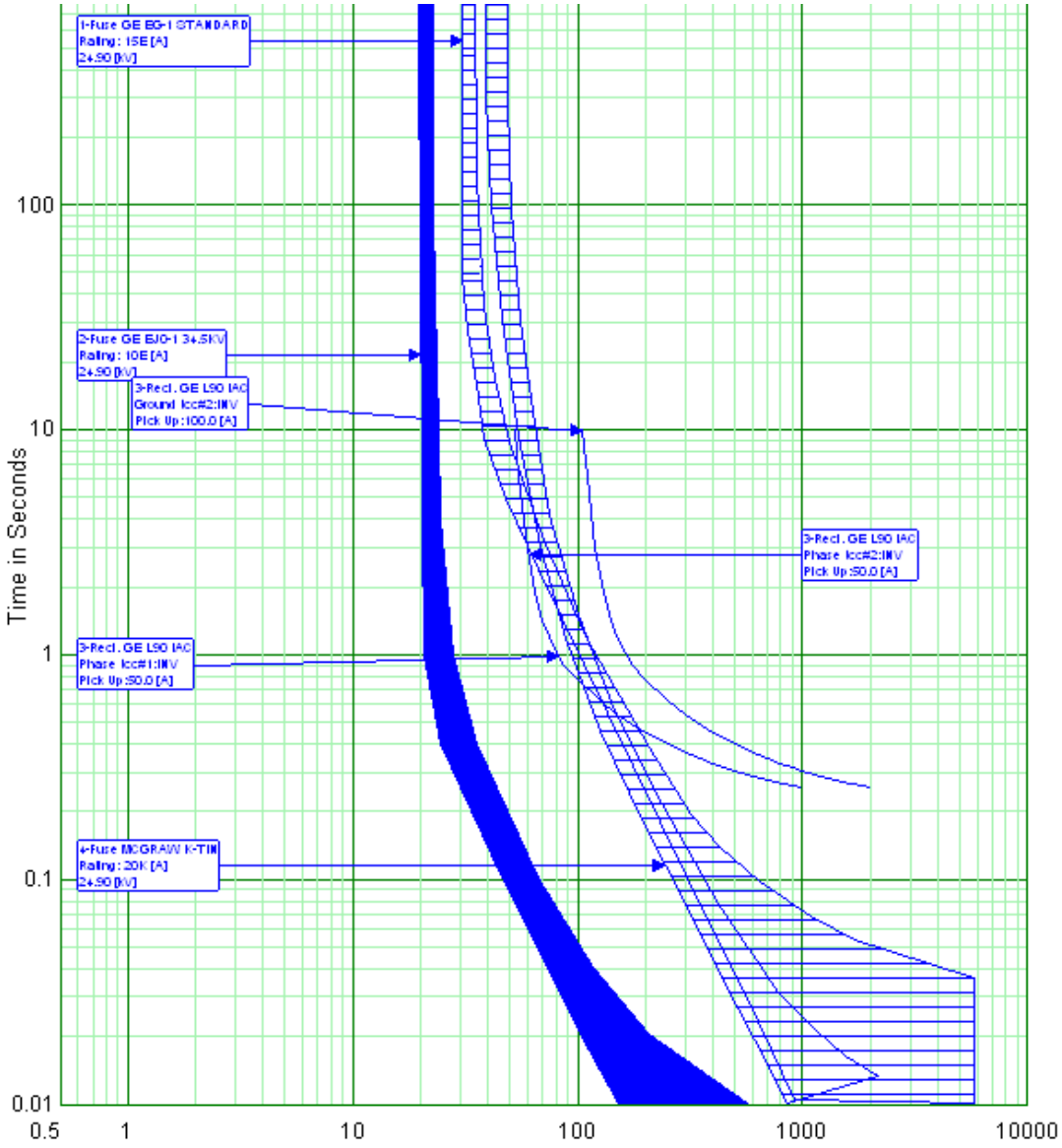

Figure 17: Fuse Recloser coordination for fault on node 848

Voltage Regulator Settings:

The system has two voltage regulators and this study involves the calculation of voltage regulator settings to avoid problems due to reverse power flow. If generation size exceeds substation loading, modifying the regulator settings can help disable the line drop compensation thus giving a crude estimate of DG current contribution.

Equation represents regulator output voltage :

$$V_{out\,(pu)} = \left(\frac{I * (R\cos 2 + X \sin 2)}{CT} + V_{float}\right) * \frac{VT\sqrt{3}}{V_{L-L}}$$

where:

V_{out} = Regulator output voltage (per unit)

I = Load current (amperes)

R = R setting of regulator (volts)

X = X setting of regulator (volts)

V_{float} = Float voltage setting of regulator (volts)

CT = CT high side amperes

VT = VT ratio of regulator

2 = Power factor angle

$V_{l\text{-}l}$ = Nominal line to line voltage (volts)

The values are predetermined for the IEEE 34 bus and if there is any change in regulator voltage it can be verified from capacitor bank current with X settings. Based on this equation the tap settings are derived and the limits don't exceed over 16 for the addition of DG's at the five nodes for our configuration. Since the tap setting regulation is not fixed when the DG's are added, initial simulation results shows DG addition at 890 as an error which means to change the tap settings.

4.6 Interconnection Overcurrent (OC) Protection Scheme:

As we discussed earlier about fuse-recloser scheme is not sufficient enough when DG's are added and hence this thesis suggests the addition of interconnection protection[25], [29] at the point of coupling (PCC) between the DG and feeder network. The existing fuse recloser scheme is modeled as shown below in figure 18adapted from [14]

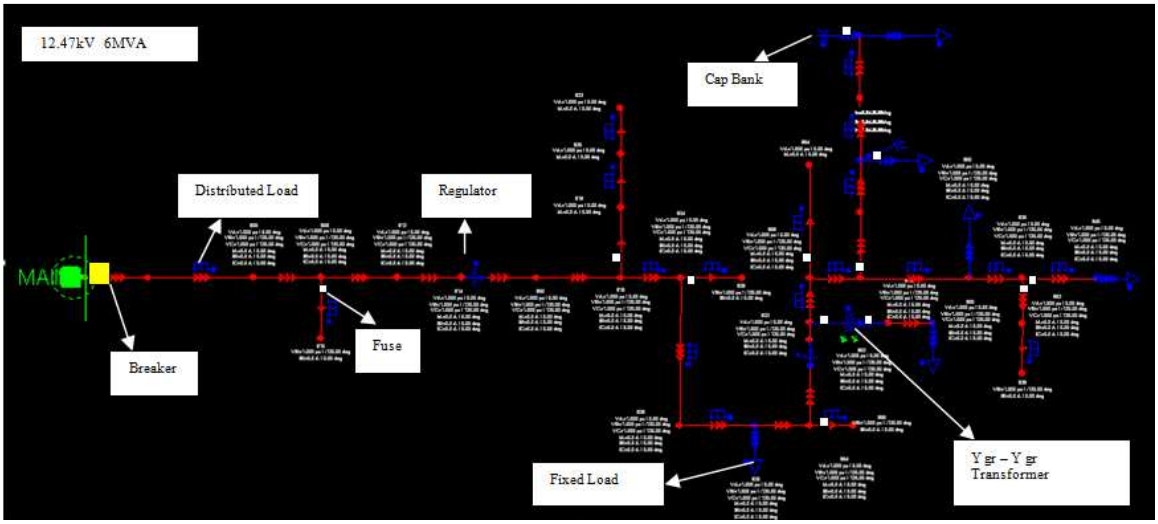

Figure 18: Complete Scaled down 12.47kV 6MVA 34 bus model in CYMDist

The results of this scheme and its affects were discussed in some of the chapters above and some of the coordination results are also shown in this chapter. On the addition of DG's the scheme adopted for protection has been changed due to the issues discussed and this work suggests the use of breakers at the point of interconnection with phase and ground overcurrent protection along with the implementation of directional overcurrent protection at node 800 since there is a possibility of reverse current flow and hence its detection is necessary. Also since there is no interconnecting transformer for the

generator with the bus 800, it is suggested to go with directional overcurrent relay. In order to simplify this protection, this chapter is divided into further parts only showing the interconnection protection. Figure 19 below shows the overall scheme in a simplified version.

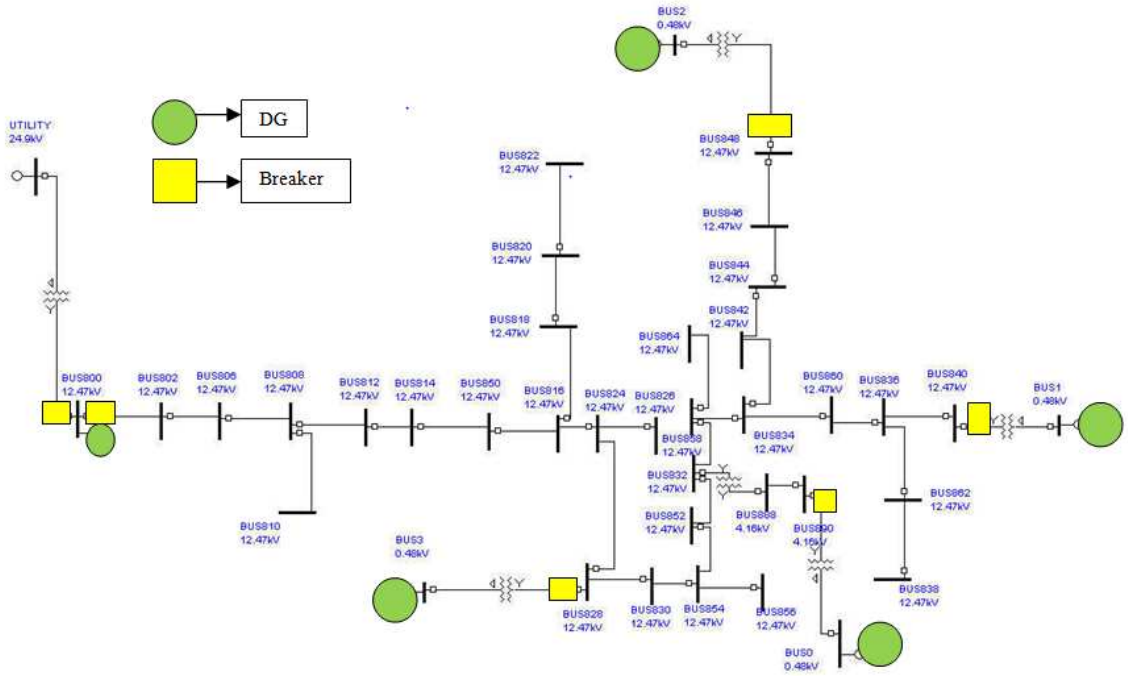

Figure 19: Interconnection Protection Scheme for DG connected to the scaled 12.47kV system

***Case 1: Interconnection Protection for Diesel Generator at Bus 800*:**

Based on IEEE 1547[25] standard and EPRI report [1], the figure below recommends the interconnection protection for the 1.5MVA diesel generator connected to bus 800. In our model since the generator is rated at 12.47kV , connected to bus 800 directly , protection in this case is crucial as the only upstream protection involves a delta-wye 24.9kV/12.47kV transformer which is from the main utility which is modeled as an infinite source. From the interconnection point of view, coordination involves coordinating the breaker on the DG side to upstream main breaker. Figure20 is adapted

from the EPRI 2001 document for integrating the DG's to radial distribution feeder and in this thesis a part of this is implemented as shown for the interconnection protection to the upstream device coordination.

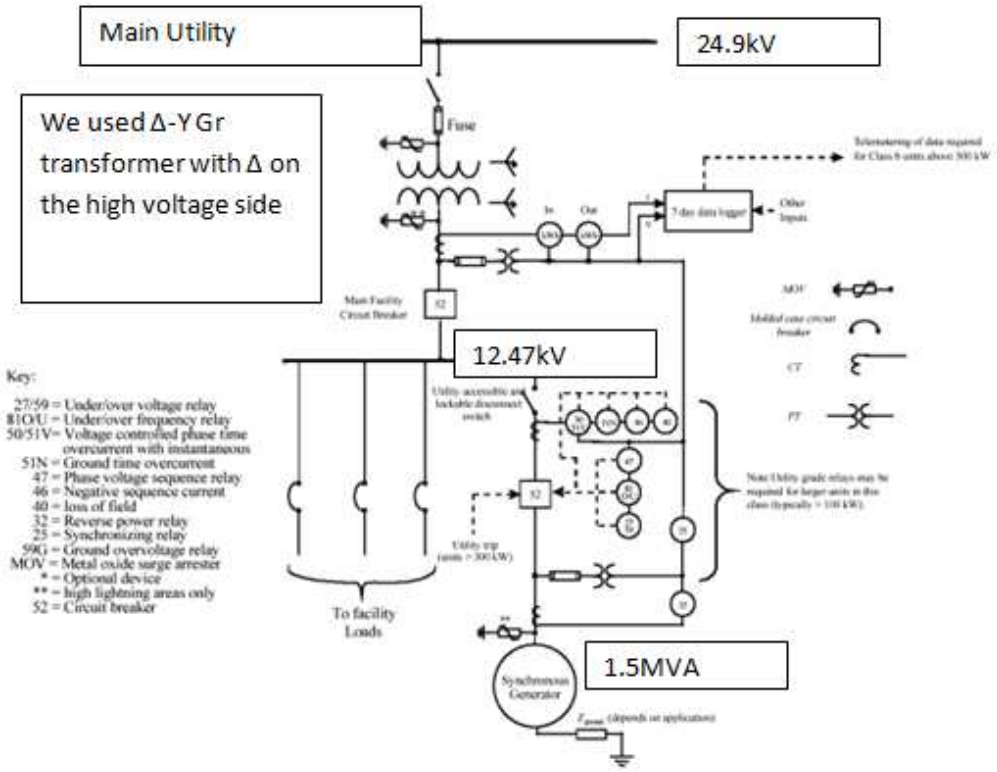

Figure 20: Interconnection Protection for Diesel Generator at Bus 800 (Adopted from [1])

The modeling of the generator in cyme involves classical model with the sub-transient, transient, positive , zero and steady state impedances inputted from the data shown in table . The equivalent impedance is obtained in per unit from cyme and modeled in Aspen for relay coordination. Overcurrent protection involves coordination of classical fault on the bus 800 and by using the design approach from the above theories, the pickup and time dial is set up to achieve coordination of the 51P and 50/51G curves

with the main breaker. Figure 21 below shows a snapshot of four main protective elements in this zone.

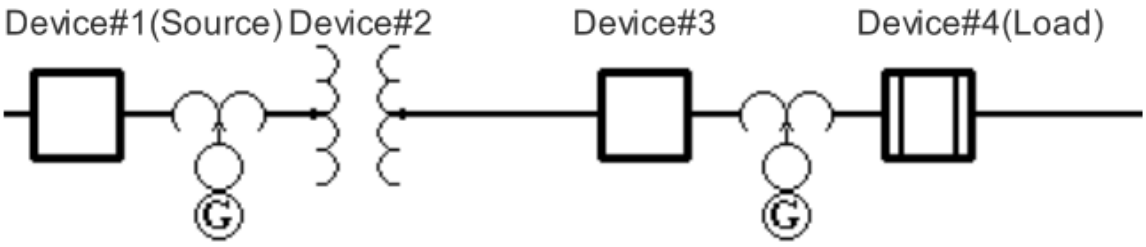

Figure 21: Section of Interconnection Protection from Bus 800 to four devices downstream modeled in S&C Coordinate Tool

The aim is for any fault type and based on the standards allowing the breaker to trip in a specified time, the settings are modeled for the phase element to trip and then for a higher magnitude of fault current, the instantaneous ground element trips as that could contribute higher ground current. Fault on the transformer is already shown for the transformer damage curve to above all curves. Inverse time Overcurrent characteristics are used belonging to the class of Very inverse and inverse curves which are mimicked to follow the fuse minimum melt and total clearing curves.

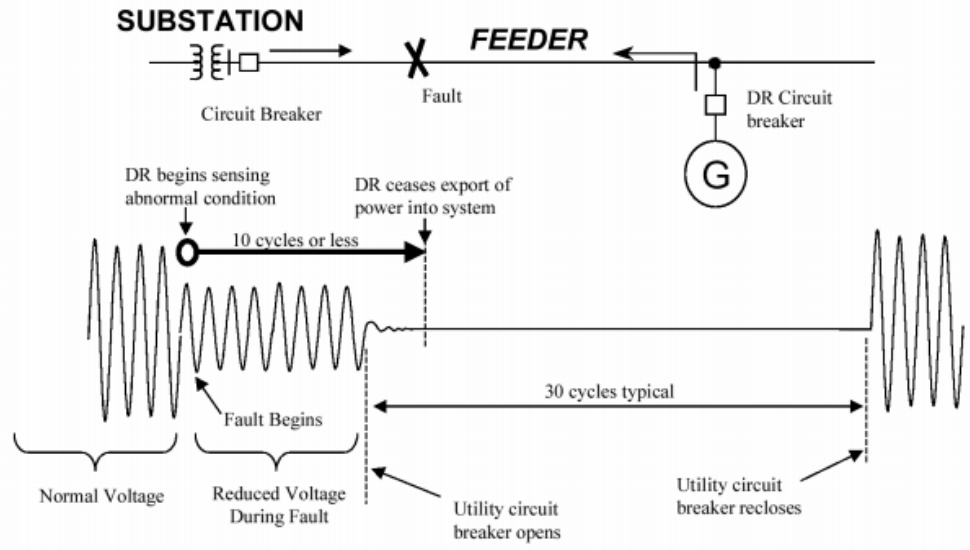

Figure 22 : Illustration of IEEE 1547 Concept for Interrupting device operation (Adopted from [1],[25])

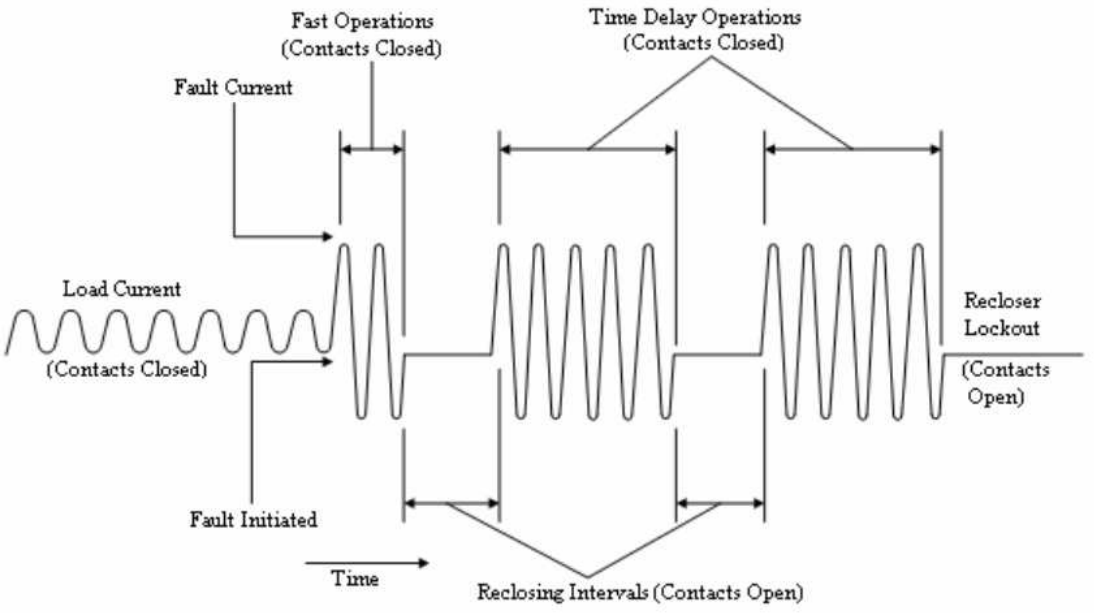

Figure 23: Operation of Recloser during Faults (Adopted from [21])

The above figures 22 and 23represent voltage and current operations for fault conditions when the breaker is operating and when the recloser is operating.

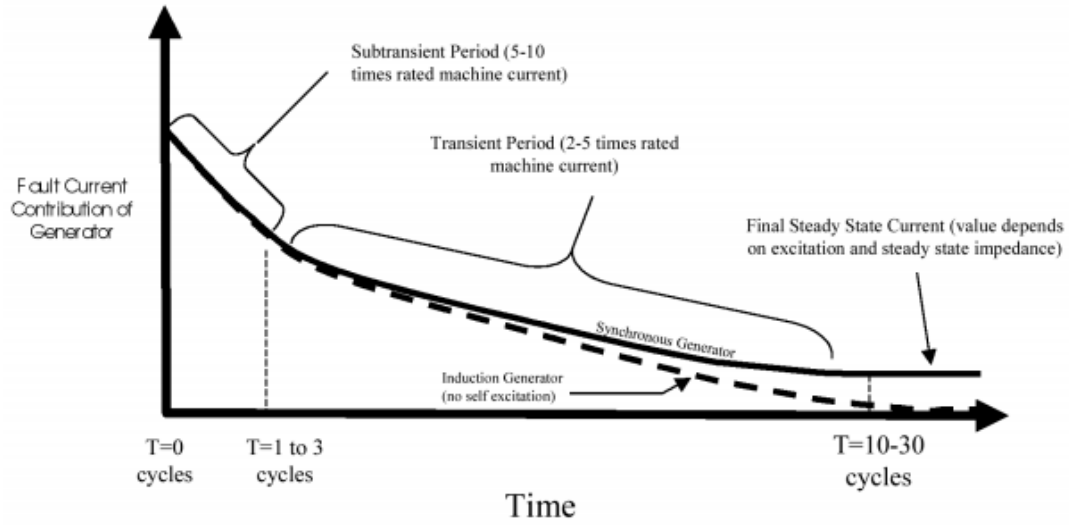

Figure 24: Fault contribution of Generator mainly during Sub-transient time (Adopted from [1])

Figure 24 shows the importance of considering sub-transient impedances in the Aspen model as they operate within 3 cycles of operation for rotating machines. Although transient and steady state impedances were inputted, their fault contribution was very less compared to that of sub-transient impedances. Figure 28 below shows the coordination results with a coordinating time interval maintained for 0.3s for safe and reliable operation. Other downstream coordination was also checked for the fault types and properly coordinated. The tool used to check the coordination is S&C Coordinate for which the curves were obtained. The fault contribution from the DG along with the generator parameters are shown in Chapter VII. In this case for a temporary line to ground fault the device 3 phase element trips and for a three phase fault, the instantaneous element trips thus protecting it from permanent faults. This is done from the utility point of protection and the DG side will have to trip once the utility breaker trips from IEEE 1547 standard. There are many challenges when it enters into an islanded mode and some of them are theoretically explained in chapter VI. The figure below

shows the coordination curves with its coordination from Phase and ground unit to transformer damage curve to fuse –recloser scheme along with the settings in Chapter VII.

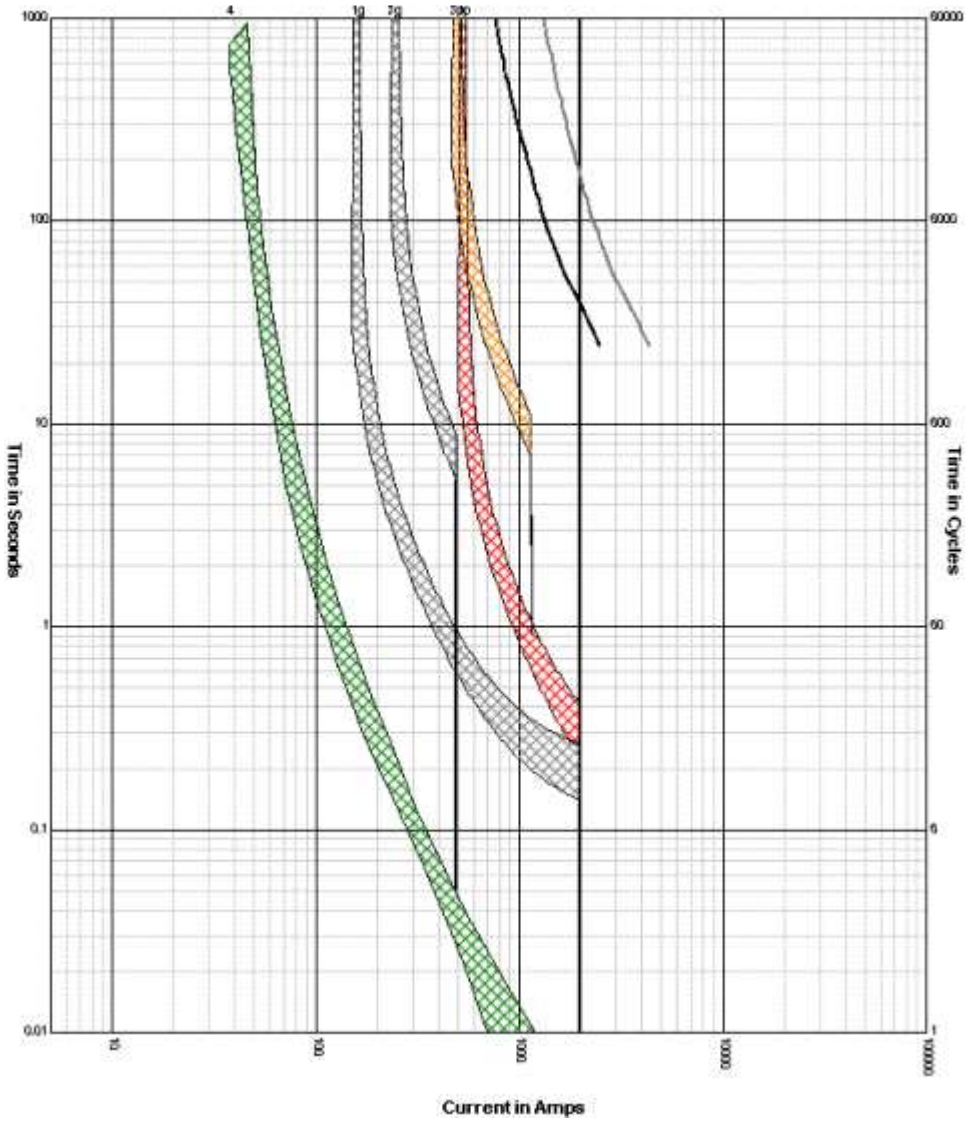

Figure 25: Inverse time non directional coordination for the four devices connected to Bus 800 with DG

Figure 26below is a post fault waveform plotted with no of cycles to phase voltages and currents when the generator breaker trips and it comes back online between 3 to 5 cycles adopted after performing event analysis from SEL website. There is yet more research to be done for generator protection and controls itself.

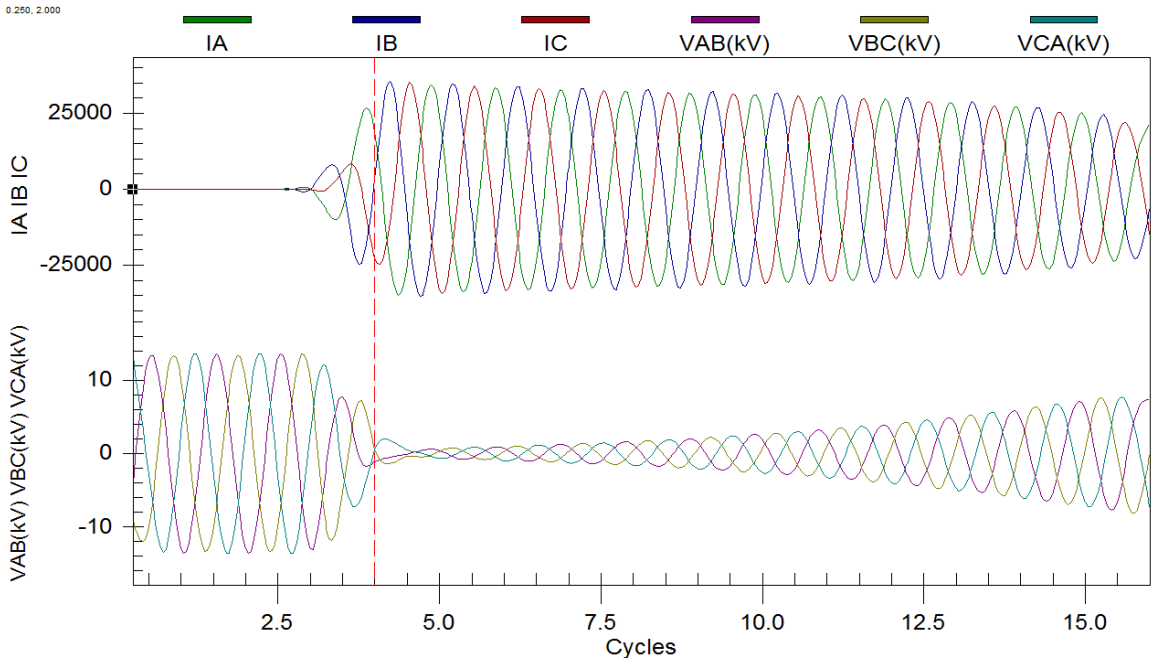

Figure 26: Post fault waveform for a Generator trip

Case 2: Interconnection Protection for Inverter based PV at Bus 890 and energy storage modeled as Inverter based PV:

This case discusses the impact of the Inverter based PV attached to node 890 of the distribution network. Also note that, since there is no specific battery model in Cyme, it has been modeled as an inverter based PV source as from interconnection point of view we need to know the fault contribution to perform coordination studies. The default PV characteristics were chosen from Cyme tabulated in Appendix C.

.

The default voltage source converter with full converter control, insolation model and long term dynamic curve were accordingly chosen to match the parameters for 250kW PV. For the short circuit analysis the fault contribution was 120% which is based on the rated current of the generator. One of the major modeling features is that the inverter current is limited to twice the maximum load current so that fault contribution is less even during islanded mode[30]. Once again, the impedances obtained from Cyme are in sequence and per unit values which are then modeled in Aspen in the per unit system for coordination studies. In the base case model, the node in 890 has a voltage below 0.95pu.As seen from the load flow analysis on addition of DG at 890, there is anincrease of voltages. The differences in voltages and currents before and after the addition of DG's are tabulated and shown in Chapter VII and these results are significant for coordination studies especially for the sensitivity of the relays or reclosers and more importantly to study fault analysis during islanded mode. While modeling in Aspen, it is crucial to also limit the fault current. This is done by checking the fault simulation options in Aspen to enforce current limiting for the generator chosen. For all modeling

conversions the per unit impedances are inputted in Aspen as sub-transient impedances and other values are chosen as default values if data is not available or cannot be calculated.

The protection scheme adopted in this case is similar to synchronous generator except for the fusing practice. Fuse saving scheme was adopted in this case as it is connected to wye – wye 12.47kV/4.16kV transformer which were modeled with fuses on both high side and low side. Since the capacity of this DG is 250kW, IEEE 1547 standard recommend proper fuse and recloser scheme. From the EPRI and IEEE standards, figure 27below shows protection scheme for three phase inverter. In our scheme, fuse to fuse coordination is checked for the wye-wye grounded transformer and the interconnect transformer is chosen as wye-delta 4.16kV/0.48kV transformer where the operating voltage of the converter is 0.48kV and transformer base kVA is 500kVA. Figure 30 adopted from the EPRI document has been used for interconnection protection scheme where the inverter protection needs anti-islanding detection techniques along with various other relaying functions as described in IEEE1547 standard. The main idea here is to coordinated the interconnect breaker with the upstream protection for various faulted conditions.

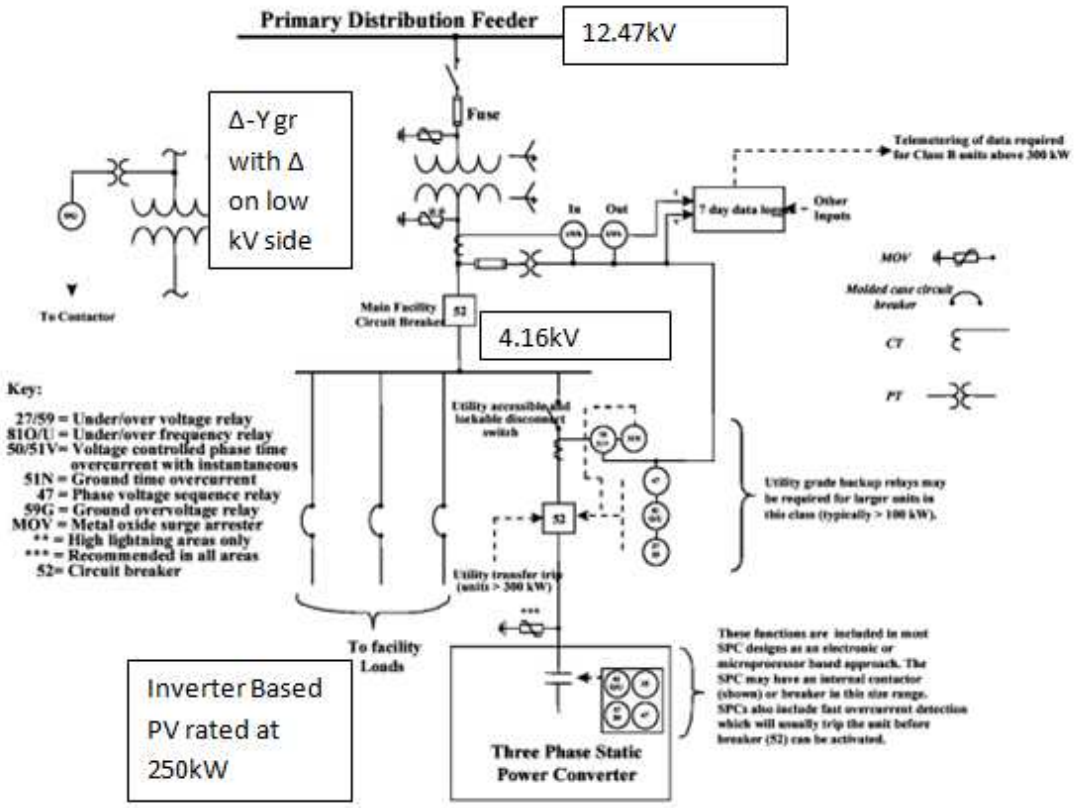

Figure 27: Inverter based Photovoltaic Interconnection Protection Schematic (Adopted from [1])

In this case fuse recloser scheme is adopted to show that since the fault contribution is lesser compared to other big sized generators in this system. Recloser phase and ground unit is chosen to be coordinated with fuses upstream. Inverter DC side has fuse protection with 15 pole 100A fuses and since the focus is for interconnection protection, the Inverter AC disconnect fuse switch is installed at the 480V terminal of the inverter rated at 400A which will provide overcurrent protection for the inverter along with Recloser phase and ground unit.

Figure 28 and 29below shows the fuse to fuse coordination for fault on node 890.

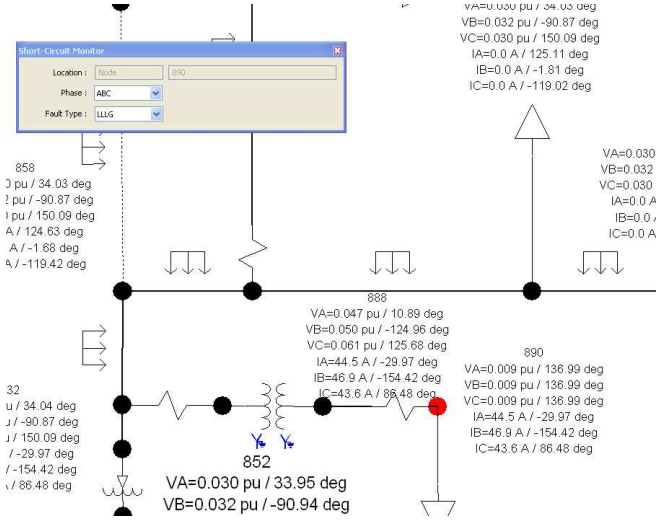

Figure 28: Classical fault on node 890 where Photovoltaic is attached

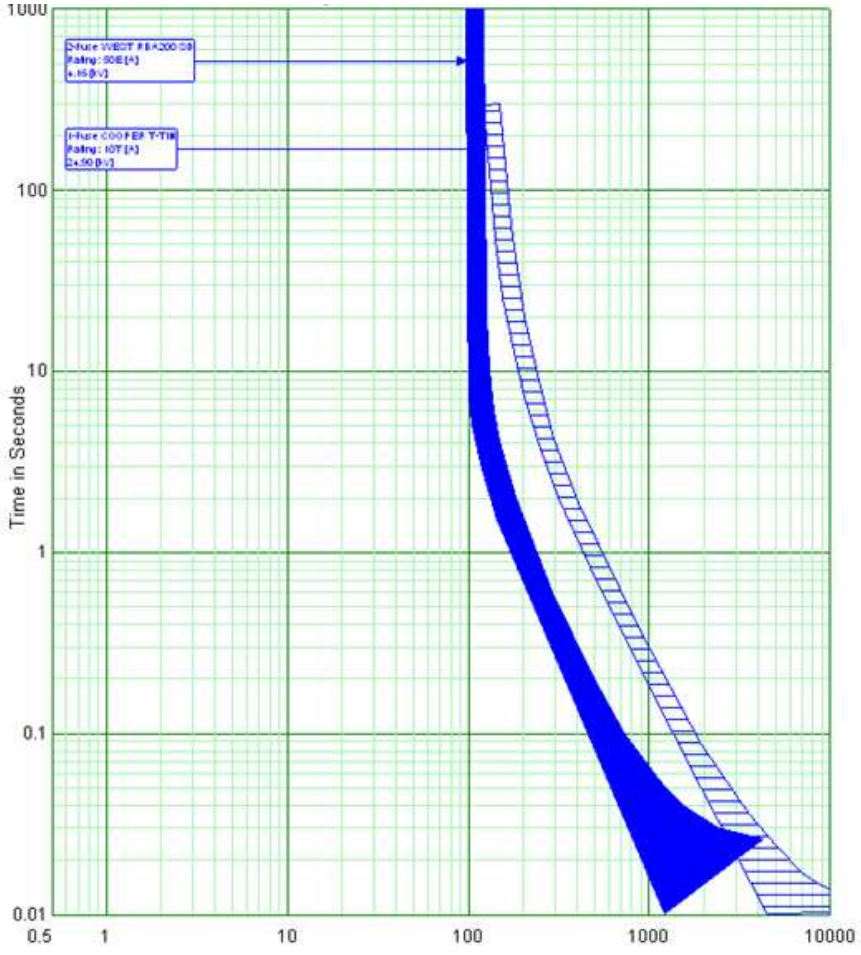

Figure 29: Fuse to Fuse coordination for fault on Bus 890

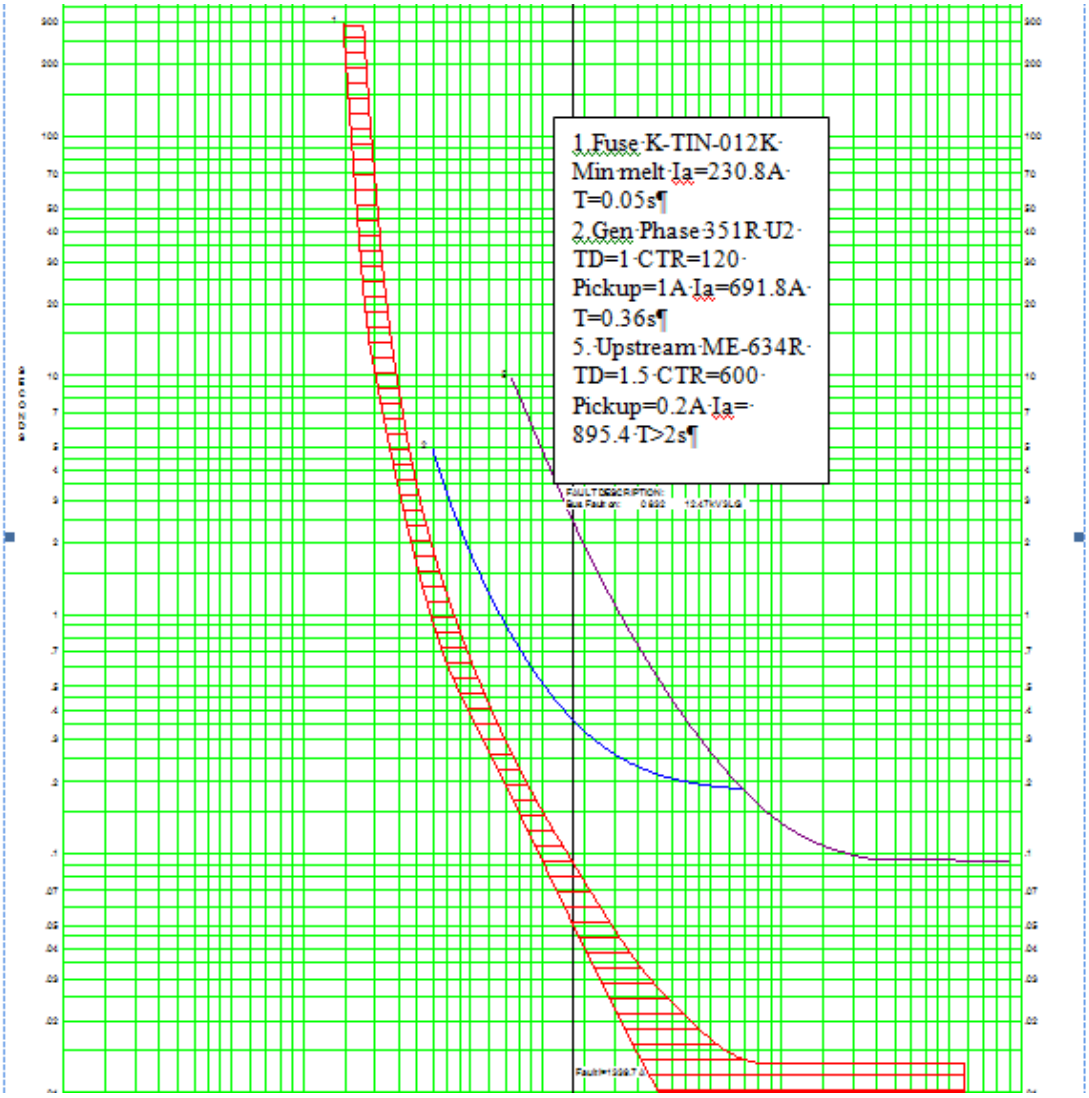

Figure 30: Coordination curve and settings for bus fault on 832 3L-G

3 phase fault at Bus 832, fuse operates first and then the phase and ground unit operateon performing post fault analysis for a distribution feeder fault on bus 832 with the curves and fuse and recloser settings as show in figure 30.

Figure 31 below shows for Fault at 888, interconnection point, for a L-G fault we expect the gen unit to operate and then fuse to operate. But the coordination sensitivity raises issues here. There seems to be many coordination issues here

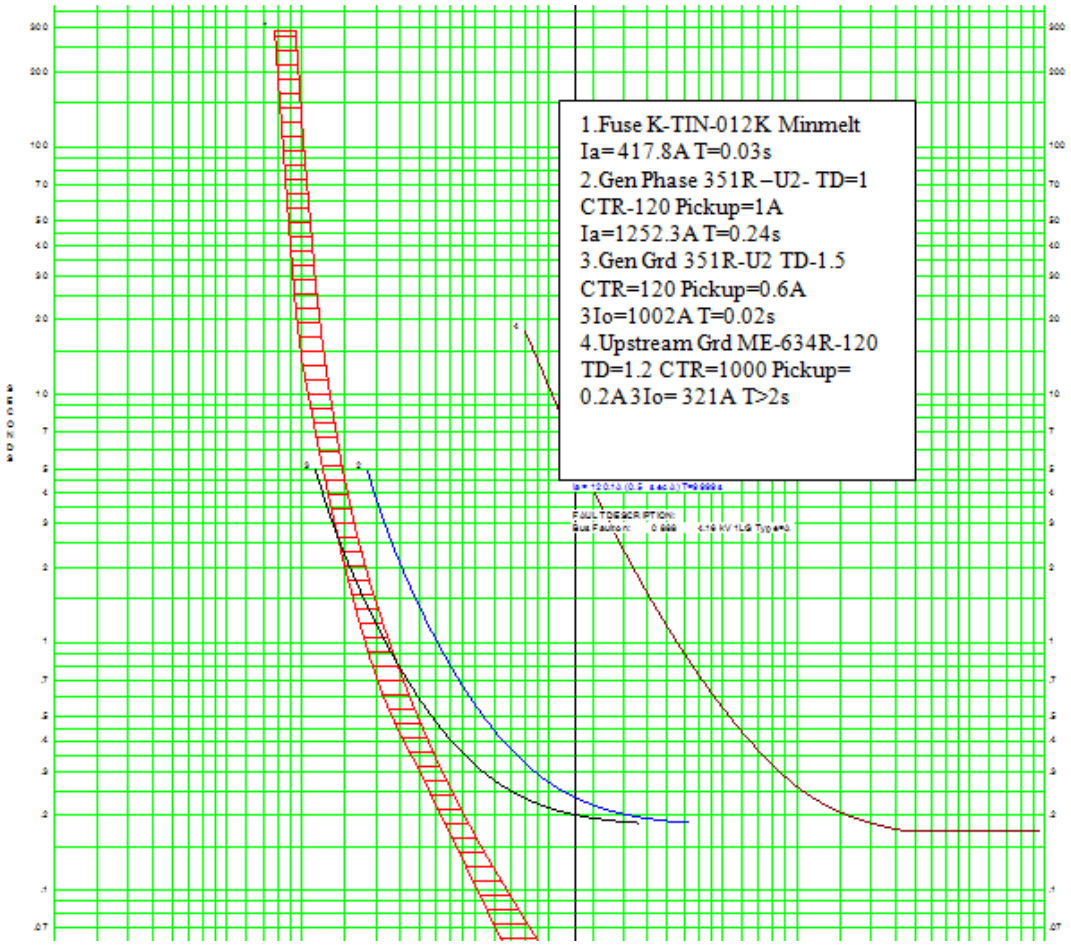

Figure 31: Improper coordination due to DG addition decreasing the sensitivity of already existing protection scheme

The similar modeling procedure was adopted for the DG at node 828 which is for the energy storage rated at 500kW, 1MWhr capacity. The fault current contribution is tabulated and shown in Appendix A.

Case 3: Interconnection Protection for the Wind Turbine at Node 840 and Node 848:

This case involves the interconnection protection study of the two Wind turbines rated at 750kW connected to node 840 and 848.The model used in Cyme is Variable speed full converter Type 4 Permanent magnet synchronous generator (PMSG). The turbine is interconnected to the distribution feeder through a delta-wye grounded 0.48kV/12.47kV transformer which is rated at 500kVA. The transformer parameters and generator parameters are listed in the Appendix C. The interconnection protection scheme is similar to the synchronous generator scheme except that since the fault contribution is not much higher compared to the DG at 800, it is suggested to use fuse recloser scheme with fuse saving approach as mentioned in the case when the DG is not interconnected.

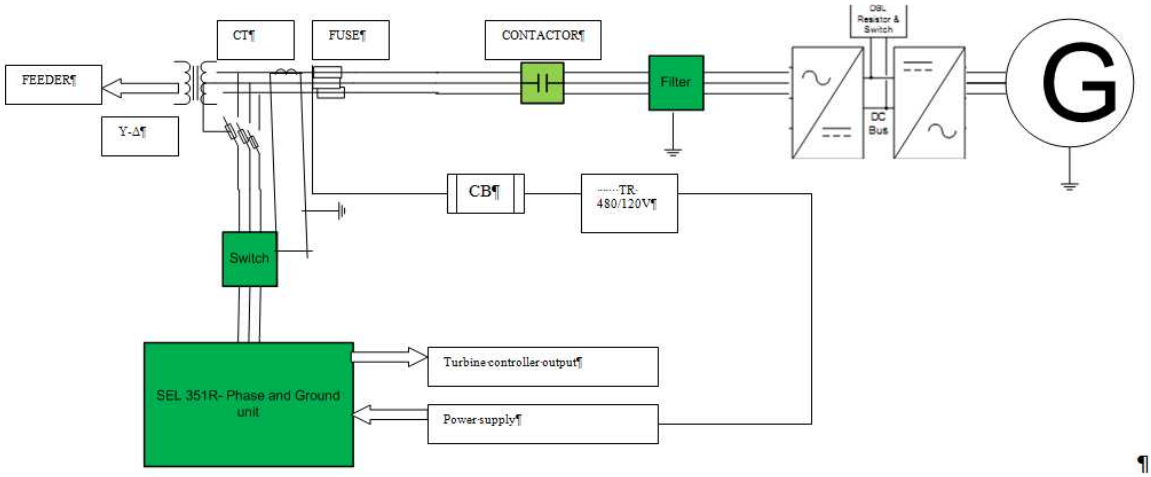

Figure 32: Schematic of Interconnection Protection for Wind Turbine at node 848 and 840

The above figure 32 shows a block diagram of the recloser 351-R which is used for reclosing phase and ground unit. SEL 351-R is common reclosing package used by SEL relay manufacturing, which is modeled in Aspen One liner. Figure 33below shows

the interconnection of Wind turbine at node 840 and change in fault current due the addition of DG

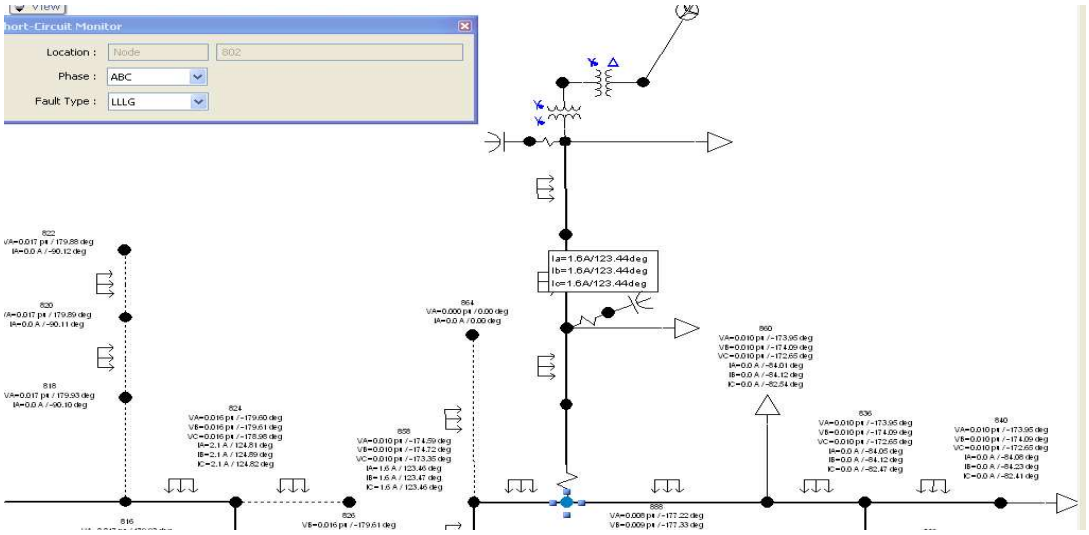

Figure 33: Fault on Bus 840 showing misoperation of Fuse due to addition of DG

One of the main issues on addition of DG at 848 causes false trip of the fuse for a fault on the main feeder as shown in figure 34 below with operating margin between the fuse and recloser less than 0.3s. For addition of DG at 840, coordination shows the fuse minimum melt time less than the instantaneous setting for the recloser for temporary classical fault on node 834 due to addition of DG at 840

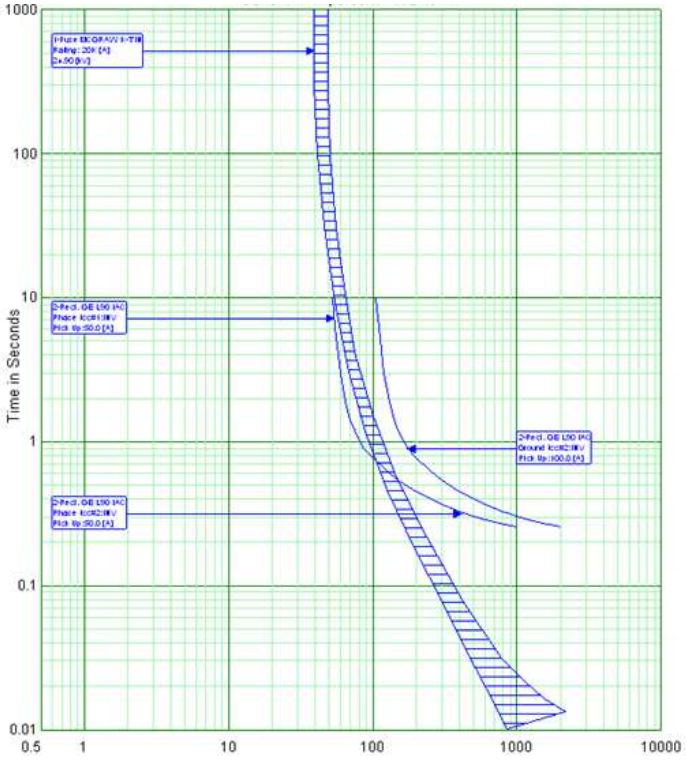

Figure 34: Coordination curve showing Min melt time is less than Instantaneous recloser phase unit for DG at 840

Figure 35 is the coordination curve obtained for the addition of DG at 848 with the recloser phase unit operating for a temporary fault with a pickup of 30A. The ground unit of the recloser and fuse curve could misoperate for ground faults and hence the recloser ground unit is set to fast operation before lockout operation.

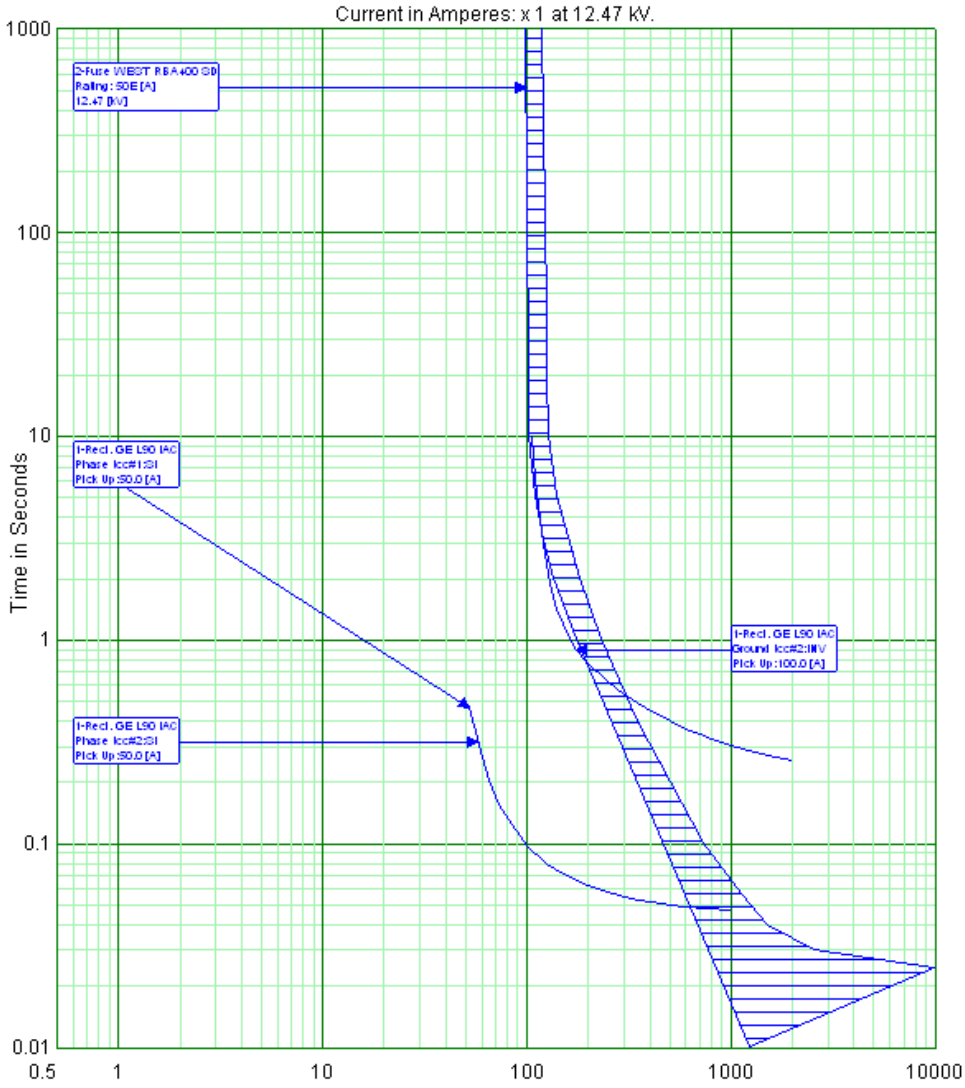

Figure 35: Coordination curve showing coordination for a close in fault at 848 with upstream devices

Short Circuit currents from Type 4 Wind turbine Generator:

Some analysis on Wind turbine modeling in grid tie mode is performed using MATLAB- Simulink [31] with the application of PWM technique with PI controller. Figure 36below shows the block diagram of Wind energy conversion system with control technique used from [32]

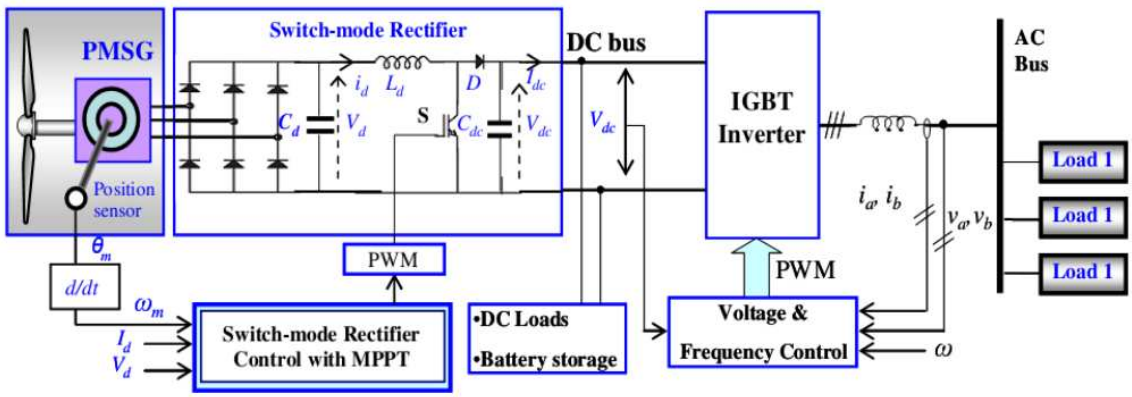

Figure 36: Block diagram of Wind Turbine PMSG connected to the Grid with Control Implementation for Short Circuit Fault study (Adopted from [32])

Control strategies involve control of pitch angle of wind turbine blades and control of electrical torque of the PMSG. Boost converter configuration is used on the generator side and PWM based inverter is used on the grid side. Since the PMSG block used is a built in block from Simulink The PMSG block is modeled as a generator in the d-q reference frame fixed to the rotor. Control strategy involves:

- The output from PMSG is rectified using the universal bridge rectifier (V_{rec})
- The boost converter is then used in controlling the load current thereby controlling generator torque and speed for different wind speeds
- From the DC-DC converter, the PWM based inverter is used for DC-AC conversion
- The Pulse width modulation (PWM) generates pulses by comparing triangular carrier waveform to a reference signal from sine wave generator, to control the AC output voltage

- The Phase locked loop (PLL) is used to synchronize a set of variable frequency, three phase sinusoidal signals
- The dq0-abc transformation technique is used to simplify the PI control technique to convert the reference signals in dq frame to abc frame of reference which can be used as modulating signal of the PWM block. This is a mathematical transformation of direct axis , quadrature and zero sequence components to phase quantities.
- The proportional Integral block is used to converge any error voltage to the minimum which is then fed as duty cycle for the boost converter gate signal.

The Wind turbine and PMSG block parameters are tabulated in the appendix along with the Simulink control loop diagrams. The idea of performing this study is to obtain the results when there is a faulted condition. Since the model does not reflect the exact parameters as the model in CYME or for this study, it is been studied to know the effects of short circuit currents from a Type 4 Wind turbine Generator [33]. A three phase fault programmable block is used from Sim Power systems [31] to obtain these conditions. The results for the Wind energy conversion is shown below with emphasis on the voltage and current waveforms for a three line to ground fault and single line to ground fault. Figure shows waveforms for fault conditions run for a simulation run time of 0.1s and duty cycle is controlled to give constant dc link voltage to the grid. The model developed is not the same as developed for the IEEE 34 bus feeder and is mainly simulated and studied for comparing the short circuit faults for further research during island mode conditions which could lead to possible out of phase reclosing issues [35] .

Simulation results for Three phase to ground fault :

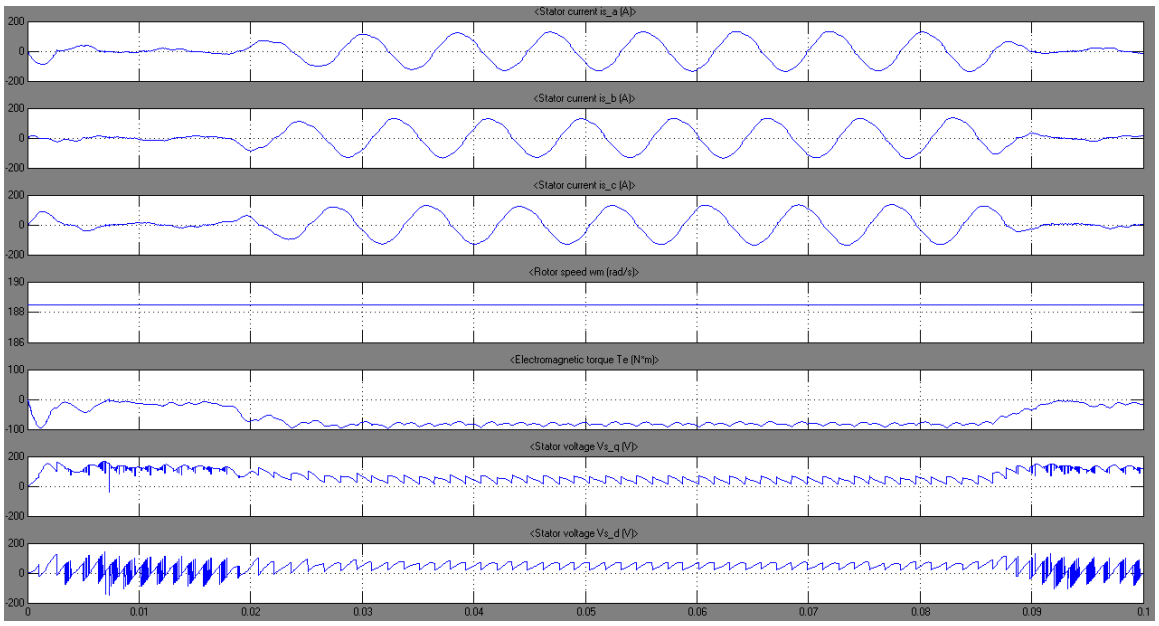

Figure 37: Stator current, Rotor current, Electromagnetic torque, Stator Voltage Waveforms

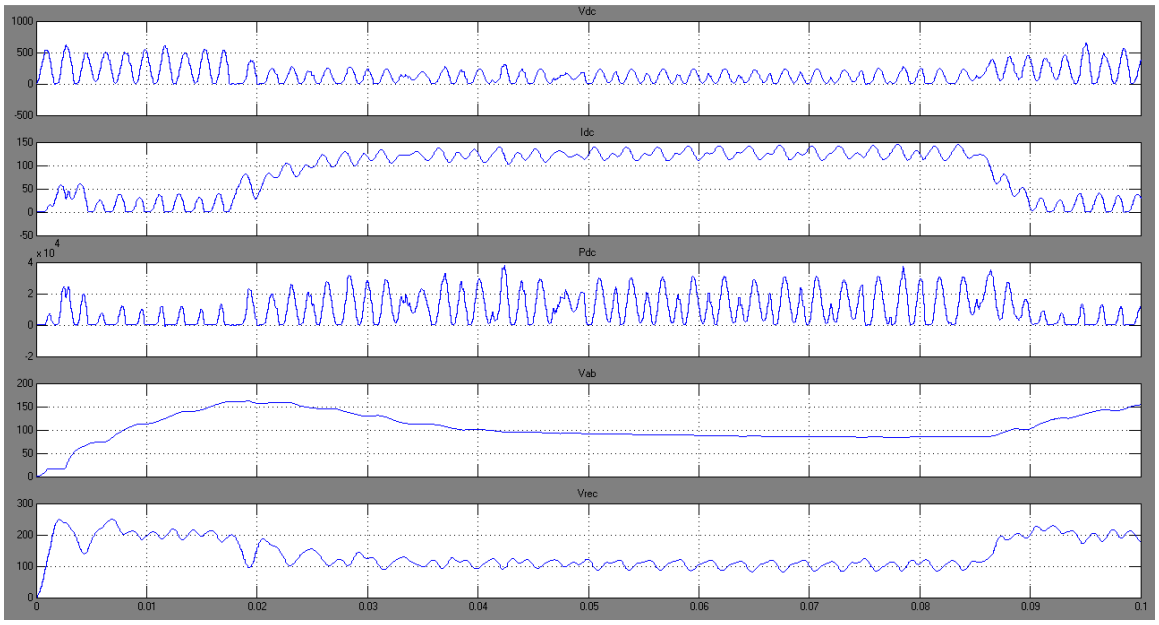

Figure 38:Waveform with emphasis on Pdc obtained after fault on grid side

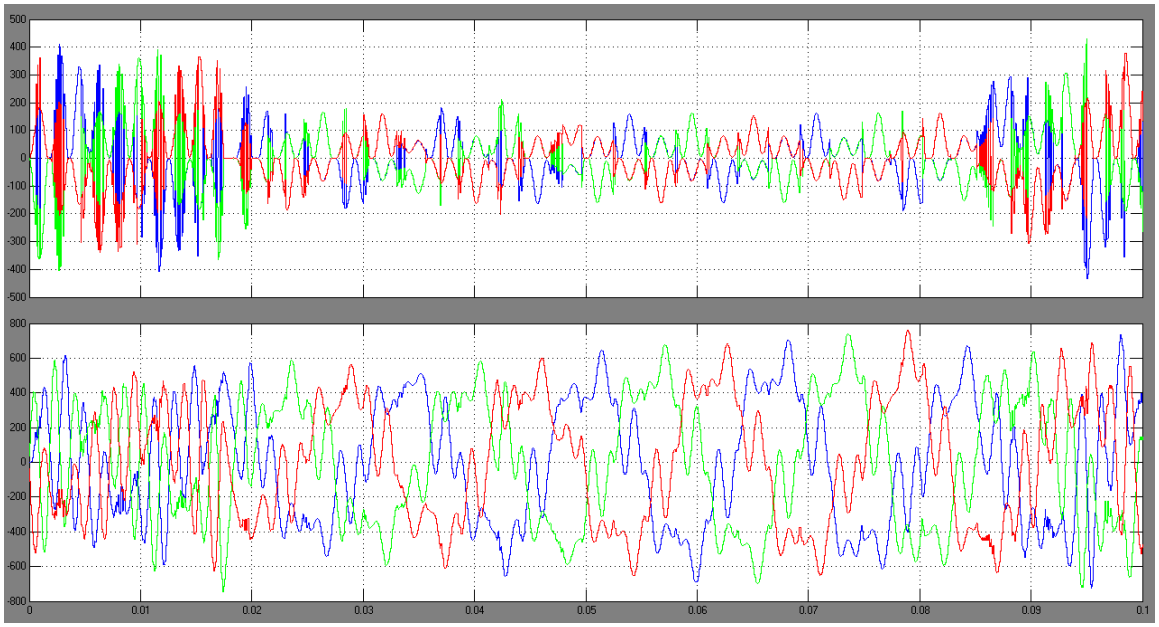

Figure 39:Vabc and Iabc waveforms after three phase fault on Grid side

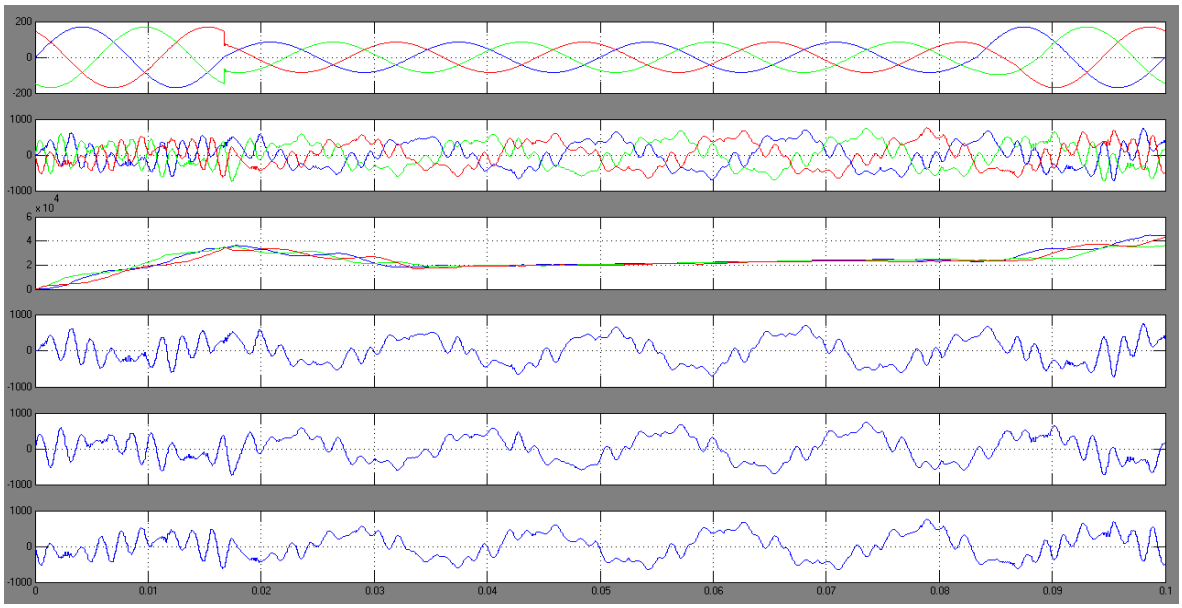

Figure 40:Vabc, Iabc, P, Ia, Ib, Ic waveforms for 3L-G fault

Simulation results for Single line to ground fault :

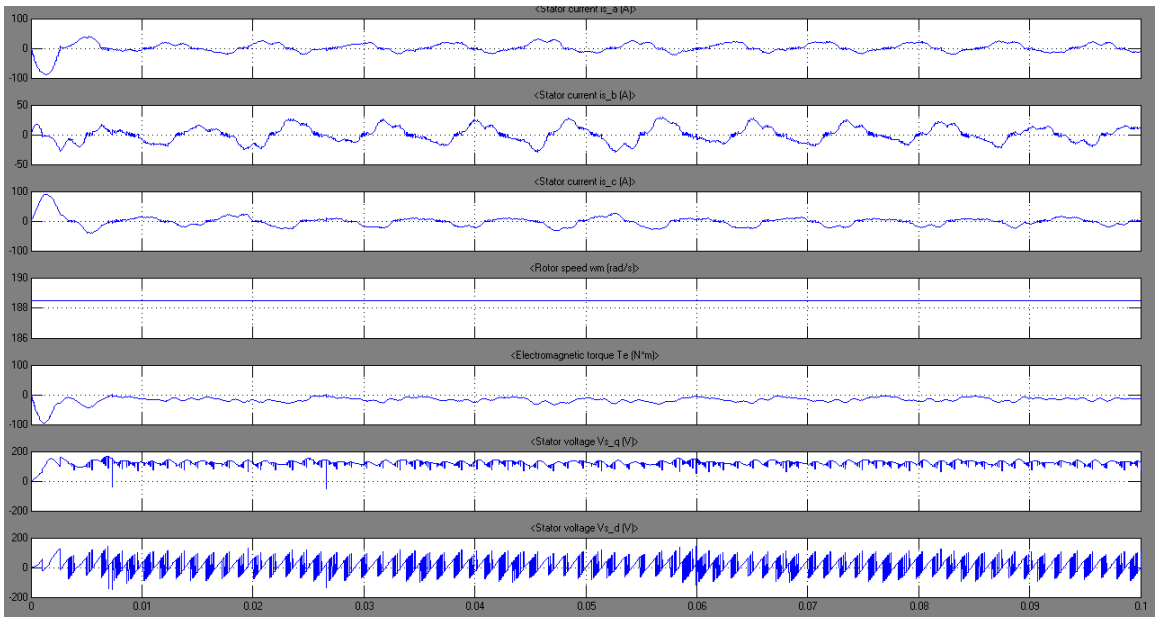

Figure 41: Stator current and Rotor current waveforms for a single line to ground fault

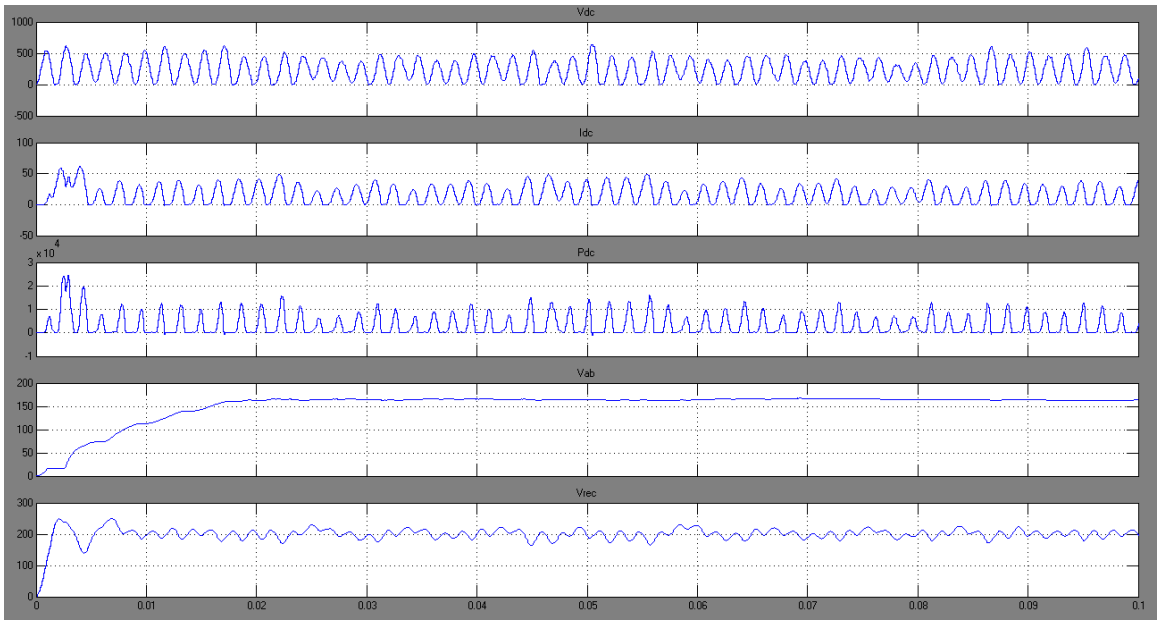

Figure 42: Waveform with emphasis on Pdc after 1L-G fault on grid side

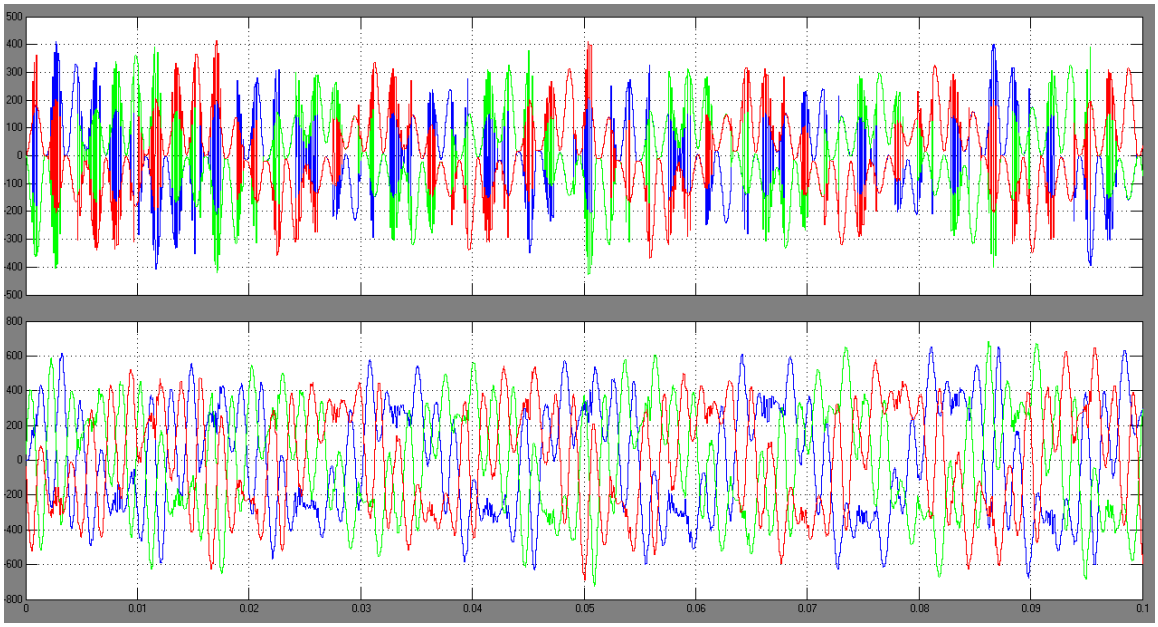

Figure 43: Vabc and Iabc waveforms after single line to ground fault on Grid side

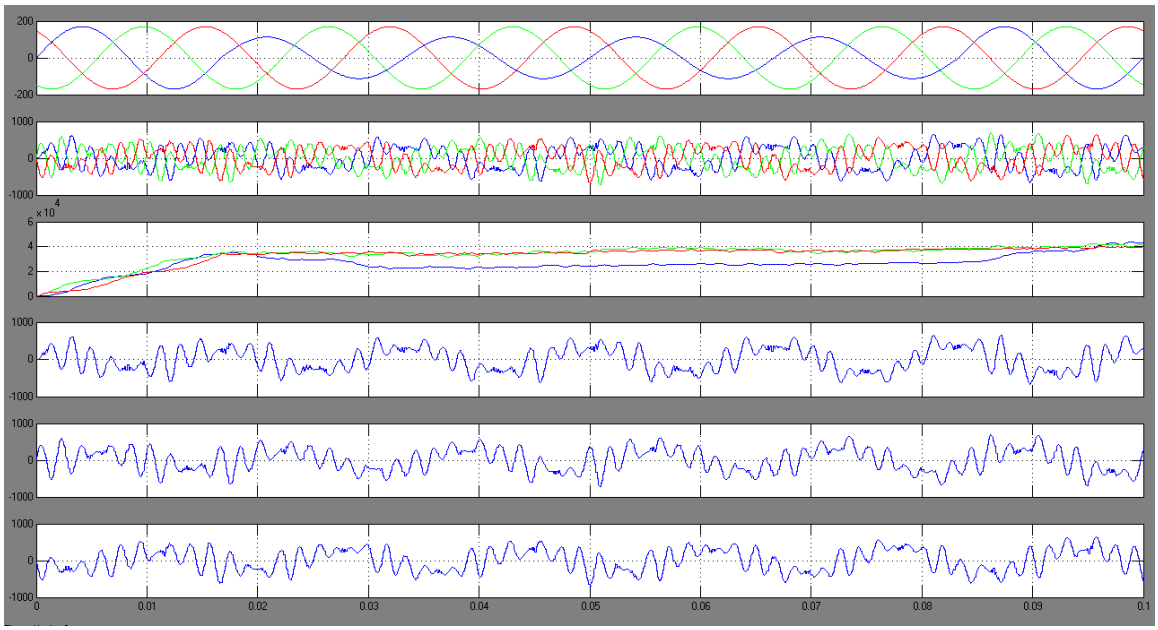

Figure 44:Vabc, Iabc, P, Ia, Ib, Ic waveforms for 1L-G fault

The objective behind this study is to see the differences and need of control strategy during faulted conditions. The short circuit current for the three phase fault is limited to the rated current. From the simulation results, when the fault is placed on the grid, the output current still stays within the current limit, but there is decrease in output power [34] and so the wind turbine must be controlled using the control strategy mentioned above.

***Implementation of Directional (67) OC Protection*:**

After analyzing the above protection schemes for various interconnections of DG's at various nodes, there seems to be coordination using Inverse time non-directional instantaneous and non-instantaneous settings for phase and ground units (50/51N) , but the addition of DG at node 800 could cause the problem of backfeed of current from other feeders on the high side if any would be connected which makes it difficult to know the direction of power flow in case there is a fault. Hence along with the 50/51N settings, the relay curve in Aspen was also checked with directional element settings. It is set for faults acting only in one direction which is from any other feeder connected to this bus on the high side. Figure 45below shows the setting from Aspen and the coordination curve with the downstream existing protection implemented before when the directional element is checked for the relay setting. In this case the fault contribution is limited to 30 cycles for the breaker operation. In this case it has approached the problem of nuisance tripping of other breakers, but in the long run for larger fault contributions, this operation is too slow and requires faster operating directional OC protection which can operate in 5 cycles [1]

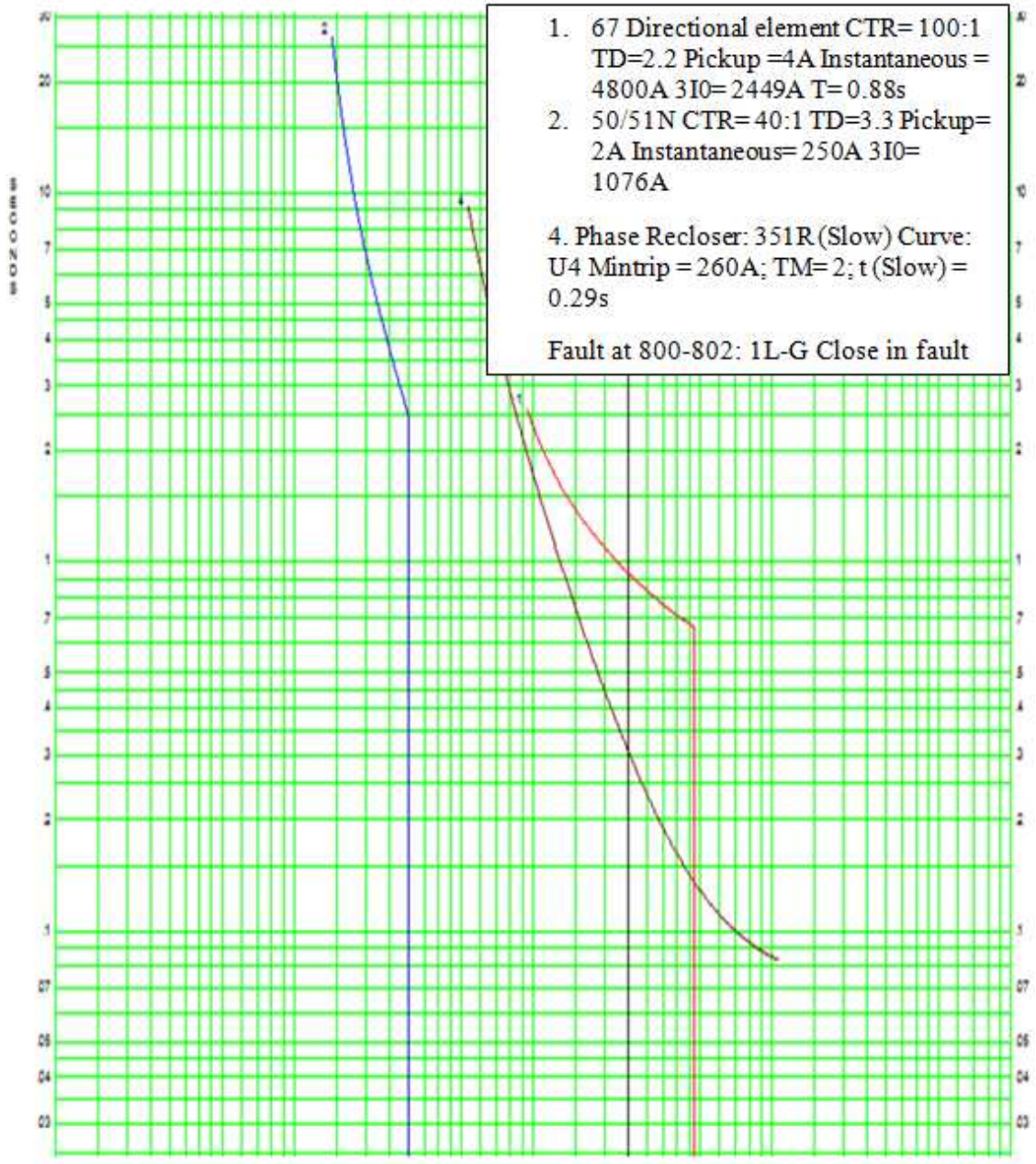

Figure 45: Directional Element 67 with settings to show detection of Backfeed current at node 800 for a parallel feeder connected to it

4.7Steady State Analysis of Faults in Waveform analysis using Wavewin:

Wavewin is a useful tool used here for post fault analysis. Once the model is built in Aspen, it can be converted to formats that can be viewable in Wavewin which has much functionality to show post fault analysis. In our case, the figures below represent the waveforms for faults at the interconnection points at the DG location to the distribution network. This can be used to analyze the time the relay operates by scrolling the data cursor for various instances of fault. It also gives an insight into the Harmonics

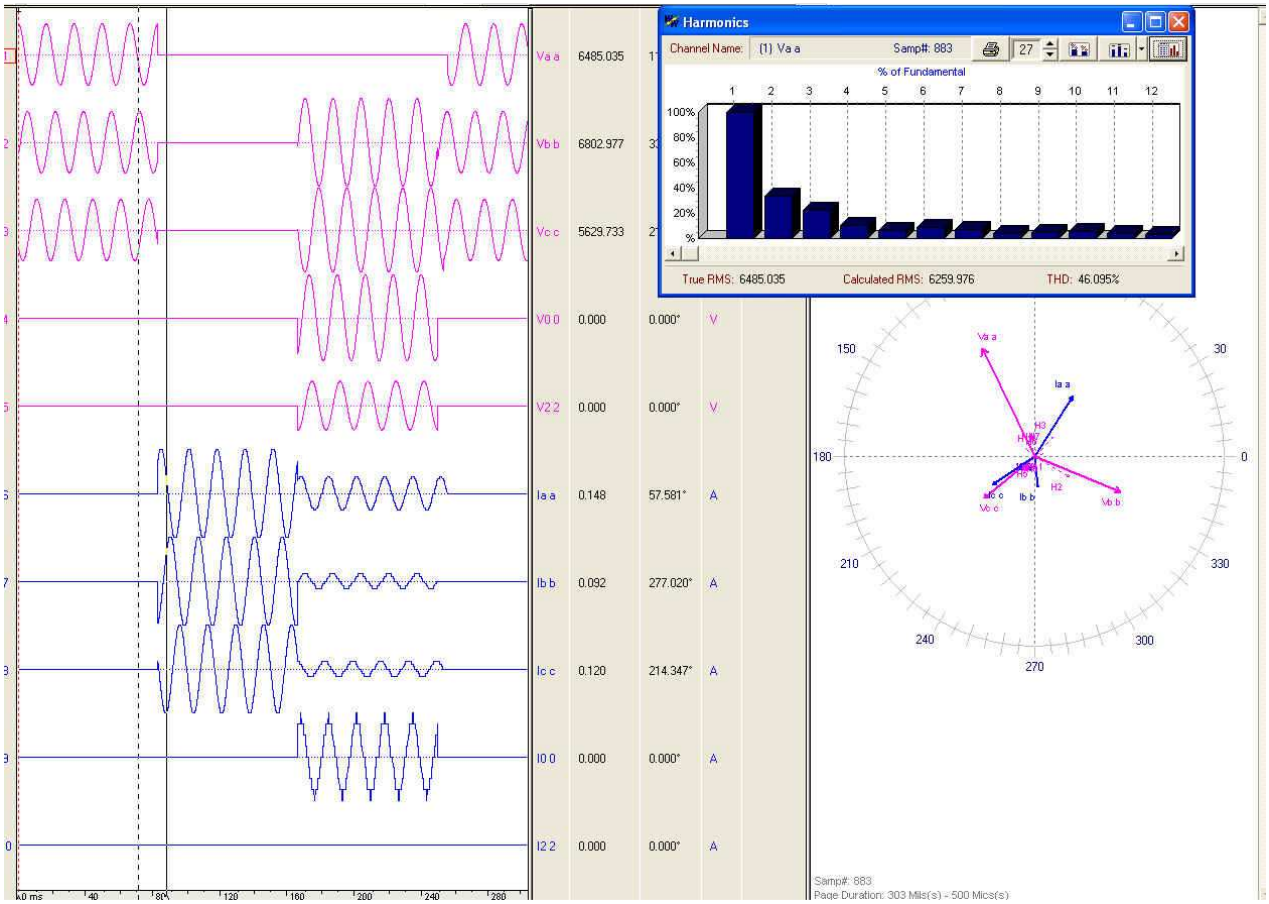

Figure 46:Waveform obtained for a close in fault on relay at node 840

Figure 46 is one of the waveforms from Wavewin tool after converting aspen test file to Wavewin compatible format for a breaker operation of 5 cycles for a faulted

condition involving either 1L-G or 3 phase fault at node 840. Waveforms obtained from this tool are Va,Vb,Vc and sequence components along with Ia,Ib,Ic and sequence current components. The figure also contains phasor rotation of vectors and Harmonics from data extrapolated.

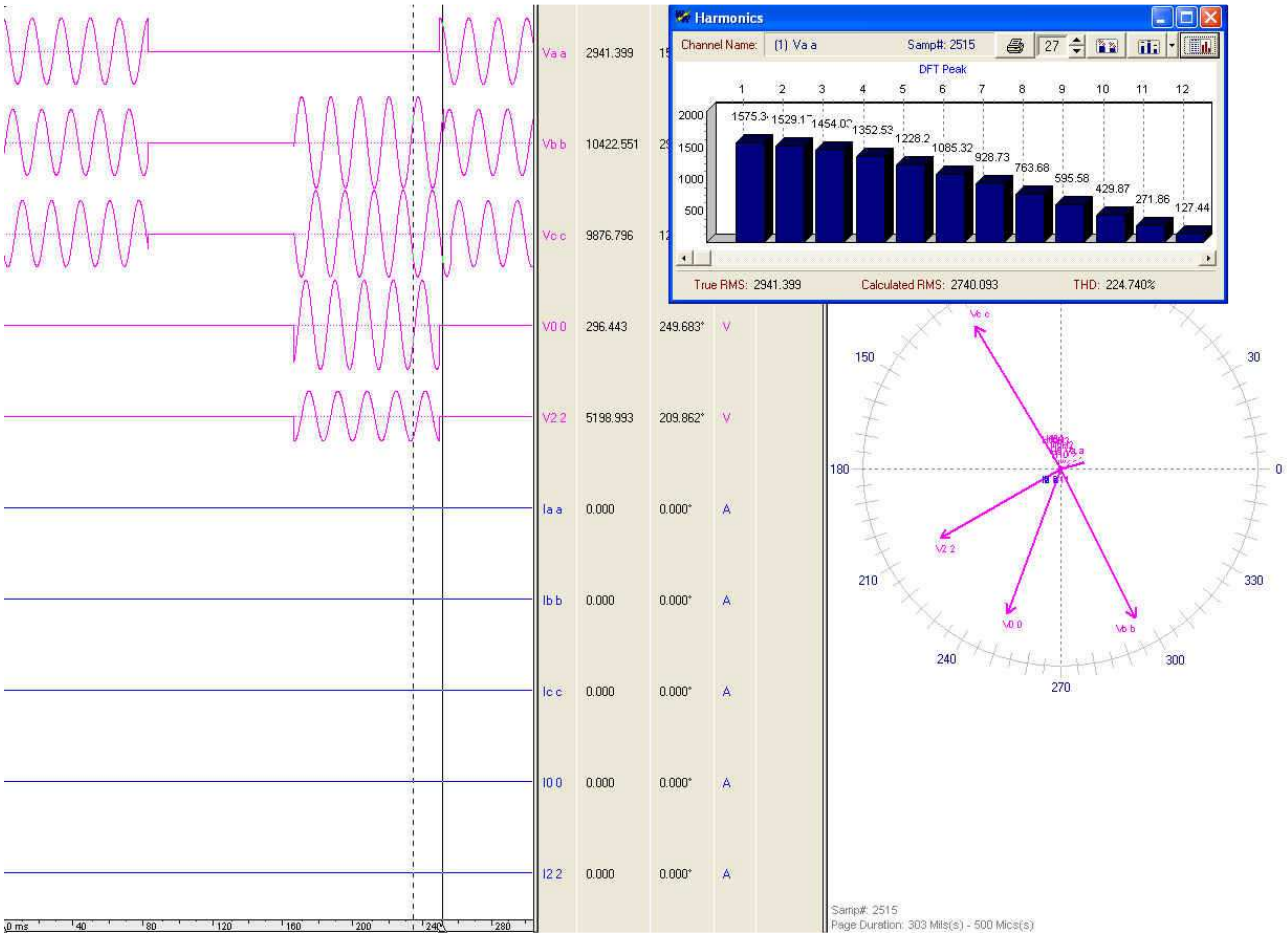

Figure 47:Waveform obtained for a close in fault on relay at node 890

Figure 47 is the waveform obtained for a faulted condition at node 890. By moving the data cursor to the waveform where the faulted condition just begins, there is a change in harmonics mainly terms from 2nd and 3rd components of the fundamental.

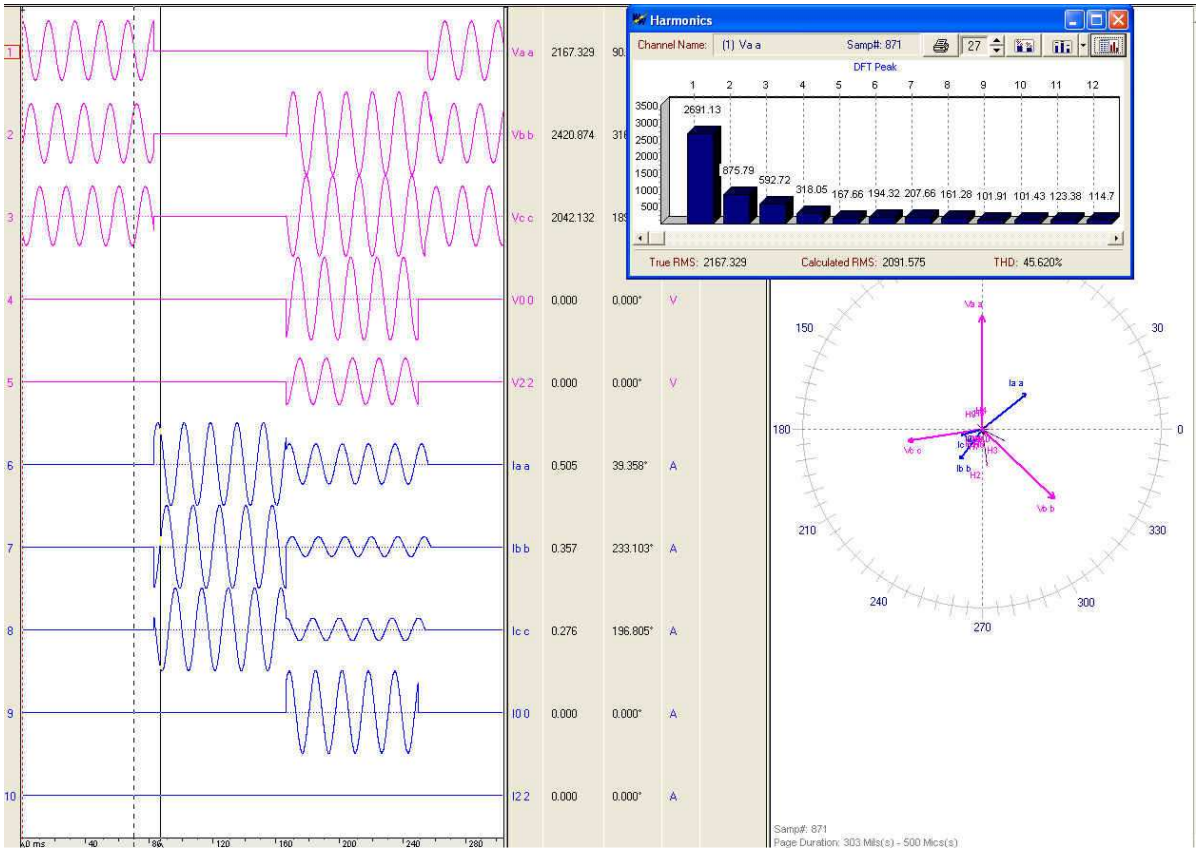

Figure 48:Waveform obtained for a close in fault on relay at node 848

Figure 48 is the waveform obtained for a faulted condition for a close in fault at node 848 containing the Wind turbine and from the waveform at an instant if close to 150ms there is sudden drop in currents possible indicating the cause to transients. This waveform is an indication of transient behavior for a faulted condition for Wind turbine behavior. In contrast to figure 50 which is also Wind turbine connected to node 840, the waveforms indicate the transient fault behavior during the operation after 144ms.

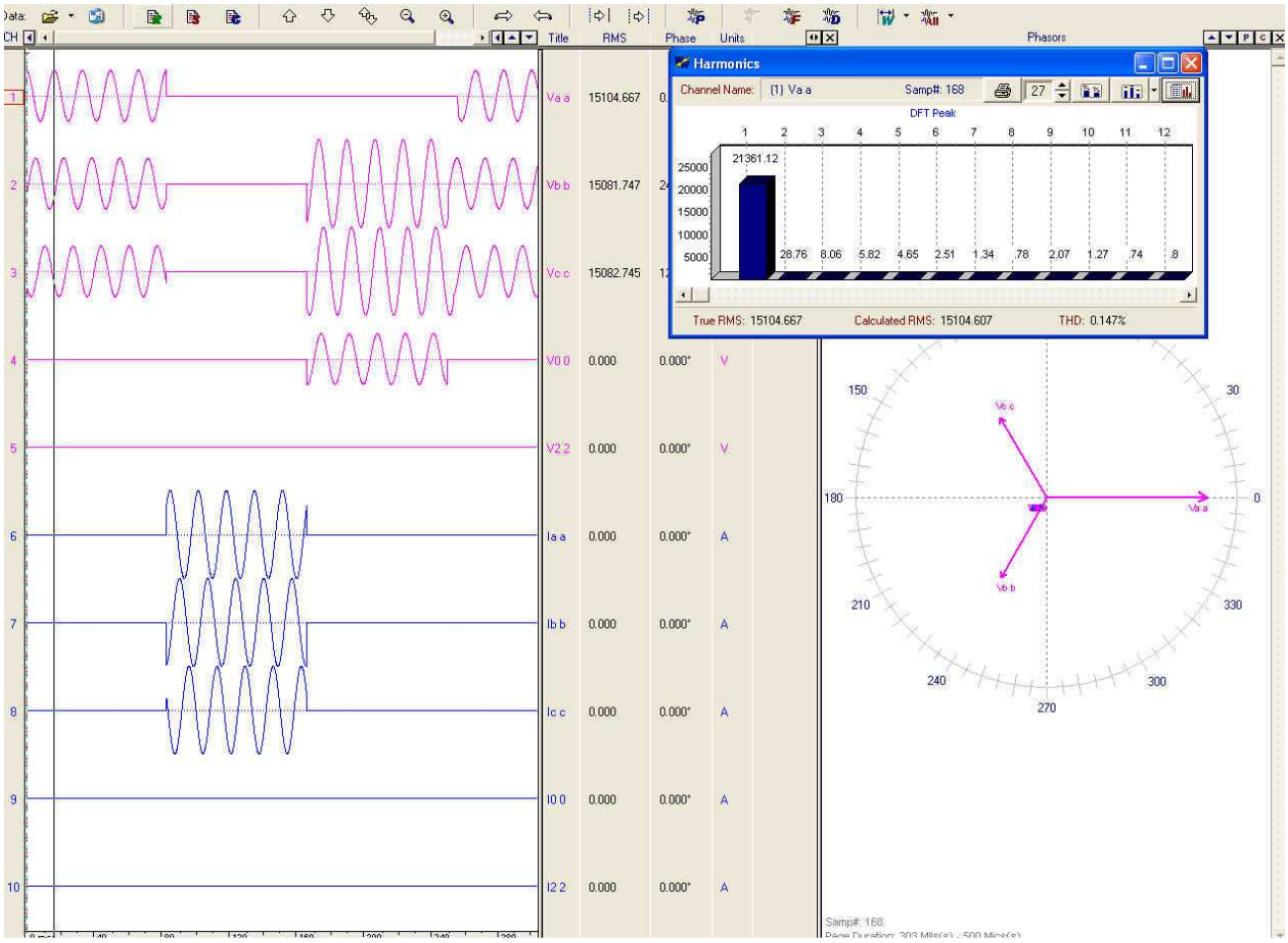

Figure 49:Waveform obtained for a close in fault on relay at node 800

Figure 49 is the waveform obtained for a relay operation faulted condition at node 800 which has the synchronous diesel generator connected. Since it is connected to the low voltage of 24.49/12/47 connected delta-wye grounded transformer, the behavior in this case is different as there is fault currents contribution from the high side which seems to higher. For this case, the waveform does not translate the nature of fault currents as described in the above chapters

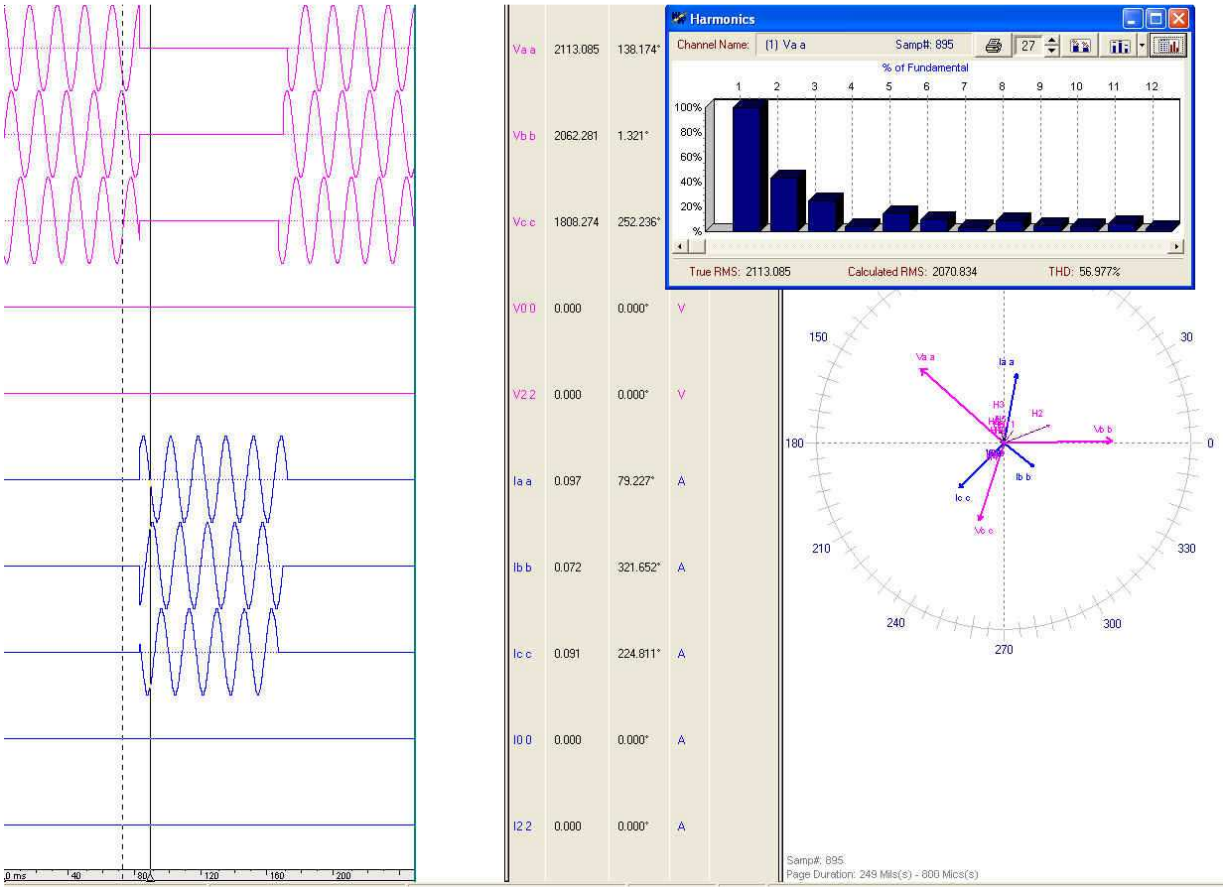

Figure 50:Waveform obtained for a close in fault on relay at node 828

Figure 50is the waveform obtained from a close in fault at node 828 which is the energy storage modeled as inverter based PV module. In all the above wavewin obtained waveforms, the phase voltage is multiplied by a security factor greater than 10 for the rms value and also includes a fault impedance of 13.33 + 13.33j. The results match Aspen per unit maximum and minimum fault currents shown in the above table 14.

4.8 Fuse and Recloser operation times:

Based on the fuse saving approach from [14] and implemented interconnection protection:

Table 7: Consolidated results for Fuse-recloser Overcurrent protection for various DG's

Location of DG	Temporary fault			Permanent fault		
	R opens	R close	Fuse	R open	R close	Fuse
800	4 cycles	13 cycle	Melts	4 cycles	13 cycle	18 cycle
840	5 cycles	15 cycle	DNM	5 cycles	15 cycle	16 cycle
848	3 cycles	12 cycle	DNM	3 cycles	12 cycle	15 cycle
890	5 cycles	16 cycle	Melts	5 cycles	16 cycle	22 cycle
828	3 cycles	13 cycle	DNM	3 cycle	13 cycle	18 cycle

DNM- Does not melt

Interconnection relay settings:

In this approach, five interconnection relays were adopted and one case for directional approach was used. The table 8 below lists the settings used for the Inverse time non directional phase and ground with time delayed and instantaneous settings and the directional element settings used

Table 8: Coordination device settings for interconnect relay at node 800 from S&C tool

Device 1	Device 2	Device 3	Device 4
Phase relay: U1-U5 Type: U2 Inverse Pick up: 500A TD: 0.5 Breaker clearing time: 0.05s Ground relay: U1-U5 Type: U3 VI Pick up: 150A	Transformer Damage curve: Delta-Wye grounded Primary/Full load amps: 24.9kV/579.67 Sec/Full load amps: 12.47kV/1157.48 Impedance: 8.06% 3 phase fault current: 1855.13A	Phase: IEEE Type: Inverse Pick up: 800A TD: 2 Ground relay: Instantaneous pick up: 848A	Fuse: Cooper Type: X Limiter kV: 8.3-23 Ampere rating: 50

CHAPTER V: ISLANDING PHENOMENON

5.1 Islanding condition:

Islanding is a condition defined when the DG is isolated from the main utility due to intentional or unintentional islanding and where in the DG continues to serve loads connected to it[36].Microgrid is a special system where the DG's are sufficient enough to feed all the loads connected to it. As formulated, the objective of the thesis is to study the protection scheme for an interconnected system to the Microgrid which is mentioned in the above chapters. This chapter is discussed to study the potential issues during islanded mode and the effect it can have on interconnection protection as it is a useful step to perform further research in isolated DG system protection, in consultation with the IEEE 1547 guidelines.

5.2 DG Unit Protection recommendations based on IEEE 1547:

In the latest IEEE standard C62.41.2, it defines that all DG interconnection systems must have the capability to withstand voltage and current surges and that the interconnection protective device should isolate the DG facility from the utility section.

-Utility companies also require that for large DG generators, it should have effective grounding system to avoid overvoltage issues. Since we have delta on the DG side with the DG grounded system, overvoltage scheme would not be required. If the primary side was wye grounded, then the neutral should be insulated and a current limiting grounding reactor is required to limit the fault current [25]

- Utility companies require a sync check device when it is out of phase with the utility

- Over and underfequency relays must meet the 1547 requirements [25]. Figure 49 and Table 7 below shows the curve for setting the thresholds for underfrequency protection for generators as adopted from NPCC [37]

Table 9: – Interconnection system response to abnormal frequencies [37]		
DR size	***Frequency range (Hz)***	***Clearing time (s)a***
≤ 30 kW	*> 60.5*	*0.16*
	< 59.3	*0.16*
> 30 kW	*> 60.5*	*0.16*
	< {59.8 - 57.0} (	*Adjustable 0.16 to 300*
	< 57.0	*0.16*
a DR ≤ 30 kW, maximum clearing times; DR > 30 kW, default clearing times		

As Per NPCC Document A-03 [37] :

"Generators should not be tripped for under-frequency conditions in the area above the curve in Figure below. And so for settings above the curve an equivalent amount of load should be shed when tripped "

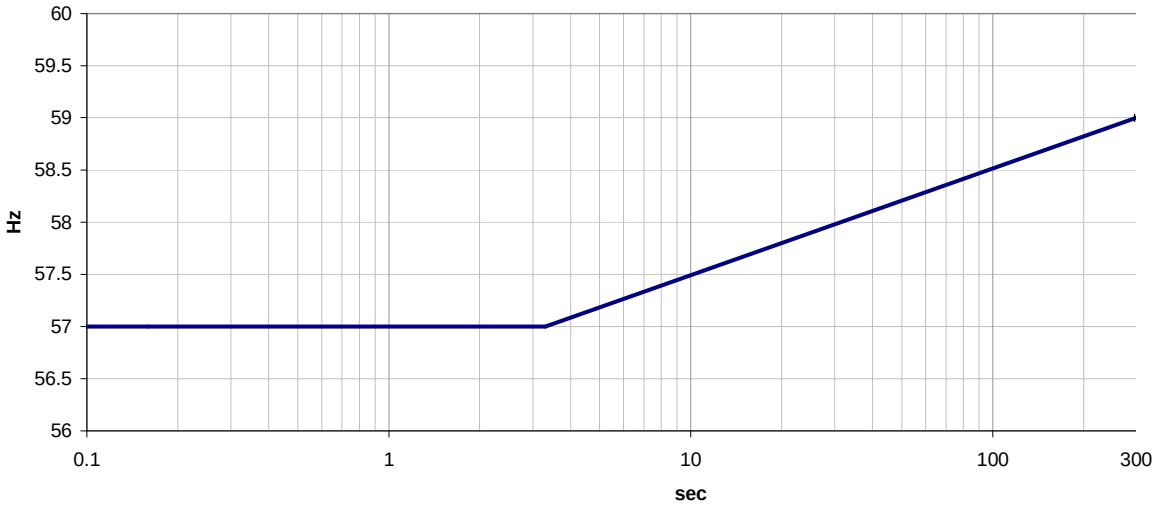

Figure 51: Underfrequency tripping conditions (Adopted from [37])

- Since the Inverter based PV is 250kW, it should be IEEE 1547 compliant and UL-1741 certified for the inverter equipped with anti-islanding internal protection. Internal relaying is considered sufficient for Inverter based PV below 500kW [1], [25]. Additional relaying adopted for inverter based protection above 500kW includes as shown in table 8 below :

Table 10: Relay Functions for various Interconnection fault conditions from DG perspective (Presented from [25], [38])

- Objective	- Relaying
- To detect Islanding	- 81o/u (Over and under frequency relay) - 27/59(Under and over voltage)
- For short circuit and overloaded conditions	- 50/51N (Instantaneous phase and ground non directional OC protection) - 67(Directional OC protection)
- Unbalances to Generator	- 46(Unbalanced currents) - 47(Unbalanced voltages)
- Reverse Power flow	- 67 or 32(Reverse power flow relay)
- Synchronizing Machine to the system	- 25 (Sync check relay)

- The IEEE 1547 states that anti-islanding protection is required for parallel generation to the utility distribution network . Further transfer trip studies and research on anti-islanding schemes is required for DG to work as an isolated system and not energize a denenergized distribution network [25], [38].

- IEEE 1547 states that, “For an unintentional island in which the DG energizes a portion of the utility , the DG interconnection shall detect and cease to energize the utility portion within 2 seconds of the island formation “

CHAPTER VI: CONCLUSIONS AND FUTURE WORK

6.1 Conclusions:

This thesis work involves the modeling and developing a protection scheme for the scaled down version of the IEEE 34 bus system with and the without Distributed Generation. The DG's are predefined at specific nodes based on various studies performed earlier. Five DG's of sizes, 250kW, 1.5MVA, 750kW, 500kW,750kW are placed in the IEEE radial distribution feeder. The first step performed was the simulation and modeling of existing IEEE 34 bus network in CYMDist 5.04 to validate the performance of the tool used. The second step performed is the scaling of the model to 12.47kV system to match the Microgrid parameters [39]. Scaling involved conversion of the ohmic values to sequence components using symmetrical component techniques and then converting to per unit system so that protection studies can be performed in Aspen One-liner by obtaining the equivalent impedances once modeled in CYME. Once the system was built, load flow and short circuit fault analysis is performed. The DG's are modeled to study the issues they have when connected to the Distribution feeder. The next step involved was to develop an interconnection protection scheme at the point of interconnection. This involves three cases studied for the Diesel generator as synchronous generator , Wind turbine and Inverter based PV protection. Each protection aspect involves coordination studies with Inverse time Overcurrent protection with instantaneous and time delayed elements along with the use of a directional element protection to detect current backfeed which could lead to nuisance tripping. Various issues related to the addition of DG's is discussed. The three cases also discuss modeling

of Wind turbine using a preset model from MATLAB to study the short circuit faults including torque control with feedback control is implemented but for a different preset model from Simulink. The thesis also includes the fusing practice for Capacitor banks in the distribution network and coordination practices with downstream an upstream protection. Post fault analysis is conducted from Aspen by converting to Wavewin supported formats which is a useful tool for relay operation time and harmonic analysis. The thesis also mentions the reasons for various choices of transformer selection and transformer phasing and also develops a chapter based on IEEE 1547 standards for relaying and protection practices to be adopted when the DG's form an island. The results are mentioned along with the relevant chapters simultaneously while other results are tabulated in the penultimate chapter.

6.2 Future Work

Going forward, the future scope of this thesis is to study the protection and stability analysis extensively for the DG's and the islanding and anti-islanding techniques as this is gaining fast importance in today's practices as there is a growing demand for alternative energy sources and storage. Since there is a lot of exciting research in the field of Renewable energy and control systems, the future work is to study the protection and transient analysis for Microgrid systems.

REFERENCES

[1] EPRI Report , “Integrating Distributed Resources into Electric Utility Distribution Systems”, 2001.[Online]. Available: http://www.epri.com/abstracts/Pages/ProductAbstract.aspx

[2] Silva, J.A.; Funmilayo, H.B.; Butler-Purry, K.L., "Impact of Distributed Generation on the IEEE 34 Node Radial Test Feeder with Overcurrent Protection," *Power Symposium, 2007. NAPS '07. 39th North American* , vol., no., pp.49,57, Sept. 30 2007-Oct. 2 2007

[3] Fu, Q.; Nasiri, A.; Bhavaraju, V.; Solanki, A.; Abdallah, T.; Yu, D.C., "Transition Management of Microgrids With High Penetration of Renewable Energy," *Smart Grid, IEEE Transactions on* , vol.PP, no.99, pp.1,11

[4] R. Kamel, A. Chaouachi and K. Nagasaka, "Detailed Analysis of Micro-Grid Stability during Islanding Mode under Different Load Conditions," *Engineering*, Vol. 3 No. 5, 2011, pp. 508-516.

[5]IEEE Distribution System Analysis Subcommittee. Radial Test Feeders[Online].Available:http://www.ewh.ieee.org/soc/pes/dsacom/testfeeders.html..

[6] Kersting, W.H., "Radial distribution test feeders," *Power Systems, IEEE Transactions on* , vol.6, no.3, pp.975,985, Aug 1991

[7] Fu, Q.; Solanki, A.; Montoya, L.F.; Nasiri, A.; Bhavaraju, V.; Abdallah, T.; Yu, D., "Generation capacity design for a microgrid for measurable power quality indexes," *Innovative Smart Grid Technologies (ISGT), 2012 IEEE PES* , vol., no., pp.1,6, 16-20 Jan. 2012

[8] Blackburn, J. L., Protective Relaying: Principles and Applications, Mercel Dekker, Inc., New York, 1987

[9]CYME Power Engineering Software, “CYME QA Validation test cases”, 2011.[Online]. Available: http://www.ipet-co.com/en/download-software/cyme-validation-tests-cases

[10] J.Burke,” Hard to Find Information about Distribution Systems ABB Inc.Consulting,,Raleigh”, 2002..[Online].Available:library.abb.com

[11] Si XinYue; Chen Qing; Gao ZhanJun; Wang Li, "The study on protection scheme for distribution system in presence of distributed generation," *Advanced Power System Automation and Protection (APAP), 2011 International Conference on* , vol.2, no., pp.857,861, 16-20 Oct. 2011

[12] ABB, Protective Relaying Theory and Applications, Mercel Dekker, Inc., New York, 2004

[13] Patterson, R. 2005. “The importance of power system event analysis”. 8th Annual Fault and Disturbance Analysis Conference. Atlanta, Georgia, USA.

[14] Funmilayo, H.B.; Silva, J.A.; Butler-Purry, K.L., "Overcurrent Protection for the IEEE 34-Node Radial Test Feeder," *Power Delivery, IEEE Transactions on* , vol.27, no.2, pp.459,468, April 2012

[15] Venkata, S.S.; Pahwa, A.; Brown, R.E.; Christie, R.D., "What future distribution engineers need to learn," *Power Systems, IEEE Transactions on* , vol.19, no.1, pp.17,23, Feb. 2004

[16] S. E. Zocholl and D. W. Smaha, “Current Transformer Concepts” Proceedings of the 46th Annual Georgia Tech Protective Relay Conference, Atlanta, GA, April 29 - May 1, 1992.

[17] “Overcurrent Protection for phase and earth faults” [Online] Available : www.fecime.org/referencias/npag/chap9-122-151.pdf

[18] IEEE Report, “Impact of Distributed Resources on Distribution Relay Protection”, A report to the Line Protection Subcommittee of the Power System Relay Committee of the IEEE Power Engineering Society prepared by working group D3, August 2004, [Online] Available: www.pes-psrc.org/Reports/wgD3ImpactDR.pdf

[19] Kasztenny, B.; Thompson, M.; Fischer, N., "Fundamentals of short-circuit protection for transformers," *Protective Relay Engineers, 2010 63rd Annual Conference for* , vol., no., pp.1,13, March 29 2010-April 1 2010

[20] Antonova, G.; Nardi, M.; Scott, A.; Pesin, M., "Distributed generation and its impact on power grids and microgrids protection," *Protective Relay Engineers, 2012 65th Annual Conference for* , vol., no., pp.152,161, 2-5 April 2012

[21] Cooper Power, Electrical Distribution-System Protection. Wisconsin: Cooper PowerSystemsInc,2005

[22] Sadeh, J.; Bashir, M.; Kamyab, E., "Effect of distributed generation capacity on the coordination of protection system of distribution network," *Transmission and Distribution Conference and Exposition: Latin America (T&D-LA), 2010 IEEE/PES* , vol., no., pp.110,115, 8-10 Nov. 2010

[23] Jun Li; Butler-Purry, K.L.; Benner, C., "Modeling of TCC-based protective devices," *Transmission and Distribution Conference and Exposition, 2003 IEEE PES* , vol.1, no., pp.150,156 Vol.1, 7-12 Sept. 2003

[24] Acharya, J.R.; Yunfei Wang; Wilsun Xu, "Temporary Overvoltage and GPR Characteristics of Distribution Feeders With Multigrounded Neutral," *Power Delivery, IEEE Transactions on* , vol.25, no.2, pp.1036,1044, April 2010

[25] IEEE Application Guide for IEEE Std 1547, IEEE Standard for Interconnecting Distributed Resources with Electric Power Systems," *IEEE Std 1547.2-2008* , vol., no., pp.1,207, April 15 2009

[26] IEEE Guide for the Protection of Shunt Capacitor Banks," *IEEE Std C37.99-2012 (Revision of IEEE Std C37.99-2000)* , vol., no., pp.1,151, March 8 2013

[27] Dawalibi, F.P.; Tee, S.; Fortin, S.; Grignon, N., "Inadequacies of the Industry-Standard IEEE C37.99-2000 Concerning Grounding Neutrals of Shunt Capacitors in High-Voltage Substations," *Power Delivery, IEEE Transactions on* , vol.26, no.2, pp.782,789, April 2011

[28] Westinghouse, *Electric Utility Engineering Reference book*, Vol. 2, Distribution Systems, 1965

[29] Mozina, C.J., "Interconnect protection of dispersed generators," *Transmission and Distribution Conference and Exposition, 2001 IEEE/PES* , vol.2, no., pp.709,723 vol.2, 2001

[30] Sortomme, E.; Mapes, G. J.; Foster, B. A.; Venkata, S.S., "Fault analysis and protection of a microgrid," *Power Symposium, 2008. NAPS '08. 40th North American* , vol., no., pp.1,6, 28-30 Sept. 2008

[31] SimPower Systems. (2007). MATLAB Manual. [Online].Available: http://www.mathworks.com.

[32] Xin Wang; Yuvarajan, S.; Lingling Fan, "MPPT control for a PMSG-based grid-tied wind generation system," *North American Power Symposium (NAPS), 2010* , vol., no., pp.1,7, 26-28 Sept. 2010

[33] Muljadi, E.; Samaan, N.; Gevorgian, V.; Li, J.; Pasupulati, S., "Different Factors Affecting Short Circuit Behavior of a Wind Power Plant," *Industry Applications Society Annual Meeting (IAS), 2010 IEEE* , vol., no., pp.1,9, 3-7 Oct. 2010

[34] Muljadi, E.; Samaan, N.; Gevorgian, V.; Jun Li; Pasupulati, S., "Short circuit current contribution for different wind turbine generator types," *Power and Energy Society General Meeting, 2010 IEEE* , vol., no., pp.1,8, 25-29 July 2010

[35] Tan, S. F.; Salman, S.K., "Investigation into the implementation of auto reclosing scheme in distribution networks with high penetration of DGs," *Universities Power Engineering Conference, 2008. UPEC 2008. 43rd International* , vol., no., pp.1,5, 1-4 Sept. 2008

[36] Feero, William E., Douglas C. Dawson, Stevens John, “White Paper on Protection Issues of The MicroGrid Concept” , March 2002 [Online] Available: http://eetd.lbl.gov/node/50097

[37] Standard PRC-006-NPCC-1 Automatic Underfrequency Load Shedding , NPCC Document A-3,” Generator Underfrequency tripping” , [Online] Available: http://www.nerc.com/files/PRC-006-NPCC-1.pdf

[38] Benato, Roberto; Caldon, Roberto; Corsi, Sandro, "Protection requirements in distribution systems with high penetration of DG and possibility of intentional islanding," *Electricity Distribution, 2005. CIRED 2005. 18th International Conference and Exhibition on* , vol., no., pp.1,4, 6-9 June 2005

[39] Ebrahimi, R.; Jamali, S.; Gholami, A.; Babaei, A., "Short circuit analysis in unbalanced distribution networks," *Universities Power Engineering Conference, 2007. UPEC 2007. 42nd International* , vol., no., pp.942,946, 4-6 Sept. 2007

Appendix A: Load flow and Fault Study Data and Results

Existing 24.9kV Load flow and Fault study:

The tables below illustrate the results after performing load flow analysis

Table 11: Load flow summary report for Regulators, Y-Y Transformer and Shunt Capacitor:

Section Id	Equipment Id	Code	Loading A (%)	Thru Power A (kW)	Thru Power A (kVAR)	VA (%)
814-850	DEFAULT	Regulator	333.4	692.1	153.5	101.77
852-832	DEFAULT	Regulator	219.8	468.6	65.4	103.59
18		Shunt Capacitor	106.2	0	-106.2	103.06
17		Shunt Capacitor	106.2	0	-159.3	103.09
832-888	XFM1_XFO_34BUS	Transformer	100.7	151.8	84.8	99.95

Table 12: Load flow report in per unit for existing 24.9kV IEEE system

Node Id	V (pu)	Angle V		QCap MVAR	PLoad MW	QLoad MVAR
800	1.05	0		0	0	0
802	1.048	-0.05		0	0.05	0.03
806	1.047	-0.08		0	0.05	0.03
808	1.024	-0.75		0	0.02	0.01
810	1.029	-120.95		0	0.02	0.01
812	0.998	-1.57		0	0	0
814	0.977	-2.26		0	0	0
850	1.021	-2.26		0	0	0
816	1.021	-2.27		0	0.01	0
818	1.016	-2.27		0	0.03	0.02
820	0.993	-2.33		0	0.17	0.09
822	0.99	-2.33		0	0.13	0.07
824	1.012	-2.38		0	0.05	0.02
826	1.016	-122.93		0	0.04	0.02
828	1.011	-2.39		0	0.01	0.01
830	0.994	-2.64		0	0.05	0.02
854	0.993	-2.65		0	0	0
852	0.963	-3.12		0	0	0
15	1.035	-3.12		0	0	0
832	1.035	-3.12		0	0.02	0.01
858	1.033	-3.18		0	0.05	0.03
834	1.031	-3.25		0	0.19	0.09
842	1.031	-3.26		0	0.01	0.01

844	1.03	-3.28		-0.32	0.48	0.36
846	1.03	-3.32		0	0.07	0.03
848	1.03	-3.33		-0.48	0.08	0.06
860	1.03	-3.24		0	0.3	0.17
836	1.03	-3.24		0	0.12	0.06
840	1.03	-3.24		0	0.07	0.04
862	1.03	-3.24		0	0.03	0.01
838	1.029	-124.39		0	0.03	0.01
864	1.034	-3.18		0	0	0
888	0.999	-4.64		0	0	0
890	0.919	-5.2		0	0.41	0.21
856	0.998	-123.41		0	0	0

Scaled 12.47kV Load flow and Fault study with and without DG's:

Table 13:Load flow report in per unit for 12.47kV scaled down system

Node Id	V (pu)	Angle V	PLoad MW	QLoad MVAR
800	1.0485	0	0	0
802	1.046	-0.08	0.05	0.03
806	1.045	-0.13	0.05	0.03
808	1.019	-1.15	0.03	0.02
812	0.99	-2.45	0	0
814	0.9675	-3.55	0	0
850	1.011	-3.55	0	0
816	1.011	-3.56	0.01	0
818	1.0055	-3.56	0.13	0.07
820	0.99	-3.62	0.27	0.14
822	0.9885	-3.62	0.14	0.07
824	1.0005	-3.84	0.1	0.05
826	1.014	-124.32	0.08	0.04
828	0.9995	-3.87	0.01	0.01
830	0.979	-4.48	0.18	0.08
854	0.9785	-4.5	0	0
852	0.9445	-5.7	0	0
15	1.0155	-5.7	0	0
832	1.0155	-5.7	0.06	0.03
858	1.013	-5.84	0.1	0.05
834	1.0095	-6.02	0.61	0.31
842	1.0095	-6.03	0.01	0.01
844	1.009	-6.08	1.7	1.31
846	1.01	-6.17	0.07	0.03
848	1.01	-6.19	0.08	0.06
860	1.009	-6.01	0.72	0.38
836	1.009	-6.01	0.16	0.08
840	1.009	-6.01	0.14	0.08

862	1.009	-6.01	0.03	0.01
838	1.028	-127.07	0.03	0.01
864	1.007	-5.84	0	0
888	0.9975	-6.98	0	0
890	0.9775	-7.12	0.88	0.44
856	0.996	-125.19	0	0
810	1.0275	-121.35	0.03	0.02

Table 14:Load Balancing report for 12.47 scaled down distribution network

	Rephasing (kVA)				Phase A (kVA)	Phase B (kVA)	Phase C (kVA)	Ineutral (A)	Total Losses (kW)	Average kVA Unbal.	Current Unbal. Factor	Voltage Unbal. Factor
Section ID	A	B	C									
816-818	to C 194.03			Before	613.18	455.91	329	16.75	349.21	31.57%	31.57%	0.00%
				After	375.05	435.17	604.76	18.91	332.76	28.22%	28.22%	0.00%
844-846	to C 0	No change	to A 22.83	Before	375.05	435.17	604.76	18.91	332.76	28.22%	28.22%	0.00%
				After	399.39	441.23	560.08	14.72	326.25	19.96%	19.96%	0.00%
802-806	to C 0	to A 33.54	to B 28.65	Before	399.39	441.23	560.08	14.72	326.25	19.96%	19.96%	0.00%
				After	421.47	438.3	526.57	10.58	324.1	13.95%	13.95%	0.00%
808-810		to A 16.77		Before	421.47	438.3	526.57	10.58	324.1	13.95%	13.95%	0.00%
				After	434.07	421.57	527.08	9.44	322.92	14.36%	14.36%	0.00%
824-828	No change	to C 0	to B 4.47	Before	434.07	421.57	527.08	9.44	322.92	14.36%	14.36%	0.00%
				After	433.34	427.32	519.55	9.04	321.64	12.93%	12.93%	0.00%

Table15: Impedances and currents are in per unit (case with no fault impedance)

		Maximum	Maximum						
BUS	KV	Phase Cur	Gnd Cur	Z+		Z2		Z0	
BUS0	0.48	0.011	0	3.83847	3.82961	157.386	134.357	4.00E+07	4.00E+07
BUS1	0.48	0.038	0	17.3924	19.8448	188.418	121.221	1.30E+07	1.30E+07
BUS2	0.48	0.037	0	17.6751	20.4434	203.713	130.655	1.30E+07	1.30E+07
BUS3	0.48	0.027	0	1.9055	1.87113	54.293	45.6122	2.00E+07	2.00E+07
BUS800	12.47	0.597	0.911	0.79459	1.72131	0.25819	6.34927	0.32431	1.12009
BUS802	12.47	0.514	0.748	0.965	1.84078	0.43433	6.48036	0.58277	1.46353
BUS806	12.47	0.427	0.573	1.24716	2.03851	0.72855	6.6993	0.99662	2.01762

BUS808	12.47	0.199	0.21	3.51451	3.62284	3.22327	8.55453	3.30817	5.32597
BUS810	12.47	0.111	0.103	6.9965	6.00212	6.70531	10.9339	7.20934	9.95501
BUS812	12.47	0.099	0.114	7.42434	6.33225	8.28024	12.3126	5.30006	8.70433
BUS814	12.47	0.069	0.086	11.3617	9.00117	15.3726	17.5779	5.98536	10.3987
BUS816	12.47	0.052	0.075	13.8306	10.3862	29.6044	28.1206	4.90061	9.52278
BUS818	12.47	0.038	0.052	21.2363	15.8222	37.0135	33.5562	8.31046	15.1874
BUS820	12.47	0.024	0.03	36.8535	25.6126	52.6347	43.346	19.9314	25.2076
BUS822	12.47	0.016	0.02	54.8109	36.6468	70.5936	54.3799	33.8935	36.4703
BUS824	12.47	0.05	0.077	11.9652	8.8907	37.7869	33.9213	3.6105	7.23708
BUS826	12.47	0.037	0.054	20.6444	14.9698	46.4673	40.0001	6.49147	12.5137
BUS828	12.47	0.051	0.083	7.64974	5.76988	46.0537	39.7651	1.92614	3.83069
BUS830	12.47	0.043	0.068	15.0003	10.5036	56.4436	46.6492	4.24077	7.01713
BUS832	12.47	0.04	0.065	22.5814	16.3681	95.3478	64.4882	3.30003	6.43857
BUS834	12.47	0.044	0.073	26.1959	19.0655	125.457	82.8576	2.61833	6.38777
BUS836	12.47	0.04	0.067	29.912	23.2915	156.779	101.902	2.27151	6.03797
BUS838	12.47	0.02	0.032	62.1207	42.9352	189.019	121.53	6.14453	15.3768
BUS840	12.47	0.046	0.078	25.6989	22.542	172.597	111.572	1.37749	3.73751
BUS842	12.47	0.038	0.063	31.6595	22.8106	140.792	92.2282	2.94067	7.55308
BUS844	12.47	0.036	0.059	33.6587	24.8651	156.249	101.676	2.86725	7.574
BUS846	12.47	0.037	0.063	32.0495	25.189	172.058	111.322	2.35587	6.34217
BUS848	12.47	0.044	0.075	26.7144	23.7162	187.896	121.007	1.39799	3.81228
BUS850	12.47	0.057	0.076	13.4983	10.3532	22.4706	22.842	5.84972	10.6703
BUS852	12.47	0.037	0.06	23.2754	15.6522	81.1263	62.3518	6.14887	8.11546
BUS854	12.47	0.039	0.062	20.081	13.7374	66.8882	53.5589	5.63511	8.34134
BUS856	12.47	0.026	0.04	34.4658	22.7692	81.2761	62.5897	12.9524	16.0279
BUS858	12.47	0.04	0.066	26.4359	18.7778	110.111	73.5198	3.16951	7.07206
BUS860	12.47	0.04	0.066	30.0286	22.1119	140.988	92.3096	2.68038	6.89937
BUS862	12.47	0.027	0.044	45.7339	32.9022	172.624	111.501	3.92367	10.4972
BUS864	12.47	0.028	0.045	41.416	27.9835	125.096	82.7232	5.36373	11.5979
BUS888	4.16	0.029	0.049	24.9957	23.1813	111.738	84.5777	2.75388	5.20117
BUS890	4.16	0.022	0.038	19.6681	20.0601	134.559	109.486	1.64797	3.06749

Table 16:Impedances and currents are in per unit (case with fault impedance)

		Maximum	Maximum					
BUS	KV	Phase Cur	Gnd Cur	Z+		Z2		Z0	
BUS0	0.48	0.007	0	3.83847	3.82961	157.386	134.357	4.00E+07	4.00E+07
BUS1	0.48	0.007	0	17.3924	19.8448	188.418	121.221	1.30E+07	1.30E+07
BUS2	0.48	0.006	0	17.6751	20.4434	203.713	130.655	1.30E+07	1.30E+07
BUS3	0.48	0.019	0	1.9055	1.87113	54.293	45.6122	2.00E+0	2.00E+0

								7	7
BUS800	12.47	0.238	0.089	0.79459	1.72131	0.25819	6.34927	0.32431	1.12009
BUS802	12.47	0.23	0.087	0.965	1.84078	0.43433	6.48036	0.58277	1.46353
BUS806	12.47	0.217	0.085	1.24716	2.03851	0.72855	6.6993	0.99662	2.01762
BUS808	12.47	0.143	0.07	3.51451	3.62284	3.22327	8.55453	3.30817	5.32597
BUS810	12.47	0.093	0.055	6.9965	6.00212	6.70531	10.9339	7.20934	9.95501
BUS812	12.47	0.086	0.054	7.42434	6.33225	8.28024	12.3126	5.30006	8.70433
BUS814	12.47	0.06	0.043	11.3617	9.00117	15.3726	17.5779	5.98536	10.3987
BUS816	12.47	0.044	0.041	13.8306	10.3862	29.6044	28.1206	4.90061	9.52278
BUS818	12.47	0.034	0.033	21.2363	15.8222	37.0135	33.5562	8.31046	15.1874
BUS820	12.47	0.023	0.023	36.8535	25.6126	52.6347	43.346	19.9314	25.2076
BUS822	12.47	0.016	0.016	54.8109	36.6468	70.5936	54.3799	33.8935	36.4703
BUS824	12.47	0.041	0.043	11.9652	8.8907	37.7869	33.9213	3.6105	7.23708
BUS826	12.47	0.032	0.034	20.6444	14.9698	46.4673	40.0001	6.49147	12.5137
BUS828	12.47	0.04	0.047	7.64974	5.76988	46.0537	39.7651	1.92614	3.83069
BUS830	12.47	0.035	0.043	15.0003	10.5036	56.4436	46.6492	4.24077	7.01713
BUS832	12.47	0.032	0.043	22.5814	16.3681	95.3478	64.4882	3.30003	6.43857
BUS834	12.47	0.032	0.046	26.1959	19.0655	125.457	82.8576	2.61833	6.38777
BUS836	12.47	0.029	0.043	29.912	23.2915	156.779	101.902	2.27151	6.03797
BUS838	12.47	0.017	0.025	62.1207	42.9352	189.019	121.53	6.14453	15.3768
BUS840	12.47	0.032	0.048	25.6989	22.542	172.597	111.572	1.37749	3.73751
BUS842	12.47	0.028	0.041	31.6595	22.8106	140.792	92.2282	2.94067	7.55308
BUS844	12.47	0.027	0.04	33.6587	24.8651	156.249	101.676	2.86725	7.574
BUS846	12.47	0.028	0.041	32.0495	25.189	172.058	111.322	2.35587	6.34217
BUS848	12.47	0.031	0.047	26.7144	23.7162	187.896	121.007	1.39799	3.81228
BUS850	12.47	0.049	0.04	13.4983	10.3532	22.4706	22.842	5.84972	10.6703
BUS852	12.47	0.031	0.041	23.2754	15.6522	81.1263	62.3518	6.14887	8.11546
BUS854	12.47	0.033	0.041	20.081	13.7374	66.8882	53.5589	5.63511	8.34134
BUS856	12.47	0.024	0.03	34.4658	22.7692	81.2761	62.5897	12.9524	16.0279
BUS858	12.47	0.031	0.044	26.4359	18.7778	110.111	73.5198	3.16951	7.07206
BUS860	12.47	0.029	0.043	30.0286	22.1119	140.988	92.3096	2.68038	6.89937
BUS862	12.47	0.022	0.032	45.7339	32.9022	172.624	111.501	3.92367	10.4972
BUS864	12.47	0.024	0.033	41.416	27.9835	125.096	82.7232	5.36373	11.5979
BUS888	4.16	0.014	0.009	24.9957	23.1813	111.738	84.5777	2.75388	5.20117
BUS890	4.16	0.012	0.009	19.6681	20.0601	134.559	109.486	1.64797	3.06749

Table 17: 24.9kV system fault currents with DG's :

Equipment Id	Phase	kVLN	LLL Kmax (Amps)	LLL Kmin (Amps)	LLG Kmax (Amps)	LLG Kmin (Amps)	LL Kmax (Amps)	LL Kmin (Amps)	LG Kmax (Amps)	LG Kmin (Amps)	Tot dista ft
800	ABC	14.4	774	642	809	672	670	556	822	682	0
150	ABC	6.9	570	473	809	671	493	410	757	629	0
802	ABC	14.4	755	626	784	651	654	542	788	654	2580
806	ABC	14.4	742	616	768	637	643	533	767	636	4310
808	ABC	14.4	549	456	532	442	476	395	495	411	3654(
810	B	14.4	0	0	0	0	0	0	452	375	4234
812	ABC	14.4	410	340	388	322	355	295	344	285	7404(
814	ABC	14.4	339	281	321	267	294	244	275	229	1037
850	ABC	14.4	339	281	321	267	294	244	275	229	1037
816	ABC	14.4	338	281	321	266	293	243	275	228	1040
818	A	14.4	0	0	0	0	0	0	270	224	1058(
820	A	14.4	0	0	0	0	0	0	180	149	1539
822	A	14.4	0	0	0	0	0	0	164	136	1676
824	ABC	14.4	314	261	299	248	272	226	254	210	1143(
826	B	14.4	0	0	0	0	0	0	247	205	1173
828	ABC	14.4	312	259	297	247	271	225	252	209	1151
137	ABC	14.4	312	259	297	247	271	225	252	209	1151
830	ABC	14.4	273	227	261	217	236	196	218	181	1355
854	ABC	14.4	272	226	261	216	236	196	217	181	1361(
852	ABC	14.4	221	183	213	177	191	159	175	145	1729
15	ABC	14.4	221	183	213	177	191	159	175	145	1729
832	ABC	14.4	221	183	213	177	191	159	175	145	1729
858	ABC	14.4	215	178	208	173	186	155	170	141	1778
834	ABC	14.4	209	173	202	168	181	150	165	137	1836
842	ABC	14.4	209	173	202	168	181	150	165	137	1839
844	ABC	14.4	207	172	201	166	179	149	164	136	1853(
846	ABC	14.4	204	169	197	164	176	146	161	134	1889
848	ABC	14.4	203	168	197	163	176	146	161	133	1894
126	ABC	0.3	4304	3573	4135	3432	3728	3094	3859	3203	1894
127	ABC	0.1	6124	5083	5304	4402	5304	4402	0	0	1894
860	ABC	14.4	207	172	200	166	179	149	164	136	1856
836	ABC	14.4	204	169	198	164	177	147	161	134	1883
840	ABC	14.4	203	169	197	163	176	146	161	133	1892
131	ABC	0.3	4306	3574	4137	3433	3729	3095	3861	3204	1892
132	ABC	0.1	6126	5084	5305	4403	5305	4403	0	0	1892
862	ABC	14.4	204	169	197	164	176	146	161	134	1886
838	B	14.4	0	0	0	0	0	0	157	131	1935
864	A	14.4	0	0	0	0	0	0	170	141	1794
888	ABC	2.4	722	600	697	579	626	519	629	522	1729
890	ABC	2.4	397	330	384	318	344	286	317	263	1835(
856	B	14.4	0	0	0	0	0	0	182	151	1594

Table 18:12.47kV system fault currents with DG's in amps :

Equipment Id	Phase	kVLN	LLL Kmax (Amps)	LLL Kmin (Amps)	LLG Kmax (Amps)	LLG Kmin (Amps)	LL Kmax (Amps)	LL Kmin (Amps)	LG Kmax (Amps)	LG Kmin (Amps)
800	ABC	7.6	942	782	1234	1024	815	677	1188	986
802	ABC	7.6	914	759	1160	963	792	657	1120	929
806	ABC	7.6	897	744	1116	926	776	644	1077	894
808	ABC	7.6	636	528	657	545	551	457	612	508
810	B	7.6	0	0	0	0	0	0	547	454
812	ABC	7.6	461	383	443	367	399	331	400	332
814	ABC	7.6	376	312	353	293	325	270	313	260
850	ABC	7.3	364	302	342	284	315	262	303	252
816	ABC	7.3	363	301	341	283	314	261	302	251
818	A	7.3	0	0	0	0	0	0	297	246
820	A	7.3	0	0	0	0	0	0	191	159
822	A	7.3	0	0	0	0	0	0	173	144
824	ABC	7.3	336	279	317	263	291	241	277	230
826	B	7.3	0	0	0	0	0	0	269	223
828	ABC	7.3	333	277	315	262	289	240	275	228
157	ABC	2.4	615	510	586	487	532	442	544	451
158	ABC	0.3	4446	3691	4262	3538	3851	3196	4008	3327
830	ABC	7.3	289	240	275	229	250	208	235	195
854	ABC	7.3	288	239	275	228	250	207	235	195
852	ABC	7.3	231	192	223	185	200	166	186	154
15	ABC	7.4	235	195	226	188	204	169	189	157
832	ABC	7.4	235	195	226	188	204	169	189	157
858	ABC	7.4	229	190	221	183	198	165	184	153
834	ABC	7.4	222	184	214	178	192	160	178	148
842	ABC	7.4	222	184	214	178	192	159	178	148
844	ABC	7.4	220	183	213	176	191	158	177	147
846	ABC	7.4	216	180	209	173	187	156	173	144
848	ABC	7.4	216	179	208	173	187	155	173	143
162	ABC	2.5	468	388	450	374	405	336	395	328
164	ABC	0.3	3539	2938	3410	2830	3065	2544	3046	2528
860	ABC	7.4	220	183	212	176	190	158	176	146
836	ABC	7.4	217	180	209	174	188	156	174	144
840	ABC	7.4	216	179	209	173	187	155	173	144
166	ABC	2.5	468	389	451	374	406	337	395	328
167	ABC	0.3	3542	2940	3412	2832	3067	2546	3049	2530
862	ABC	7.4	217	180	209	174	188	156	174	144
838	B	7.4	0	0	0	0	0	0	169	141
864	A	7.4	0	0	0	0	0	0	184	153
888	ABC	2.5	496	412	477	396	430	357	422	350
890	ABC	2.5	390	324	375	311	338	280	320	265
170	ABC	0.8	369	307	360	299	320	265	345	286
171	ABC	0.1	2367	1964	2319	1925	2050	1701	2248	1865
856	B	7.3	0	0	0	0	0	0	194	161

Arc flash and Voltage sag analysis:

Table 19: Arc flash report using IEEE 1584 :

Voltage (V)	Bolted Fault [kA]	I (arc) seen by device [A]	Clearing Time (s)	Minimum Approach Distance (in)
12470	0.211	0.22	0.4	26
12470	15.569	14.65	0.4	26
12470	9.32	9.06	0.4	26
12470	1.1	1.1	0.4	26
12470	0.875	0.89	0.4	26
12470	0.543	0.55	0.4	26
12470	0.387	0.4	0.4	26
12470	0.386	0.4	0.4	26
12470	0.376	0.39	0.4	26
12470	0.217	0.22	0.4	26
12470	0.193	0.22	0.4	26
12470	0.344	0.35	0.4	26
12470	0.33	0.34	0.4	26
12470	0.341	0.35	0.4	26
12470	0.28	0.29	0.4	26
12470	0.211	0.22	0.4	26
12470	0.197	0.2	0.4	26
12470	0.191	0.2	0.4	26
12470	0.186	0.19	0.4	26
12470	0.19	0.2	0.4	26
12470	0.197	0.2	0.4	26
12470	0.195	0.2	0.4	26
12470	0.191	0.2	0.4	26
12470	0.19	0.2	0.4	26
12470	0.387	0.4	0.4	26
12470	0.211	0.22	0.4	26
12470	0.279	0.29	0.4	26
12470	0.22	0.23	0.4	26
12470	0.204	0.21	0.4	26
12470	0.194	0.2	0.4	26
12470	0.191	0.2	0.4	26
12470	0.202	0.21	0.4	26
4160	0.435	0.45	0.4	26
4160	0.325	0.33	0.4	26

Table 20 :Voltage sag Analysis

Faulted Item	Fault Type	Vmin (pu)
838	LG	0.3471
826	LG	0.4293
862	LG	0.335
862	LLL	0.0977
862	LL	0.4998
862	LLG	0.2063
822	LG	0.6452
836	LG	0.3343
836	LLL	0.0962
836	LL	0.4997
836	LLG	0.206
824	LG	0.4162
824	LLL	0.0016
824	LL	0.4987
824	LLG	0.2727
840	LG	0.3365
840	LLL	0.101
840	LL	0.5
840	LLG	0.2071
818	LG	0.4557
820	LG	0.6145
860	LG	0.3275
860	LLL	0.0808
860	LL	0.4987
860	LLG	0.203
816	LG	0.4482
816	LLL	0.0019
816	LL	0.4985
816	LLG	0.2888
848	LG	0.3371
848	LLL	0.1023
848	LL	0.5002
848	LLG	0.2075
850	LG	0.4493
850	LLL	0.0019
850	LL	0.4985
850	LLG	0.2893
846	LG	0.3357
846	LLL	0.0994
846	LL	0.4999
846	LLG	0.2067
812	LG	0.5409
812	LLL	0.0023
812	LL	0.4982
812	LLG	0.3329

814	LG	0.4493
814	LLL	0.0019
814	LL	0.4985
814	LLG	0.2893
844	LG	0.3265
844	LLL	0.0785
844	LL	0.4986
844	LLG	0.2027
808	LG	0.7178
808	LLL	0.0029
808	LL	0.4977
808	LLG	0.4053
834	LG	0.3224
834	LLL	0.0689
834	LL	0.4982
834	LLG	0.2015
842	LG	0.3231
842	LLL	0.0705
842	LL	0.4982
842	LLG	0.2017
810	LG	0.7347
802	LG	0.9757
802	LLL	0.0034
802	LL	0.4973
802	LLG	0.4902
832	LG	0.2949
832	LLL	0
832	LL	0.5
832	LLG	0.2067
806	LG	0.9598
806	LLL	0.0034
806	LL	0.4973
806	LLG	0.4855
858	LG	0.3075
858	LLL	0.0327
858	LL	0.4981
858	LLG	0.2013
800	LG	1
856	LG	0.4505
15	LG	0.2949
15	LLL	0
15	LL	0.5
15	LLG	0.2067
890	LG	0.7075
890	LLL	0
890	LL	0.5
890	LLG	0.4075

854	LG	0.3609
854	LLL	0.001
854	LL	0.4992
854	LLG	0.2438
864	LG	0.3137
852	LG	0.2949
852	LLL	0
852	LL	1
852	LLG	0.2067
888	LG	0.7758
888	LLL	0
888	LL	1
888	LLG	0.4323
828	LG	0.4137
828	LLL	0.0016
828	LL	0.4987
828	LLG	0.2715
830	LG	0.3621
830	LLL	0.001
830	LL	0.4992
830	LLG	0.2444

APPENDIXB:

Calculations involving symmetrical component analysis:

```
>> a = -0.5 + 0.866j

a =  -0.5000 + 0.8660i

>> a*a

ans =  -0.5000 - 0.8660i

>> A= [ 1 1 1 ; 1 a a*a ; 1 a*a a ]


A = 1.0000            1.0000            1.0000
  1.0000           -0.5000 + 0.8660i  -0.5000 - 0.8660i
 1.0000           -0.5000 - 0.8660i  -0.5000 + 0.8660i

>> inv(A)

ans = 0.3333 - 0.0000i   0.3333 + 0.0000i   0.3333 + 0.0000i
0.3333 + 0.0000i  -0.1667 - 0.2887i  -0.1667 + 0.2887i
0.3333 + 0.0000i  -0.1667 + 0.2887i  -0.1667 - 0.2887i

>> Z = [ 0 0 0 ; 0 1.922 + 1.421j 0 ; 0 0 0 ]

Z = 0                0                0
       0           1.9220 + 1.4210i       0
       0                0                0

>> Zsym = A * Z * inv(A)

Zsym = 0.6407 + 0.4737i   0.0899 - 0.7917i  -0.7305 + 0.3180i
  -0.7305 + 0.3180i   0.6407 + 0.4737i   0.0899 - 0.7917i
  0.0899 - 0.7916i  -0.7305 + 0.3180i   0.6406 + 0.4737i

>> B= [0 0 0; 0 4.364i 0 ; 0 0 0 ]


B = 0                0                0
```

```
      0                0 + 4.3640i      0
      0                0                0
>> A * Z * inv(A)
ans = 0.6407 + 0.4737i   0.0899 - 0.7917i  -0.7305 + 0.3180i
  -0.7305 + 0.3180i   0.6407 + 0.4737i   0.0899 - 0.7917i
0.0899 - 0.7916i  -0.7305 + 0.3180i   0.6406 + 0.4737i
>> A * B * inv(A)
ans = -0.0000 + 1.4547i   1.2598 - 0.7274i  -1.2598 - 0.7273i
-1.2598 - 0.7273i   0.0000 + 1.4547i   1.2598 - 0.7273i
  1.2598 - 0.7273i  -1.2598 - 0.7273i        0 + 1.4546i
>> Z = [ 0 0 0 ; 0 2.8 + 1.486j 0; 0 0 0 ]
Z = 0                0                0
      0           2.8000 + 1.4860i    0
      0                0                0
>> A * Z * inv(A)
ans = 0.9333 + 0.4953i  -0.0377 - 1.0560i  -0.8956 + 0.5607i
-0.8956 + 0.5606i   0.9333 + 0.4953i  -0.0377 - 1.0559i
-0.0377 - 1.0559i  -0.8956 + 0.5606i   0.9333 + 0.4953i
>> B= [0 0 0; 0 4.225i 0 ; 0 0 0 ]
B = 0                0                0
      0                0 + 4.2250i      0
      0                0                0
>>  A * B * inv(A)
ans = -0.0000 + 1.4084i   1.2197 - 0.7042i  -1.2197 - 0.7041i
  -1.2196 - 0.7042i   0.0000 + 1.4084i   1.2196 - 0.7042i
 1.2196 - 0.7041i  -1.2196 - 0.7042i  -0.0000 + 1.4083i

>> Z = [ 0 2.8 + 1.486j 0 ; 0 0 0 ; 0 0 0 ]
```

```
Z = 0            2.8000 + 1.4860i        0
      0                0                0
      0                0                0

>> Z = [  2.8 + 1.486j 0 0; 0 0 0 ; 0 0 0 ]
Z = 2.8000 + 1.4860i        0                0
      0                0                0
      0                0                0
>> A * Z * inv(A)
ans = 0.9333 + 0.4953i   0.9333 + 0.4953i   0.9333 + 0.4953i
  0.9333 + 0.4953i   0.9333 + 0.4953i   0.9333 + 0.4953i
 0.9333 + 0.4953i   0.9333 + 0.4953i   0.9333 + 0.4953i
>> B= [0 0 0; 0 4.225i 0 ; 0 0 0 ]
B = 0                0                0
      0                0 + 4.2250i        0
      0                0                0

>> B= [4.225i 0 0; 0 0 0 ; 0 0 0]
B = 0 + 4.2250i        0                0
      0                0                0
      0                0                0

>> A * B * inv(A)
ans = 0.0000 + 1.4083i  -0.0000 + 1.4084i  -0.0000 + 1.4084i
  0.0000 + 1.4083i  -0.0000 + 1.4084i  -0.0000 + 1.4084i
 0.0000 + 1.4083i  -0.0000 + 1.4084i  -0.0000 + 1.4084i
```

APPENDIX C:

Distributed Generation source parameters:

Diesel Generator : (Fixed Q Limits)

Parameter	Value
Rated line voltage	12.47kV
Rated Power	1.5MVA
Armature Resistance	0.002pu
Armature Time constant	0.332pu
Potier Reactance	0.0110pu
Airgap factor	1.0
Steady State impedances	0.13 + j0.51 pu
Transient impedances	0.03 + j0.228 pu
Sub transient impedances	0.022 + j0.290 pu
Zero sequence impedances	0.001 + j0.001 pu
Negative impedance	0.001 + j0.002 pu

Photovoltaic model:

Parameter in Standard test conditions	Value
Current at Maximum Power Point	4.6A
Short circuit current	5A
Shot circuit temperature coefficient	0.0314 %/ºC
Open circuit voltage temperature coefficient	-0.357%/ºC
Normal operating cell temperature	45ºC
Reference Ambient temperature	20ºC
STC Temperature	25ºC
STC Insolation	1000 W/m^2
PV Panel rated power	250kW
Fault contribution	120%
Voltage source converter rating	500kVA
DC Capacitor	15000 µF
Rated DC Voltage	0.5kV
Grid side coupling Inductance	0.006H

Wind Turbine Model:

Parameter	Value
Rated Wind speed	19.685 ft/s
Cut-in Wind speed	9.8425 ft/s
Cut-out Wind speed	39.370 ft/s
Number of blades	3
Rotor Radius	65.61 ft
Generator capacity	859.11 kVA
Generator rated voltage	0.48kV

Generator rated Power	750kW
Rated speed	1800rpm
Synchronous Reactance's	
Xd	1.2pu
Xl	0.1pu
Xq	0.9pu
Transient Reactance's	
X'd	0.3pu
X'q	0.6pu
T'do	5s
T'qo	1.5s
Sub-transient reactance's	
X''d	0.15pu
X''q	0.2pu
T''do	0.04s
T''qo	0.08s
Fault contribution	100%

Transformer Ratings:

kVA	% Resistance	% Reactance	% Impedance	X/R Ratio	Type
300	1.48	4.77	5.0	3.22	3phase shell, Liquid filled, self-cooled
500	1.30	4.83	5.0	3.71	3phase shell, Liquid filled, self-cooled
750	1.28	5.6	5.75	4.37	3phase shell, Liquid filled, self-cooled
1000	1.21	5.62	5.75	4.37	3phase shell, Liquid filled, self-cooled
1500	1.06	5.64	5.75	5.32	3phase shell, Liquid filled, self-cooled
2500	0.97	5.67	5.75	5.85	3phase shell, Liquid filled, self-cooled

APPENDIX D:

Fuse, Recloser and Relay curves:

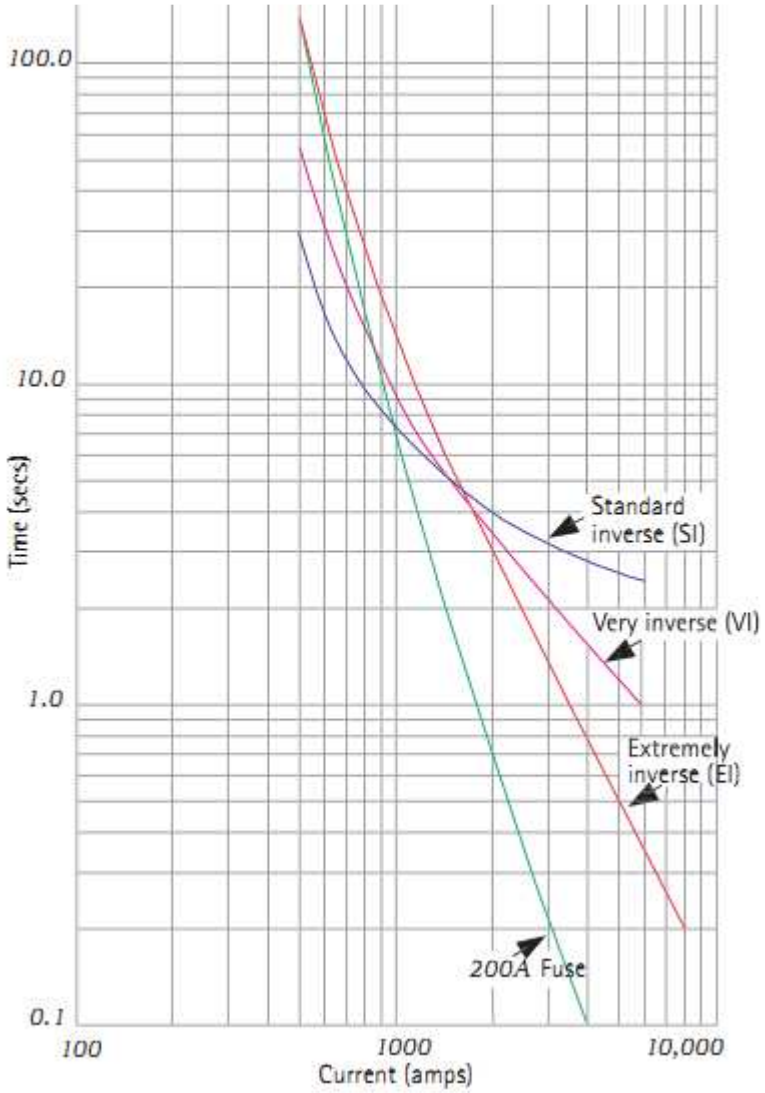

Figure 52: Example of time inverse characteristic curves mimicking fuse curve (Adopted from [17])

Coordination Report for Fuse recloser Overcurrent Protection on the Section 800 downstream:

OVERCURRENT GRD relay on BUS800- 12.47KV-0 BUS802 12.47KV 2L
Type=351R-U3 (SEL.RLY) CTR=240
TD=3.300 Tap=1.200A Nondirectional
Inst ele: none
Time mult. =1.0 Time adder= 0.0 Reset= 0.0

OVERCURRENT PHASE RELAY on BUS800-12.47KV-BUS802 12.47KV 2L
Type=351R-U3 (SEL.RLY) CTR=240
Time ele: TD=1.500 Tap=3.900A Nondirectional
Inst ele: none
Time mult. =1.0 Time adder= 0.0 Reset= 0.0

OVERCURRENT GRD RELAY onBUS808 12.47KV - BUS812 -12.47KV 1L
Type=ME-634R-120(COOPER.RLY) CTR=1000
Time ele: TD=1.000 Tap=0.200A Nondirectional
Inst ele: none
Time mult. =1.8 Time adder= 0.0 Reset= 0.0

OVERCURRENT PHASE RELAY on BUS808 12.47KV -BUS812-12.47KV 1L
Type=ME-634R-120(COOPER.RLY) CTR=1000
Time ele: TD=1.000 Tap=0.500A Nondirectional
Inst ele: none
Time mult. =1.0 Time adder= 0.0 Reset= 0.0

RECLOSER on BUS800-12.47KV - BUS802-12.47KV 2L
Operating cycles: Slow-10s-Slow-Lockout
Fast curve=N/A (SEL.RLY) Min.trip=1A time=0 Time mult. =1 adds. =0
Slow curve=351R-U4 (SEL.RLY) Min.trip=280A time=0 Time mult. =2 add. =0
High curr.trip=0A Delay=0

RECLOSER on BUS828-12.47KV -BUS824-12.47KV 1L
Operating cycles: Slow-Lockout
Fast curve=N/A (SEL.RLY) Min.trip=1A time=0 Time mult. =1 add. =0
Slow curve=351R-U3 (SEL.RLY) Min.trip=50A time=0 Time mult. =5 add. =0
High curr.trip=0A Delay=0

RECLOSER on BUS828 12.47KV - BUS824 12.47KV 1L
Operating cycles: Slow-Lockout
Fast curve=N/A (SEL.RLY) Min.trip=1A time=0 Time mult. =1 add. =0
Slow curve=351R-U4 (SEL.RLY) Min.trip=140A time=0 Time mult. =0.5 add. =0
High curr.trip=0A Delay=0

RECLOSER on BUS808 12.47KV - BUS812 12.47KV 1L
Operating cycles: Slow-10s-Slow-Lockout
Fast curve=N/A (SEL.RLY) Min.trip=1A time=0 Time mult. =1 add. =0
Slow curve=351R (SEL.RLY) Min.trip=100A time=0 Time mult. =1 add. =0
High curr.trip=0A Delay=0

RECLOSER on BUS808 12.47KV BUS812 12.47KV 1L
Operating cycles: Slow-10s-Slow-Lockout
Fast curve=N/A (SEL.RLY) Min.trip=1A time=0 Time mult. =1 add. =0
Slow curve=351R (SEL.RLY) Min.trip=280A time=0 Time mult. =1 add. =0
High curr.trip=0A Delay=0

Some of the curves discussed:

Westinghouse CO-5 relay, long time
Westinghouse CO-6 relay, definite time
Westinghouse CO-7 relay, moderate inverse
Westinghouse CO-8 relay, inverse,
Type COL and CIL capacitor fuse. 15 Amps K Link
BE1-1051_E2 Basler Electric BE1-1051 inverse time-overcurrent relay. 51P, 51Q, 51N
Chance Type "K" (FAST) 15 amp fuse link in cutout.
Chance Type "K" (FAST) 20 amp fuse link in cutout.
Cooper 8.3, 15.5,23 kV (10 amp) X-Limiter Full Range Fuse.
M-E fuse links: EEI-NEMA TYPE K-TIN. 10K,
KEARNEY TYPE X 1.25A FUSE LINKS
ME-221-A
McGraw-Edison recloser type L. TCC-221-A. 200A.
ME-221-BME-301-A
McGraw-Edison recloser types 4H, V4H, PV4H (Single Phase); 6H, V6H (
Three Phase) 25A. TCC-301-A.
ME-634R-101
Recloser Form 4A and 4C,
GE IAC-51 Relay, Inverse curves.
KRNY-K015 Kearney "K" type fuse 15 Amps
Mitsubishi Over-Current Relay CO Time dial: 0.5 - 10
S&C Liquid Power Fuse 100E Slow speed, size 3, 4, 5 7.5kV and 23kV 119-5-3-125E
S&C Liquid Power Fuse 125E Slow speed, size 3, 4, 5 7.5kV and 23kV 119-5-3-150E
Schweitzer 351R Electronic recloser. Curve A